ABSTRACT

KITCHENER, REBECCA LYNN. Recombinant Expression and Characterization of Industrial Enzymes from Thermophilic Archaea. (Under the direction of Dr. Amy M. Grunden).

Extremophiles are microorganisms that are capable of surviving in harsh environments such as temperature extremes, high or low pH, high salt, high metal concentration, or anoxic conditions. Enzymes from extremophiles are often functional under these conditions and therefore have particular value in industrial processing applications. The relative ease with which these enzymes can be expressed recombinantly in common host organisms such as *Escherichia coli* has allowed for extensive research into the myriad ways they can be used to improve current industrial processes. Thermophilic (optimal temperature above 45°C) or hyperthermophilic (optimal temperature above 60°C) biocatalysts are used in several industries including detergents, food, animal feed, starch, textiles, pulp and paper, and pharmaceuticals. These enzymes exhibit increased stability and hydrophobicity at elevated temperatures, and tend to be easy to column purify due to the fact that a pre-column heat treatment allows for removal of most host cell proteins. In this research, two hyperthermophilic enzymes (a hydrolase and an oxidoreductase) were utilized in two very different applications with the intention of improving upon current processes.

Prolidase, or proline dipeptidase, from the hyperthermophilic archaeon *Pyrococcus horikoshii* has been shown to hydroyze the P-O or P-F bonds found in harmful organophosphorus pesticides and nerve agents in addition to its native substrate, Xaa-Pro dipeptides. Prolidase from *Alteromonas* sp. is currently being used as a component of a biodecontamination foam; however, its activity is limited during exposure to high temperatures

or solvents, making formulation and storage problematic. Variants of *P. horikoshii* prolidase (*Ph1*prol) were created using random mutagenesis to generate a prolidase that could withstand temperature and solvent exposure, but would also have catalytic activity over a broad range of temperatures instead of its normal optimal temperature of 100°C. Four variants were biochemically characterized and demonstrated improved catalytic properties at lower temperatures while maintaining stability at high temperatures, making them excellent candidates for use in a biodecontamination strategy.

Superoxide reductase (SOR) from *Pyrococcus furiosus* is capable of reducing toxic intracellular reactive oxygen species (ROS), specifically the superoxide anion, to water without generating molecular oxygen when expressed in exogenous hosts. Superoxide is generated in plants and microorganisms as a result of abiotic stress or as a by-product of oxygenic photosynthesis, and is capable of damaging macromolecules, negatively impacting cellular metabolism, or generating more ROS. Endogenous enzymes for superoxide detoxification are expressed once concentrations build up within the cell; however, molecular oxygen is produced as a by-product of this mitigation process. Accumulation of molecular oxygen can be harmful due to the ease with which it can be reduced to form more superoxide, particularly under persistent stress conditions. Expression of SOR in the cyanobacterium *Synechococcus elongatus* PCC 7942, resulted in improved tolerance to and recovery from abiotic stress such as high temperature, UV-B exposure, high salt concentration, and exposure to solvents. Cyanobacteria have value as producers of biofuels and commodity chemicals using atmospheric CO_2 as a carbon source. It is most desirable to cultivate them in seawater in outdoor photobioreactors on non-arable land to avoid competition with food crops for water or

land, therefore the ability to tolerate abiotic stress increases the economic value of this production strategy.

The use of extremophilic enzymes for these applications supported superior function over a broader range of conditions for OP decontamination in the case of the bioengineered *P. horikoshii* prolidase, and enhanced superoxide detoxification for cyanobacteria expressing *P. furiosus* SOR. The results generated by these studies provide the basis for the development of improved applications in two important research areas of biodecontamination and abiotic stress management.

Recombinant Expression and Characterization of Industrial Enzymes from Thermophilic Archaea

by

Rebecca Lynn Kitchener

A dissertation submitted to the Graduate Faculty of
North Carolina State University
in partial fulfillment of the
requirements for the degree of
Doctor of Philosophy

Microbiology

Raleigh, N.C.

2017

APPROVED BY:

_____

Amy M. Grunden, Ph.D.
Chair of Advisory Committee

_____ _____

Nathaniel G. Hentz, Ph.D. Gary L. Gilleskie, Ph.D.

_____ _____

José M. Bruno-Bárcena, Ph.D. Michael R. Hyman, Ph.D.

DEDICATION

This dissertation is dedicated to my grandfather, Dr. James Joseph Napier, Ph.D. (1921 – 2010). He was an English professor on a life-long quest for knowledge regardless of the subject. His love of learning was something he instilled in me at a young age. Most admirably, he completed his doctorate with a wife and small children at home after serving our country as a Marine in World War II. Were he still here today, I'm certain he would have become an expert in microbiology, read this document from cover to cover, and probably subjected me to a mock defense at home.

I also dedicate this work to my son, Oren James Kitchener. His presence in my life has constantly helped me to maintain perspective, and has never let me lose sight of the fact that it is he, not this research, that will be my greatest accomplishment.

BIOGRAPHY

Rebecca Lynn (Becky) Kitchener was born in the great state of New Jersey, where she lived for ten years before moving to southwest Florida, and eventually relocating to North Carolina where Raleigh became her forever home. Despite growing up in several states, she is living proof of the veracity of the adage; "you can take the girl out of New Jersey, but you can't take New Jersey out of the girl." Just ask her husband (or her lab mates).

Becky's road to completing a Ph.D. in Microbiology was neither short, straight, nor simple. After graduating from North Carolina State University in 2003 with a Bachelor's Degree in Animal Science, Becky spent the next few years working in the pharmaceutical industry as a laboratory technician in quality control. In 2007, she accepted a position at her alma mater as a Laboratory Manager at the Biomanufacturing Training and Education Center (BTEC), a collaborative training facility designed to prepare students - both from N.C. State and around the world - to excel in the biopharmaceutical industry.

Working in the Analytical Services Laboratory at BTEC gave Becky the chance to expand her knowledge of bioprocessing science as it related to the biopharmaceutical industry. She had the excellent fortune to work with Dr. Nathaniel Hentz - friend, mentor, life coach, and science guru - and together they transformed the BTEC Analytical Services Laboratory from an empty room to a fully-functional analytical testing lab. They worked together to design, develop, and execute several short courses and a suite of analyses that supported both BTEC courses as well as industry clients. With Dr. Hentz's guidance (and somewhat regular

pep talks), Becky gained skill and confidence as a scientist while learning, developing, and teaching new analysis methods at BTEC.

After completing a few graduate-level science courses with the intention of brushing up on her scientific knowledge, Becky began to consider the possibility of obtaining a graduate degree. She was accepted into the Microbiology program and kicked off her graduate career as a part-time student, while continuing to work full-time at BTEC. After completing a particularly challenging yet interesting course in microbial metabolic regulation taught by Dr. Amy Grunden, Becky joined the Grunden lab and began working to biochemically characterize recombinant archaeal hydrolases that had been mutated to improve function at lower temperatures. Upon completion of this project, and with Dr. Grunden's encouragement, Becky decided to change her degree track from Master of Science to Doctor of Philosophy. Shortly after making the switch, Becky met and married her wonderful husband, Jacob Kitchener. Their son Oren James was born in 2014.

After Oren's birth, Becky made the incredibly difficult decision to leave her position at BTEC and join the Grunden lab as a full-time student so that she could focus on her research as well as her new family. She began her second research project: transforming cyanobacteria with an archaeal antioxidant gene to improve its tolerance to oxidative stress, with the ultimate goal of creating a more robust producer of next generation biofuels. While the challenges associated with research were numerous, and at times seemingly endless, the benefits – such as gaining strength and confidence as a scientist – far outweighed any hardship.

ACKNOWLEDGEMENTS

I would first like to thank my advisor, Dr. Amy Grunden, for taking a chance on a non-traditional graduate student and allowing me to join her lab. I am incredibly grateful for the patience she showed me, and I am honored to have studied under her guidance. I must also acknowledge my graduate committee members: Drs. Nat Hentz, Gary Gilleskie, Michael Hyman, and José Bruno-Bárcena for their time, advice, and constructive feedback.

Sincere gratitude is owed to the past and present members of the Grunden Lab; particularly Dr. Stephanie Mathews, Caroline Smith-Moore, and Hannah Wapshott for welcoming me into their lab and their lives. These three women, with their constant encouragement, humor, patience, assistance, and empathy, are largely responsible for the existence of this document. Thanks to Jacob Dums as well for being an incredible teaching buddy, inspiration, and friend.

I've made countless jokes with Dr. Nat Hentz about any challenges associated with my research being directly attributable to him, since he was the one to originally suggest that I had potential to be successful as a graduate student. There is, however, quite a bit of truth in that joke. As cliché as it sounds, Nat believed in me as a scientist before I would have ever thought to believe in myself. I would not have applied to graduate school without his encouragement, and I certainly wouldn't have stayed there. It is a rare occurrence for a supervisor to transform into a mentor and a dear friend; my luck in knowing him has not escaped me.

Finally, endless appreciation and gratitude is due to my husband, Jacob Kitchener, for providing patience, love, and support throughout this lengthy endeavor. We met after I had

begun graduate school and, for some reason, he married me anyway. I could not and would not have stayed the course without him.

"All of us are driven by a simple belief that the world as it is just won't do – that we have an obligation to fight for the world as it should be." – Michelle Obama

TABLE OF CONTENTS

LIST OF FIGURES

CHAPTER 4. Expression of Antioxidant Superoxide Reductase from *Pyrococcus furiosus* Enhances Stress Tolerance in the Cyanobacterium *Synechococcus elongatus* PCC 7942

LIST OF TABLES

CHAPTER 1.

Prolidase Function in Proline Metabolism and its Medical and Biotechnological Applications

Rebecca L. Kitchener and Amy M. Grunden

Citation: Kitchener, R.L. and Grunden, A.M. (2012). Prolidase function in proline metabolism and its medical and biotechnological applications. *J Appl Microbiol, 113*: 233–247.

1.1. Abstract

Prolidase is a multifunctional enzyme that possesses the unique ability to degrade imidodipeptides in which a proline or hydroxyproline residue is located at the C-terminal end. Prolidases have been isolated from archaea and bacteria, where they are thought to participate in proline recycling. In mammalian species, prolidases are found in the cytoplasm and function primarily to liberate proline in the final stage of protein catabolism, particularly during the biosynthesis and degradation of collagen. Collagen comprises nearly one-third of the total protein in the body, and it is essential in maintaining tissue structure and integrity. Prolidase deficiency (PD), a rare autosomal recessive disorder in which mutations in the PEPD gene affect prolidase functionality, tends to have serious and sometimes life-threatening clinical symptoms. Recombinant prolidases have many applications and have been investigated not only as a possible treatment for PD, but also as a part of anti-cancer strategies, a component of biodecontamination cocktails and in the dairy industry. This review will serve to discuss the many *in vivo* functions of prokaryotic and eukaryotic prolidases, as well as the most recent advances in therapeutic and biotechnological applications of prolidases.

1.2. Introduction

Proteases are enzymes that catalyze the breakdown of proteins into smaller peptides and amino acids. The unique structure of proline induces conformational constraints on the peptide bond, protecting it from general degradation processes (Cunningham and O'Connor, 1997). The existence of a small number of special proteases capable of hydrolyzing the bond between proline and other amino acids, in addition to the tissue distribution and localization of

these proteases suggests that proline plays a role in the regulation of key biological processes (Phang et al., 2010, Wu et al., 2011). Prolidase, or proline dipeptidase, is one of these unique enzymes capable of degrading dipeptides in which a proline or hydroxyproline residue is located at the C-terminal position (Xaa-Pro) (Lowther and Matthews, 2002). Prolidases are ubiquitous in nature and have been isolated from archaeal, bacterial, and several eukaryotic sources.

In bacteria and archaea, prolidase is thought to function in the degradation of intracellular proteins and in proline recycling in concert with other endo-and exo-peptidases (Du et al., 2005). In humans, cytosolic prolidase is involved in the final step of protein catabolism where it serves to liberate proline from proline-rich dietary and endogenous proteins such as extracellular collagen. Fluctuations in prolidase activity can indicate a disruption in collagen metabolism which is characteristic of many disease states as well as the progression of disease (Viglio et al., 2006, Phang et al., 2010). The connection between prolidase and collagen biosynthesis and degradation can be better understood by studying prolidase deficiency (PD), a rare hereditary condition affecting humans in which mutations in the PEPD gene on the 19th chromosome result in inactive or impaired prolidases. The mutated prolidase present in PD patients is unable to hydrolyze certain Xaa-Pro substrates resulting in their accumulation and excretion in the urine causing a major loss of proline that would otherwise be utilized in the body. PD patients suffer from an array of clinical symptoms such as skin ulcerations due to defective wound healing, immunodeficiency, mental retardation, splenomegaly and recurrent respiratory infections (Viglio et al., 2006, Phang et al., 2010).

Thus, it can be surmised that prolidase is somehow involved in the metabolic disturbances leading up to these symptoms.

Enzyme replacement therapy using recombinant prolidases has been considered as a possible treatment for prolidase deficiency (Viglio et al., 2006), and determination of the optimal method of enzyme administration is currently ongoing. High substrate specificity and differential expression of prolidase during certain disease states make it an excellent target as a prodrug therapeutic agent in alleviating these conditions. Outside of the medical field, prolidase has been studied extensively for several biotechnological applications. In the food industry, prolidase and other peptidases can be added during the cheese fermentation process to improve the flavor of the cheese by hydrolyzing peptides responsible for bitter flavor (Courtin et al., 2002). Recombinant bacterial prolidases such as organophosphorus acid anhydrolase (OPAA), a prolidase isolated from *Alteromonas* sp. strain JD6.5, are currently being studied to better understand their enzymatic and structural properties for use in the degradation of organophosphorus (OP) compounds present in certain pesticides and chemical warfare agents (CWAs). In this application, prolidases have shown promise as biosensors to detect OP contamination or as part of an environmentally-friendly biodecontamination strategy (Cheng and DeFrank, 2000, Simonian et al., 2001).

1.3. General properties of prolidase

Prolidases are metallopeptidases that require binding of a metal cofactor near the active site in order for catalysis to occur. More specifically, the occupancy of two metal ions (a dinuclear metal center) is needed for full prolidase activity, whereas other metallopeptidases

such as methionine aminopeptidase (MetAP) employ only one metal ion for activity and the other metal ion participates in activity modulation (Lowther and Matthews, 2002). The presence of divalent metal cations helps to stabilize the enzyme as well as to secure the substrate in the binding pocket. Crystal structure analysis has revealed five conserved amino acids important for metal binding that have been identified in several prolidases (Gonzales and Robert-Baudouy, 1996, Maher et al., 2004, Alberto et al., 2011). Metallopeptidases can be further classified by their structural homologies as well as their substrate preferences, and based on this, prolidase is classified as a member of the "pita-bread" family of enzymes. Pita-bread enzymes contain a highly-conserved characteristic fold in their C domain where the metal center is located, and is flanked by a well-defined substrate binding pocket (Lowther and Matthews, 2002). This family of enzymes exhibits very narrow substrate specificity, cleaving only a small number of N-terminal peptide bonds, suggesting that these enzymes function more to regulate biological processes instead of participating in general protein degradation (Lowther and Matthews, 2002). Figure 1-1 depicts the structures of the prolidases from *Pyrococcus furiosus* and *Pyrococcus horikoshii* as well as a stereoview of the five conserved amino acids in the *P. furiosus* active site. Prolidases hydrolyze the structurally unique bond between a hydrophobic amino acid residue in the N-terminus and a proline residue in *trans* conformation in the C-terminus (Cunningham and O'Connor, 1997, Lupi et al., 2008). They will also cleave dipeptides where proline is replaced by hydroxyproline, but their hydrolytic activity is decreased (Cunningham and O'Connor, 1997, Lupi et al., 2008).

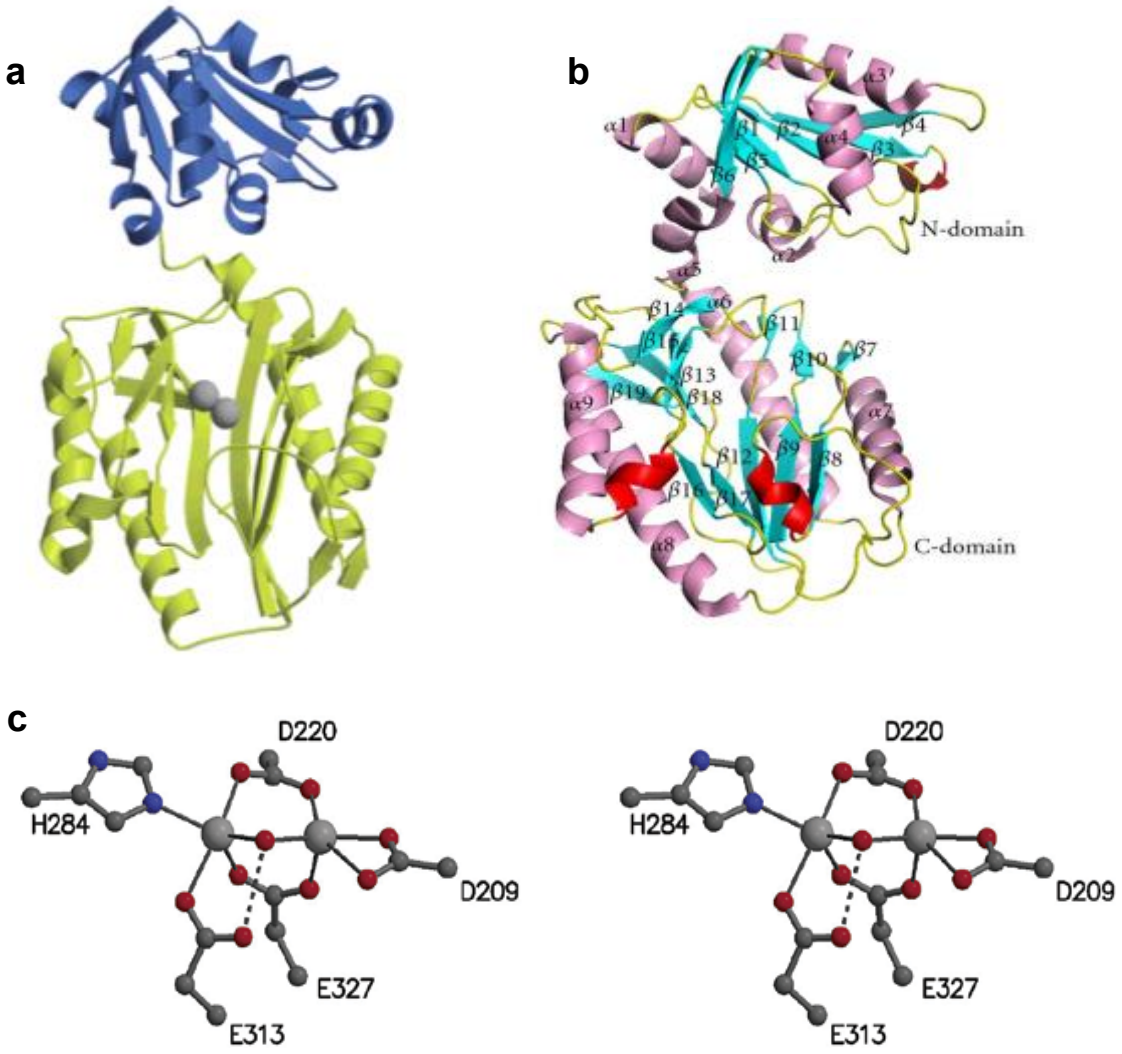

Figure 1-1. a) Monomeric structure of the prolidase from *Pyrococcus furiosus* in which the Zn atoms are shown as gray spheres (from Maher et. al. 2004). **b)** Monomeric structure of the prolidase from *Pyrococcus horikoshii* in which the active site is located between two 3_{10} helices (residues 191-195 and 281-284) shown in red (from Jeyakanthan et al., 2009. **c)** Stereoview of the active site of *Pyrococcus furiosus* showing the five conserved amino acids and the two zinc atoms of the metal center (from Maher et al., 2004).

Figure 1-2 shows the general prolidase reaction in which the affected bond between proline and glycine is highlighted. The proposed mechanism of the prolidase reaction has been discussed in detail in several reviews (Lowther and Matthews, 2002, Theriot et al., 2009, Alberto et al., 2011). In short, once substrate is bound to the active site, the reaction is initiated by a nucleophilic attack from a hydroxide group associated with the metal center on the scissile bond. Protons are shifted by a conserved glutamate residue that acts as a proton shuttle allowing the amide bond between proline and the Xaa residue to be cleaved. Upon the release of free proline, the prolidase active site is fully regenerated (Theriot et al., 2009).

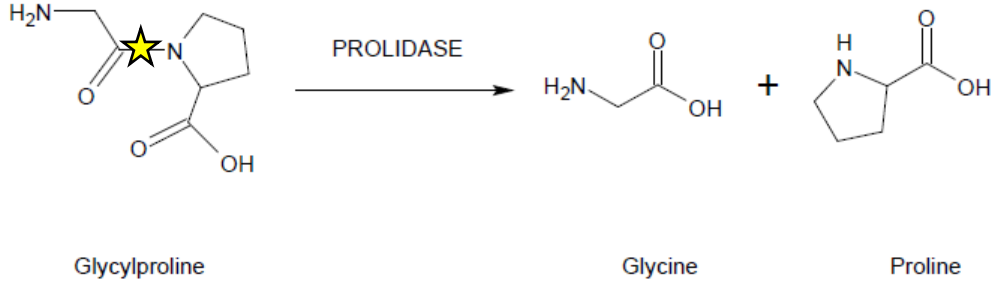

Figure 1-2. The prolidase reaction involving the dipeptide Gly-Pro in which the amide bond is highlighted.

Table 1-1. Properties of various biochemically characterized prolidases.

Domain	Organism	Prolidase	Metal Requirement[a,b]	Native Structure	Optimal Temperature	Optimal pH	References
Archaea	*Pyrococcus furiosus*	*Pf* prolidase PF1343	Co^{2+} (100), Mn^{2+} (80)	Homodimer	100°C	7.0	(Ghosh et al., 1998, Du et al., 2005)
Archaea	*Pyrococcus horikoshii*	*Ph* prolidase PH1149/*Ph1* prolidase PH0974	Co^{2+} (100)Mn^{2+} (35, 70)[c]	Homodimer	100°C	7.0	(Theriot et al., 2010b)
Bacteria	*Alteromonas* sp. Strain JD6.5	OPAA	Mn^{2+} (100), Co^{2+} (85)	Tetramer	50°C	8.0	(DeFrank and Cheng, 1991, Cheng et al., 1993, Vyas et al., 2010)
Bacteria	*Lactobacillus casei*	PepQ prolidase	Mn^{2+} (100), Co^{2+} (52)	Monomer	55°C	6.5 - 7.5	(Fernandez-Espla et al., 1997)
Bacteria	*Lactobacillus delbrueckii* subsp. *bulgaricus* CNRZ 397	PepQ prolidase	Zn^{2+}	Homodimer	50°C	6.0	(Morel et al., 1999)
Bacteria	*Lactococcus lactis*	*Lc. lactis* prolidase	Zn^{2+} (100), Mn^{2+} (22)	Homodimer	35 - 55°C	7.0	(Yang and Tanaka, 2008)
Bacteria	*Xanthomonas maltophilia*	Prolidase	Mn^{2+}	Dimer	37°C	7.5	(Suga et al., 1995)
Eukarya	*Aspergillus nidulans*	PepP	Mn^{2+}	Homodimer	na	7.0	(Jalving et al., 2002)
Eukarya	*Bos primigenius* (Cow)	Prolidase	na	Homodimer	40°C	7.0 – 7.2	(Yoshimoto et al., 1983)
Eukarya	*Cavia porcellus (*Guinea Pig)	Prolidase	Mn^{2+}	Dimer	na	8.0	(O'Cuinn and Fottrell, 1975)
Eukarya	*Homo sapiens* (Human)	Prolidase I (PD I)/Prolidase II (PD II)/PepD	Mn^{2+} (100), Zn^{2+} (<30)	Dimer	50°C	7.8	(Lupi et al., 2006, Besio et al., 2010)

[a]The relative percent activity for prolidase loaded with the indicated metal is provided in parentheses.
[b]Various dipeptide substrates used to assay activity for all prolidases except OPAA. OPAA activity was assayed with diisopropyl fluorophosphate (DFP).
[c]Activity with Mn^{2+} is 35% that of Co^{2+} for *Ph* prolidase and 70% that of Co^{2+} for *Ph1* prolidase

Several prokaryotic and eukaryotic prolidases have been biochemically characterized (Table 1-1). Prolidases differ greatly in their substrate specificities, metal requirements, native structure and optimal temperature for catalysis; however, they all seem to operate within a relatively narrow pH range of 6.0 – 8.0, with the optimal pH being dependent on the species of origin. Optimal temperatures for catalysis are in the range of 35°C – 55°C for prolidases obtained from mesophilic sources, whereas prolidases isolated from hyperthermophilic archaea *Pyrococcus* spp. show optimal activity at 100°C. The majority of prolidases studied are homodimeric, although the prolidase from *Lactobacillus casei* is thought to be a monomer, and OPAA has recently been shown to be a tetramer (Fernandez-Espla et al., 1997, Vyas et al., 2010). While prolidases are highly specific in the type of substrate that they hydrolyze, there are differences in dipeptide substrate specificities among the prolidases. Human prolidase shows the highest activity with Gly-Pro, although it is also active with Ala-Pro, Met-Pro, Phe-Pro, Leu-Pro and Val-Pro (Lupi et al., 2008). Wild-type prolidase from *Pyrococcus horikoshii* is most active with Val-Pro and shows very little activity with Gly-Pro (Theriot et al., 2011). OPAA prolidase prefers Met-Pro and has very little activity with both Gly-Pro and Val-Pro (Kitchener, 2011. Unpublished data).

Several organisms possess more than one prolidase. When more than one prolidase is present the enzymes typically differ in substrate preference as well as the conditions under which they are expressed (Theriot and Grunden, 2011). Two prolidases from *P. horikoshii* have been isolated and characterized; *Ph* prolidase (*Ph*prol) and *Ph* prolidase homolog 1 (*Ph1*prol) (Theriot et al., 2010b). Both prolidases are similar in metal requirement and molecular weight (39.27 kDa and 40.04 kDa, respectively); however, differences in relative

activities and substrate specificities suggest the *in vivo* roles of the two prolidases may differ (Theriot et al., 2010b). Humans also have two forms of prolidase: Isoform I (PD I) and Isoform II (PD II) which differ in their molecular weight (56 kDa and 95 kDa, respectively), their metal requirement, heat stability and substrate specificities (Uramatsu et al., 2009, Liu et al., 2007). In humans, PD I is most active with Gly-Pro, whereas PD II has higher activity with Met-Pro and has little activity against Gly-Pro. Two prolidase isoforms also exist in rats, where PD I is more active with Ser-Pro and Ala-Pro than Gly-Pro, and PD II still shows very little activity with Gly-Pro (Liu et al., 2007).

It is the existence of these two prolidase isoforms in humans that explains why prolidase activity in patients suffering from prolidase deficiency is indeed present, but modified. Prolidase isolated from PD patients shows very little activity with Gly-Pro while its activity against other substrates remains unchanged indicating that the mutations of the PEPD gene associated with PD affect PD I and not PD II (Uramatsu et al., 2009). Additionally, concentrations and activities of PD I and PD II can differ based on their location in the body. In rats, PD I is the most concentrated in the small intestine and kidney, suggesting that PD I functions mainly in the absorption and reabsorption of proline (Liu et al., 2007).

1.4. Prolidase function

The exact physiological role of prolidase in prokaryotic species remains undefined; however, it is generally thought that prolidase functions in the liberation and recycling of free proline from protein. In bacterial proteolytic systems, peptidases with broad specificity are required for the initial steps of protein degradation in which protein is broken down into smaller

peptides (Miller and Green, 1983). The cyclic structure of proline and its presence and position in a peptide chain can protect biologically active peptides from proteolysis since there are only a select few peptidases that can hydrolyze the bond between proline and another amino acid (Cunningham and O'Connor, 1997). It has been suggested that both proline and the highly substrate-specific class of enzymes capable of degrading proline-containing peptides could serve as a way to regulate these biologically active peptides (Lowther and Matthews, 2002). Prolidase and prolinase are the only known enzymes capable of degrading proline-containing dipeptides to produce free proline as a product. Prolinase hydrolyzes dipeptides in which a prolyl residue is located at the N-terminus (Pro-Xaa) while prolidase hydrolyzes only Xaa-Pro dipeptides. In one study, a mutant strain of *Salmonella typhimurium* lacking both aminopeptidase P (PepP), a broad-specificity aminopeptidase, and prolidase (PepQ) showed an 85% decrease in ability to produce free proline from protein (Miller and Green, 1983).

The primary physiological role of prolidase (PepD) in humans is somewhat better understood. During protein catabolism, prolidase and prolinase catalyze the end stage of the degradation of intracellular collagen, procollagen, and other proline-containing peptides in which proline-containing dipeptides are hydrolyzed releasing free proline into the cytoplasm (Surazynski et al., 2008b). Proline acts as a stress substrate and is able to participate in metabolic signaling. Collagen breakdown typically occurs during conditions of metabolic stress such as compromise of the blood supply during tissue damage (Phang et al., 2010). Free proline is also required for collagen biosynthesis indicating prolidase could be a step-limiting factor in the rate at which new collagen is formed (Surazynski et al., 2008b). Collagen is critical for the maintenance of connective tissue and is the most abundant protein in the body (Phang

et al., 2008). Proline and hydroxyproline comprise 25% of the amino acid residues in collagen; thus, collagen is essentially a proline reservoir (Phang et al., 2008). Collagen degradation is initiated by activation of matrix metalloproteinases (MMPs) resulting in smaller proteins and peptides which are degraded into tripeptides and dipeptides by endopeptidases and exopeptidases (Phang et al., 2008). Endopeptidases cleave bonds within the peptide chain, while expoeptidases cleave amino acid residues from the N and C termini (Gonzales and Robert-Baudouy, 1996). As illustrated in Figure 1-3, the penultimate step of collagen degradation results in the production of imidodipeptides, the most abundant of which contain proline (Xaa-Pro and Pro-Xaa) and are degraded only by prolidase and prolinase, respectively (Zanaboni et al., 1994). Therefore, prolidase and prolinase have important functions in a critical step in extracellular matrix (ECM) turnover (Phang et al., 2010).

Degradation of cellular components by the cell itself to maintain required bioenergy levels under conditions of nutrient stress is called autophagy (Phang et al., 2008). This process, as it relates to proline, is referred to as ecophagy. Ecophagy, whether in the case of normal collagen turnover in bone or ECM, or under conditions of nutrient stress such as wound healing or tumor progression, is recognized as the cytokine-mediated activation of MMPs and subsequent increase in prolidase activity leading to the degradation of collagen and release of free proline (Phang et al., 2008). Much is known about MMPs; their function, regulation and ability to modulate cell behaviors have been thoroughly examined, but are beyond the scope of this review. The link between MMPs and the effects of prolidase cannot be ignored, however, and will be addressed.

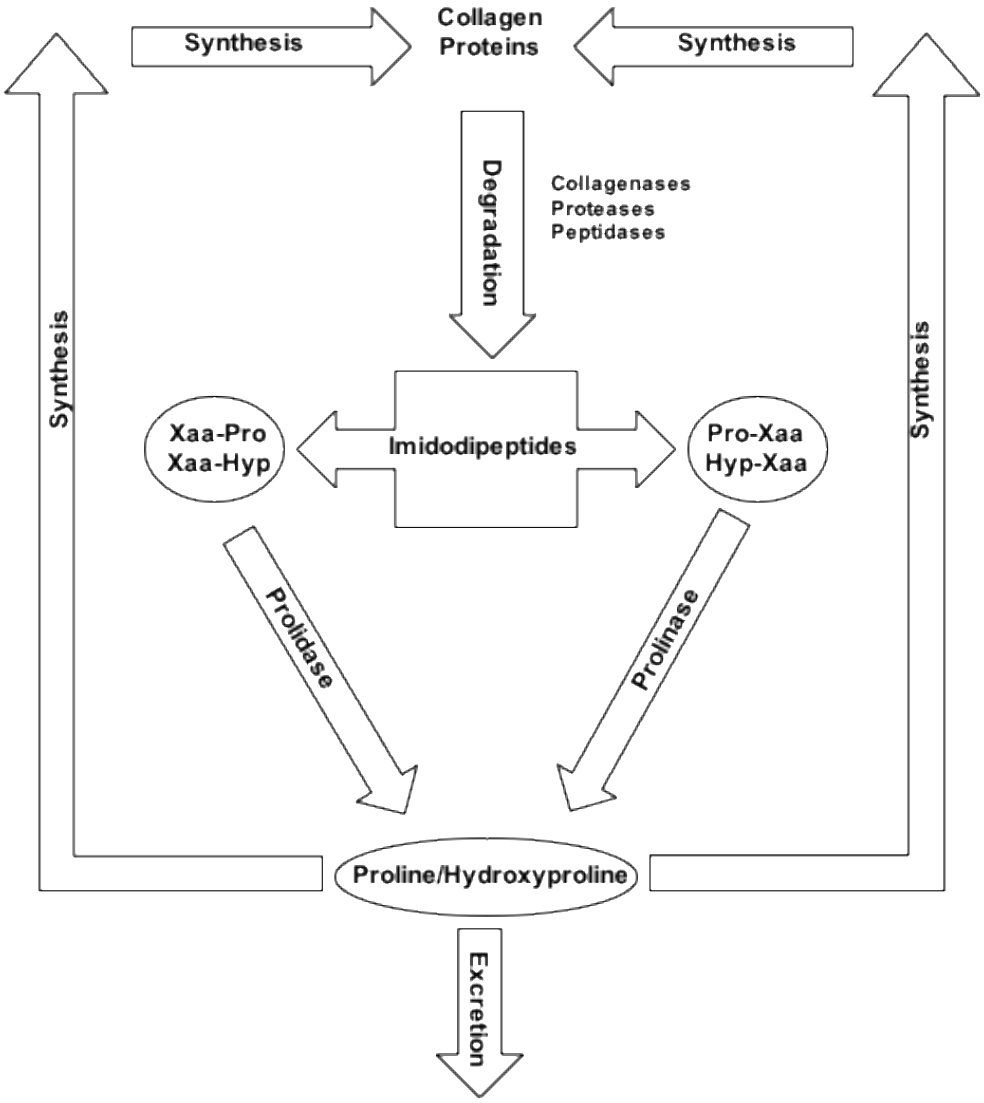

Figure 1-3. Diagram of collagen degradation resulting in imidodipeptides that are hydrolyzed by prolidase and prolinase. Modified from Zanaboni et al., 1994.

Prolidase deficiency, or PD, is a rare autosomal recessive genetic condition affecting a small percentage of humans. Molecular characterization of 30 PD patients revealed a variety of mutations in the 15-exon, 130 kb prolidase gene or PEPD located on chromosome 19 (Tanoue et al., 1990) including: point mutations leading to amino acid substitutions or

premature stop codons, deletions causing missing amino acids, or even deletion of the entire exon 14 (Tanoue et al., 1990, Lupi et al., 2008). Figure 1-4 shows a map of the human PEPD gene and highlights some of the point mutations, deletions, exon splicing and duplications that are known to be associated with PD. Some of these point mutations and deletions have been shown to occur in amino acids that are highly conserved in other prolidase sequences, which could explain why the end result is an inactive prolidase isoform I (Zanaboni et al., 1994, Cunningham and O'Connor, 1997, Maher et al., 2004). Isoform II seems to remain functional in patients with PD (Ohhashi et al., 1990); therefore, metabolically, PD manifests as the excretion of large amounts of proline dipeptides, specifically Gly-Pro, in the urine (imidodipeptiduria). Clinically, PD patients present with a spectrum of chronic symptoms ranging from mild to severe. Phenotypic symptoms are varied and can include skin ulcerations, mental retardation, splenomegaly, recurrent infections, photosensitivity, hyperkeratosis, and unusual facial appearance (Kokturk et al., 2002, Viglio et al., 2006, Mitsubuchi et al., 2008). Typically, PD patients develop symptoms in early childhood which progress into adulthood; however, some late-onset cases have also been reported (Dyne et al., 2001).

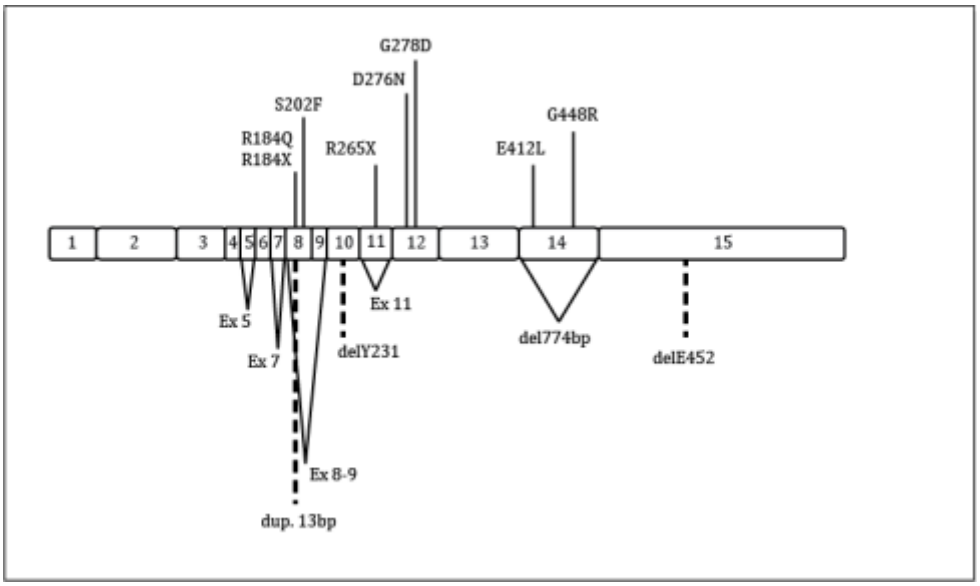

Figure 1-4. Diagram of the human PEPD gene in which the point mutations (top), deletions, duplications, and exon splicing (bottom) known to be associated with PD are indicated. Modified from Lupi et al., 2008.

PD falls into the "orphan" category of diseases, affecting less than 5 in every 10,000 people. Unfortunately, this classification means that PD and other disorders with similar incidence generally attract little interest from pharmaceutical companies, and therefore, often lack effective treatments or a definitive cure (Perugini et al., 2005). Such is the case with PD, as there is currently no cure or effective treatment for the associated symptoms. The incidence of PD is estimated to be 1-2 cases per million births. This is likely an underestimation of the actual number of cases worldwide since many physicians are unfamiliar with the condition and as a result patients suffering from PD are often misdiagnosed (Viglio et al., 2006, Lupi et al., 2008). Several methods are available for diagnosing PD; the oldest and most common of which is a spectrophotometric method first described by Chinard et al., which is used to determine prolidase activity in erythrocytes, lymphocytes, or skin fibroblast cultures (Viglio et al., 2006).

This method is time-consuming and susceptible to variability between samples, test runs, technicians, and laboratories, making the assay results difficult to compare. Additional analytical methods such as capillary electrophoresis (CE), high-performance liquid chromatography (HPLC), and matrix-assisted laser desorption/ionization time-of-flight mass spectrometry (MALDI-TOF MS) have been used successfully to determine prolidase activity in human samples (Viglio et al., 2006). Another option for PD diagnosis is to screen urine samples for excess imidodipeptides, particularly Gly-Pro. Isotachophoresis (ITP), amino acid analysis, HPLC with atmospheric pressure ionization mass spectrometry (API-MS) and CE have been used successfully to identify and quantify imidodipeptides in the urine of PD patients (Viglio et al., 2006). Prenatally, a PD diagnosis can be obtained by sequencing the prolidase gene (Lupi et al., 2008).

1.5. Prolidase as a marker for disease

The fact that several of the symptoms present in PD patients are angiopathic (relating to irreparably diseased or damaged blood vessels and improper wound healing) is an indicator that prolidase could play an important role in angiogenic signaling. Angiogenesis, or the growth of new blood vessels from existing vessels, is a normal process in wound healing; however, it is also a fundamental step in the transition of a tumor from dormancy to an invasive malignancy. Recently it was proposed that increased prolidase activity, as a result of MMPs activated by tumor-secreted cytokines, could up-regulate the activity of hypoxia-inducible factor-1 (HIF-1), a transcription factor known to play a role in stress-induced gene expression and angiogenic signaling (Surazynski et al., 2008a). Under normal conditions, HIF-1 is

inactive because its α subunit is being continually targeted for ubiquitination and degradation by hydroxylation of specific proline residues in the oxygen-dependent degradation (ODD) domain and their interaction with the von Hippel-Lindau (VHL) complex (Jaakkola et al., 2001). When prolidase activity is increased, the resulting free proline can inhibit the degradation of HIF-1α by interfering with the interaction between the hydroxylated proline residues in the ODD domain with the VHL complex (Karna et al., 2012). The result is an active HIF-1α which increases angiogenic signaling by up-regulating expression of inflammatory response mediators such as vascular endothelial growth factor (VEGF) (Surazynski et al., 2008a).

Another signaling molecule, nitric oxide (NO) is secreted in excess by activated macrophage cells as part of the immune response, and is also elevated in tissues undergoing repair (Nunoshiba et al., 1993, Surazynski et al., 2005). NO has also been shown to play a role in the regulation of collagen metabolism, but the mechanism linking collagen and NO was not previously understood (Surazynski et al., 2005). Recently it was shown that in the presence of NO, prolidase activity increases but prolidase expression remains unchanged. It was determined that NO is able to regulate prolidase activity through phosphorylation of serine/threonine sites on the prolidase enzyme via the cGMP kinase pathway (Surazynski et al., 2005).

Changes in prolidase activity have been documented in several diseases and cancers. An increase or decrease in prolidase activity can indicate not only the presence of a disease state but also progression of the condition. Table 1-2 lists some of the many medical conditions where prolidase activity has been monitored and reported. This table is not intended to be an

exhaustive list of every medical condition involving prolidase, but serves to illustrate the importance of prolidase function *in vivo* and to suggest that monitoring prolidase activity could be beneficial in not only diagnosis of disease but also in tracking disease progress. Prolidase activity has been shown to be elevated in several cancers, such as breast cancer, endometrial cancer, lung cancer and melanoma (Karna et al., 2000, Mittal et al., 2005, Cechowska-Pasko et al., 2006, Arioz et al., 2009). The increase in prolidase activity in these cancers is thought to be due to the increased collagen breakdown and turnover that occurs as a tumor metastasizes and spreads. In most cancers, the benefit of early detection is obvious and the chance of survival post-diagnosis is greatly increased by early detection. If these conditions have already been diagnosed in a patient, monitoring prolidase activity could be a way to evaluate success of a treatment or cancer progression. Understanding elevated prolidase activity in cancer offers an appealing treatment option as well such as with proline-containing prodrugs, which can be targeted to cancer cells and hydrolyzed by prolidase (Mittal et al., 2005). This exciting avenue for cancer treatment is discussed in the next section of this review.

Several other disorders are characterized by excessive collagen turnover and therefore show increased levels of prolidase activity. In both hypertension and erectile dysfunction (ED), increased collagen deposition in blood vessels (leading to the side effects that characterize each disorder) can be indicated by elevated serum prolidase activity levels (Demirbag et al., 2007, Savas et al., 2010). Since prolidase activity would need to increase in order for collagen degradation and synthesis to increase, monitoring prolidase activity levels could be a way to achieve an earlier and more definitive diagnosis in some of these conditions.

Table 1-2. Prolidase activity as a marker for disease

Medical condition	Resulting prolidase activity*	References
Bipolar disorder	Increase	(Andreazza et al., 2008, Selek et al., 2011)
Breast cancer	Increase	(Cechowska-Pasko et al., 2006)
Endometrial cancer	Increase	(Arioz et al., 2009)
Keloid scar formation	Increase	(Duong et al., 2006)
Erectile dysfunction (ED)	Increase	(Savas et al., 2010)
Thalassemia major	Increase	(Cakmak et al., 2010)
Helicobacter pylori (Intestinal bacterial infection)	Increase	(Aslan et al., 2007)
Liver disease	Increase	(Myara et al., 1984, Abraham et al., 2000)
Lung cancer	Increase	(Karna et al., 2000)
Hypertension	Increase	(Demirbag et al., 2007)
Melanoma	Increase	(Mittal et al., 2005)
Early Pregnancy Failure - Placenta	Increase	(Namiduru et al., 2001, Toy et al., 2010, Vural et al.,
Early Pregnancy Failure - Mother	Decrease	(Namiduru et al., 2001, Toy et al., 2010, Vural et al.,
Asthma	Decrease	(Cakmak et al., 2009)
Chronic Obstructive Pulmonary Disease (COPD)	Decrease	(Gencer et al., 2011)
Dilated Cardiomyopathy (DCM)	Decrease	(Sezen et al., 2010)
Osteoarthritis	Decrease	(Altindag et al., 2007)
Chronic Pancreatitis	Decrease	(Palka et al., 2002)
Pancreatic cancer	Decrease	(Palka et al., 2002)

*Change in prolidase activity relative to healthy control.

There are some situations in which a decrease in prolidase activity is seen; such as when collagen deposition has advanced to the point of fibrosis or hardening of the tissue due to the presence of scarring, resulting in reduced fluid flow through the tissue. In advanced chronic obstructive pulmonary disease (COPD), the airway tissue gradually becomes fibrotic during which collagen turnover slows and prolidase activity drops (Gencer et al., 2011). A similar situation occurs in dilated cardiomyopathy (DCM) where the vasculature surrounding the heart becomes fibrotic and prolidase activity is decreased (Sezen et al., 2010). Decreased prolidase activity is evident in both pancreatitis and pancreatic cancer, and it is hypothesized that collagen degradation products, when in excess, can somehow inhibit prolidase activity (Palka et al., 2002).

In addition to collagen turnover, oxidative status and oxidative stress have also been shown to correlate with prolidase activity levels under certain conditions (Aslan et al., 2007, Cakmak et al., 2009, Cakmak et al., 2010, Selek et al., 2011). Oxidative stress and the presence of reactive oxygen species (ROS) or free radicals is a significant part of the pathogenesis of several diseases in that it can modify cell receptor activity and signaling as well as cause the release of endogenous mediators of inflammation (Kaleli et al., 2006). Oxidative stress has been demonstrated in endometrial cancer and, as with other cancers, could be due to impaired enzymatic antioxidant function such as superoxide dismutase and catalase (Arioz et al., 2009). The coupling of oxidative stress with the lack of antioxidant response could explain why prolidase is elevated in this situation. In thalassemia major, an autosomal recessive blood disorder characterized by widening of the bone marrow cavities and decreased bone mass, elevated prolidase activity has been documented (Cakmak et al., 2010). Thalassemia patients

also experience elevated total oxidant status (TOS) relative to the amount of antioxidants present in the serum (Cakmak et al., 2010). Alternatively, with bronchial asthma, oxidative stress is prevalent, and there is an active antioxidant response, but prolidase activity is decreased (Cakmak et al., 2009). It is possible that in the presence of antioxidant enzymes, prolidase activity is inhibited. Oxidative stress in the intestine is a known component of *Helicobacter pylori* infection, and oxidative stress in the brain has been demonstrated in cases of bipolar disorder (Aslan et al., 2007, Andreazza et al., 2008, Selek et al., 2011). In both of these cases, prolidase activity is elevated as well; however, antioxidant status was not studied.

An interesting case involving both an increase and decrease in prolidase activity is that of early pregnancy loss (EPL), or first trimester miscarriage, the most common complication of human reproduction (Toy et al., 2010). In pregnant women undergoing EPL, a reduction in serum prolidase activity was documented, as was an increase in oxidative stress and a decrease in antioxidant response (Toy et al., 2010). While this contradicts the previous hypothesis that decreased presence of antioxidant enzymes would allow prolidase activity to increase, the prolidase levels and oxidative status of the failing fetus must also be considered. In cases of EPL, prolidase activity in the placenta was found to be significantly increased when compared to that of the mother (Vural et al., 2011). It is hypothesized that the increase in fetal collagen turnover characteristic of EPL could be detected by the associated increase in placental prolidase activity, especially when compared to maternal serum prolidase activity and that prolidase activity could serve as a clinical marker for EPL (Vural et al., 2011).

1.6. Therapeutic and biotechnological applications of prolidase

As mentioned previously, there is no definitive cure for prolidase deficiency although several treatments have been evaluated with varying degrees of success at alleviating the clinical symptoms of PD and improving patient quality of life. Some treatments directed towards alleviating the symptoms of PD that have been utilized so far are occlusive dressings, topical antiseptics and antibiotics, topical glycine and proline, topical growth hormone, oral supplements of manganese and ascorbic acid, oral corticosteroids, blood transfusions as enzyme replacement therapy and skin grafts (Kokturk et al., 2002, Lupi et al., 2002, Lupi et al., 2008). All of these treatments have shown limited success, with short-lived results. In a study performed by Lupi et al., blood transfusions containing functional prolidase coupled with topical therapy demonstrated the most success of the treatments listed, as patients experienced improvement and healing of skin ulcerations (Lupi et al., 2002). Blood transfusions, in addition to being somewhat hazardous and extremely expensive, must also be performed on a regular basis in order to achieve the desired result bringing into question whether a treatment of this nature would actually be considered an improvement.

A promising avenue for treatment of PD using enzyme replacement therapy involves employing micro- and nanoparticles to deliver prolidase directly to the cells. Prolidase cannot be administered freely, as it has no specific membrane carriers and could not be independently transported into the cell (Colonna et al., 2008a). Several targeted prolidase delivery systems have been tested with some success including: enzyme microencapsulation in biodegradable microspheres, enzyme-loaded liposomes intended for injection, and enzyme-loaded chitosan glutamate nanoparticles intended for topical application (Lupi et al., 2004, Perugini et al., 2005,

Colonna et al., 2007). Several challenges exist in targeted enzyme replacement therapy. The delivery particle must be biodegradable and non-toxic. The enzyme must be kept stable inside its delivery particle and must not be degraded prior to it reaching its intended destination. Prolidase is a cytosolic enzyme, so the formulation must allow for or facilitate the enzyme crossing the cell membrane or being endocytosed. Additionally, controlled release of the enzyme from encapsulation is desirable to increase length of time between needed treatments.

Microspheres made of poly (lactic-*co*-glycolic acid) or PLGA loaded with prolidase from pig kidney were initially tested against fibroblasts from PD patients and proved to be somewhat inefficient as the amount of enzyme entering the cells was significantly lower than the amount of enzyme initially dosed (Genta et al., 2001, Lupi et al., 2004). The PGLA microspheres were also of varying sizes and controlled release was not possible as microspheres are susceptible to bursting. Encapsulating prolidase in liposomes, or artificially-created particles comprised of lipid bilayer, was more successful as liposomes can be made in smaller and more uniform sizes. Liposomes are also easily endocytosed and are commonly used for targeted drug delivery whether administered systemically, parenterally or topically.

Most recently, nanoparticles composed of chitosan, a polysaccharide common in nature, have been tested as candidates for targeted prolidase delivery (Colonna et al., 2007, Colonna et al., 2008a). Chitosan is biodegradable and non-toxic, and has been studied extensively as a drug delivery system for complex molecules such as proteins and plasmids (Janes et al., 2001). Chitosan particles have bioadhesive properties which significantly improve their likelihood of cellular uptake and can protect the molecules they are carrying from environmental degradation (Colonna et al., 2008a). When incubated with prolidase deficient

fibroblasts, prolidase-loaded chitosan nanoparticles increased prolidase activity to a maximum of nearly 70% of control activity in fibroblasts for up to 6 days (Colonna et al., 2008a). After 5 days of incubation, the prolidase enzyme was still active indicating chitosan was indeed protecting the functionality of the enzyme (Colonna et al., 2008a). In an attempt to further stabilize the prolidase enzyme prior to loading into chitosan particles, site-directed PEGylation at sulfhydryl groups was performed (Colonna et al., 2008b). PEGylation of prolidase increased the stability of the enzyme and prolonged its activity in the cytoplasm to 10 days (Colonna et al., 2008b), making this combination of PEGylated prolidase and chitosan nanoparticles an extremely promising candidate for treatment of PD.

Prolidase has additional therapeutic value outside of prolidase deficiency. While Xaa-Pro dipeptides are the preferred substrate for these enzymes, various prolidases have been shown to have activity against toxic organophosphorus (OP)-containing compounds such as diisopropylfluorophosphate (DFP), and the chemical warfare agents sarin, soman and tabun (DeFrank and Cheng, 1991). Prolidases from various bacteria and archaea, as well as human prolidase, can hydrolyze these compounds and render them harmless (DeFrank and Cheng, 1991, Wang et al., 1998, Park et al., 2004, Theriot et al., 2010a). OP compounds are biodegradable, yet they are extremely toxic to mammals because they bind to acetyl cholinesterase and inactivate it, leading to a buildup of the neurotransmitter acetylcholine in the synapses. Acetylcholine then produces a continuous signal resulting in hyper salivation, confusion, convulsions, respiratory complications, respiratory failure, coma and death. OP compounds exist mainly in the form of pesticides and chemical warfare agents (CWAs), and it is estimated that 38% of the pesticides used worldwide contain OP, and approximately

200,000 tons of OP nerve agents are stockpiled worldwide (Singh, 2009). Annually, there are an estimated 3 million poisonings and 300,000 human deaths owing to OP compounds (Singh, 2009). There is a need for OP detoxification strategies that are safe for humans and the environment. Enzymes from several microorganisms have been shown to degrade a range of OP compounds; however, an ideal enzyme or combination of enzymes to be used in a decontamination cocktail would be able to degrade all OP compounds while remaining stable for an extended period of time at a range of temperatures and pH.

Several microbial enzymes, such as organophosphorus acid anhydrolase (OPAA) and phosphotriesterase (PTE), are capable of degrading OP compounds and have been extensively studied for their high activity and specificity against G-type nerve agents (Singh, 2009). The stability of these enzymes, however, is limited when incorporated into formulations containing solvents and other denaturants. Additionally, high concentrations of metals must be added to formulations containing these enzymes in order to maximize their activity which poses further complications (Theriot et al., 2011). More recent studies have included recombinant prolidases from hyperthermophilic archaea (Vyas et al., 2010, Theriot and Grunden, 2010). Wild type and mutant prolidases from *Pyrococcus horikoshii* have been characterized and show promising enzymatic properties as candidates for OP decontamination in that they are highly thermostable with broad substrate specificity. Further characterization of *P. horikoshii* prolidases is ongoing.

In addition to OP decontamination strategies, prolidases are useful in both detection and antagonism of OP contamination. OPAA has high activity toward OP compounds containing P-F bonds and minimal activity with compounds containing P-S or P-O bonds. This

specificity for a single substrate can be used in discriminative detection of fluorine-containing OPs (Simonian et al., 2001). Current biosensors utilize technology based on cholinesterase inhibition and are successful in detection of OP compounds, although this method does not enable unequivocal determination of compound identity. It is essential that, in detection of OP contamination, the source of the contamination can be determined to ensure that contamination from OP pesticides is never confused with that of chemical warfare. Fluorine-containing OPS such as the CWAs sarin and soman and the pesticide DFP are substrates for OPAA. Thus, OPAA can be used in concert with other enzymes to detect and distinguish between OP compounds in a biosensor unit (Simonian et al., 2001).

Recombinant microbial prolidases can be administered as an antidote or as a prophylactic measure in the case of OP exposure; however, when the enzyme is injected in its free form, it is susceptible to immunologic reactions and degradation which limit its effectiveness (Petrikovics et al., 2000a). Successful experiments have been performed in which OPAA has been encapsulated in sterically stable, long circulating liposomes and remained stable in blood for several days (Petrikovics et al., 2000a). The liposomes can be safely injected into the bloodstream, as they are non-toxic and biodegradable. OP compounds diffuse through the liposomal membrane, are hydrolyzed by the encapsulated prolidase, and the harmless reaction products diffuse back out of the liposome (Petrikovics et al., 2000b). This application of liposomes and prolidase together as an OP antagonist has obvious military implications, as it can be employed to protect military personnel from the harmful results of exposure to nerve gas.

There are several instances where inhibition of prolidase can be beneficial as well. Prolidase deficiency is not known to occur in any species other than humans, and as such, there are no naturally-occurring PD animal models that can be used in the research of this condition or to gain a better understanding of the biological functions of prolidase (Lupi et al., 2005). *N*-benzyloxycarbonyl-L-proline (Cbz-Pro) has been shown to inhibit prolidase activity in human fibroblasts and in mice *in vivo*, and could be useful in development of a successful animal model to mimic PD (Lupi et al., 2005). Additionally, elevated prolidase activity four times that of normal skin is seen during the formation of keloid scars, an abnormal accumulation of ECM at the wound site following traumatic injury (Duong et al., 2006). It is possible that partial inhibition of prolidase at the wound site could be a way to reduce or limit keloid scar formation. Since prolidase is necessary for successful healing (Surazynski et al., 2008a), it would be critical not to inhibit prolidase activity altogether in the case of keloid scar formation but merely to limit it.

Prolidase has also been identified as a potential target for anti-cancer prodrugs both for its differential expression in cancer cells and for its high substrate specificity (Mittal et al., 2005, Mittal et al., 2007). A study by Mittal et al. showed that prolidase is overexpressed in melanoma cell lines indicating that it might be overexpressed *in vivo* melanoma cases as well (Mittal et al., 2005). Prodrugs, or drugs that are inactive when administered and become activated when metabolized, are a particularly promising form of anti-cancer therapy, as they offer a way to target the specific cancer cells of interest with limited effect on surrounding cells. Melphalan is a chemotherapeutic agent with effective antineoplastic activity, but it has the unpleasant side effects often associated with chemotherapy. Melphalan coupled with

proline (Mel-Pro or prophalan) is a proline prodrug that mimics prolidase substrate and is inactive until it is taken up into cells and hydrolyzed into melphalan by prolidase (Chrzanowski et al., 2004). Both acetylsalicylic acid and Cbz-Pro are capable of inhibiting prolidase activity and could be used in conjunction with prophalan to concentrate delivery and activation of the prodrug in cancer cells while limiting activity of the drug in normal cells (Chrzanowski et al., 2004, Mittal et al., 2005).

Table 1-3. Biotechnological applications of prolidase

Industry	Application	Prolidase	Mode of utilization	References
United States Military	Degradation of toxic OP compounds	OPAA	When used as a component of biodecontamination cocktail, prolidases hydrolyze OP compounds rendering them harmless	(Cheng and DeFrank, 2000)
United States Military	Detection of toxic OP nerve agents	OPAA	Enzyme serves as a biosensor for fluorine-containing OP compounds such as DFP, soman and sarin	(Simonian et al., 2001)
United States Military	OP Antagonism	OPAA	When encapsulated in liposomes and injected into the bloodstream, OPAA can serve to prevent effects of toxic OP exposure or can act as an antidote in the event of poisoning.	(Petrikovics et al., 2000a, Petrikovics et al., 2000b)
Food /Dairy	Cheese ripening	PepQ	Adding recombinant prolidases to cheese fermentation process increases proteolysis of bitter peptides (mostly proline containing peptides)	(Courtin et al., 2002)
Medical	Enzyme replacement therapy	Human, Pig	Prolidase encapsulated in liposomes or chitosan nanoparticles is a promising treatment for prolidase deficiency.	(Perugini et al., 2005, Colonna et al., 2007, Colonna et al., 2008a, Colonna et al., 2008b)

Several native and recombinant prolidases have important biotechnological applications which are summarized in Table 1-3. In the food industry, prolidase can be added during the cheese fermentation process to reduce the bitter flavor of proline dipeptides (Courtin et al., 2002). The addition of proline-specific peptidases from *Lactobacillus* species to *Lactococcus lactis* cultures during cheese ripening has been shown to increase the amount of free amino acids in the culture by three-fold (Courtin et al., 2002). Lactobacilli have higher proteolytic activity overall because they possess additional peptidases compared to *L. lactis*, and those peptidases are expressed at higher levels. By augmenting the proteolytic capabilities of *L. lactis* with peptidases from lactobacilli, the flavor of the cheese can be improved and the ripening time shortened (Courtin et al., 2002).

1.7. Conclusion

Prolidase, a metalloenzyme responsible for hydrolysis of proline-containing imidodipeptides, is critical for the liberation of free proline in protein metabolism. In humans, prolidase is essential for maintenance, rebuilding and degradation of collagen-containing connective tissue, and dysregulation of prolidase activity manifests as disruptions in collagen metabolism. Prolidase deficiency, a rare genetic condition affecting humans in which one of the prolidase isoforms is inactive, provides a model system in which to study the metabolic implications of this enzyme. The uncomfortable and chronic nature of the symptoms associated with PD provides motivation to develop accurate diagnoses and definitive treatment options for this condition. Aberrations in prolidase activity are present in many disease states such as cancers and fibrotic processes, and prolidase activity can be a useful marker in the early

detection and monitoring of these conditions. Further understanding and study of prolidase and prolidase inhibition strategies is warranted as it has applications for use in the activation of proline prodrugs in anticancer therapy, for topical and parenteral treatments for prolidase deficiency, and for prophylactic or post-exposure treatment of OP poisoning. Recombinant microbial prolidases have medical, military, and industrial value and are currently being studied extensively in these areas.

Acknowledgements

The authors thank Dr. Sherry Tove for her helpful comments on the manuscript. Support for some of the studies described in this review was provided by the Army Research Office (contract number 44258LSSR).

References

Abraham, P., Wilfred, G. & Ramakrishna, B. 2000. Plasma prolidase may be an index of liver fibrosis in the rat. *Clin Chim Acta,* 295**,** 199-202.

Alberto, M. E., Leopoldini, M. & Russo, N. 2011. Can human prolidase enzyme use different metals for full catalytic activity? *Inorganic Chemistry,* 50**,** 3394-3403.

Altindag, O., Erel, O., Aksoy, N., Selek, S., Celik, H. & Karaoglanoglu, M. 2007. Increased oxidative stress and its relation with collagen metabolism in knee osteoarthritis. *Rheumatol Int,* 27**,** 339-44.

Andreazza, A. C., Kauer-Sant'anna, M., Frey, B. N., Bond, D. J., Kapczinski, F., Young, L. T. & Yatham, L. N. 2008. Oxidative stress markers in bipolar disorder: a meta-analysis. *J Affect Disord,* 111**,** 135-44.

Arioz, D. T., Camuzcuoglu, H., Toy, H., Kurt, S., Celik, H. & Aksoy, N. 2009. Serum prolidase activity and oxidative status in patients with stage I endometrial cancer. *Int J Gynecol Cancer,* 19**,** 1244-7.

Aslan, M., Nazligul, Y., Horoz, M., Bolukbas, C., Bolukbas, F. F., Aksoy, N., Celik, H. & Erel, O. 2007. Serum prolidase activity and oxidative status in *Helicobacter pylori* infection. *Clin Biochem,* 40**,** 37-40.

Besio, R., Alleva, S., Forlino, A., Lupi, A., Meneghini, C., Minicozzi, V., Profumo, A., Stellato, F., Tenni, R. & Morante, S. 2010. Identifying the structure of the active sites of human recombinant prolidase. *Eur Biophys J,* 39**,** 935-45.

Cakmak, A., Soker, M., Koc, A. & Aksoy, N. 2010. Prolidase activity and oxidative status in patients with thalassemia major. *J Clin Lab Anal,* 24**,** 6-11.

Cakmak, A., Zeyrek, D., Atas, A., Celik, H., Aksoy, N. & Erel, O. 2009. Serum prolidase activity and oxidative status in patients with bronchial asthma. *J Clin Lab Anal,* 23**,** 132-8.

Cechowska-Pasko, M., Palka, J. & Wojtukiewicz, M. Z. 2006. Enhanced prolidase activity and decreased collagen content in breast cancer tissue. *Int J Exp Pathol,* 87**,** 289-96.

Cheng, T.-C., & Defrank, J. J. (2000). Hydrolysis of organophosphorus compounds by bacterial prolidases. B. Zwanenburg, M. Mikołajczyk, & P. Kiełbasiński (Eds.), In *Enzymes in Action: Green Solutions for Chemical Problems* (pp. 243–261). Dordrecht: Springer Netherlands.

Cheng, T. C., Harvey, S. P. & Stroup, A. N. 1993. Purification and properties of a highly active organophosphorus acid anhydrolase from *Alteromonas undina*. *Appl Environ Microbiol,* 59**,** 3138-40.

Chrzanowski, K., Bielawska, A., Bielawski, K., Palka, J. & Wolczynski, S. 2004. Acetylsalicylic acid as a potential regulator of prolidase-convertible pro-drugs in control and neoplastic cells. *Farmaco,* 59**,** 679-84.

Colonna, C., Conti, B., Perugini, P., Pavanetto, F., Modena, T., Dorati, R. & Genta, I. 2007. Chitosan glutamate nanoparticles for protein delivery: development and effect on prolidase stability. *J Microencapsul,* 24**,** 553-64.

Colonna, C., Conti, B., Perugini, P., Pavanetto, F., Modena, T., Dorati, R., Iadarola, P. & Genta, I. 2008a. Ex vivo evaluation of prolidase loaded chitosan nanoparticles for the enzyme replacement therapy. *Eur J Pharm Biopharm,* 70**,** 58-65.

Colonna, C., Conti, B., Perugini, P., Pavanetto, F., Modena, T., Dorati, R., Iadarola, P. & Genta, I. 2008b. Site-directed PEGylation as successful approach to improve the enzyme replacement in the case of prolidase. *Int J Pharm,* 358**,** 230-7.

Courtin, P., Nardi, M., Wegmann, U., Joutsjoki, V., Ogier, J. C., Gripon, J. C., Palva, A., Henrich, B. & Monnet, V. 2002. Accelerating cheese proteolysis by enriching *Lactococcus lactis* proteolytic system with lactobacilli peptidases. *International Dairy Journal***,** 447 - 454.

Cunningham, D. F. & O'connor, B. 1997. Proline specific peptidases. *Biochim Biophys Acta,* 1343**,** 160-86.

DeFrank, J. J. & Cheng, T. C. 1991. Purification and properties of an organophosphorus acid anhydrase from a halophilic bacterial isolate. *J Bacteriol,* 173**,** 1938-43.

Demirbag, R., Yildiz, A., Gur, M., Yilmaz, R., Elci, K. & Aksoy, N. 2007. Serum prolidase activity in patients with hypertension and its relation with left ventricular hypertrophy. *Clin Biochem,* 40**,** 1020-5.

Du, X., Tove, S., Kast-Hutcheson, K. & Grunden, A. M. 2005. Characterization of the dinuclear metal center of *Pyrococcus furiosus* prolidase by analysis of targeted mutants. *FEBS Lett,* 579**,** 6140-6.

Duong, H. S., Zhang, Q. Z., Le, A. D., Kelly, A. P., Kamdar, R. & Messadi, D. V. 2006. Elevated prolidase activity in keloids: correlation with type I collagen turnover. *Br J Dermatol,* 154**,** 820-8.

Dyne, K., Zanaboni, G., Bertazzoni, M., Cetta, G., Viglio, S., Lupi, A. & Iadarola, P. 2001. Mild, late-onset prolidase deficiency: another Italian case. *British Journal of Dermatology,* 144**,** 635-636.

Fernandez-Espla, M. D., Martin-Hernandez, M. C. & Fox, P. F. 1997. Purification and characterization of a prolidase from *Lactobacillus casei* subsp. *casei* IFPL 731. *Appl Environ Microbiol,* 63**,** 314-6.

Gencer, M., Aksoy, N., Dagli, E. C., Uzer, E., Aksoy, S., Selek, S., Celik, H. & Cakir, H. 2011. Prolidase activity dysregulation and its correlation with oxidative-antioxidative status in chronic obstructive pulmonary disease. *J Clin Lab Anal,* 25**,** 8-13.

Genta, I., Perugini, P., Pavanetto, F., Maculotti, K., Modena, T., Casado, B., Lupi, A., Iadarola, P. & Conti, B. 2001. Enzyme loaded biodegradable microspheres *in vitro ex vivo* evaluation. *J Control Release,* 77**,** 287-95.

Ghosh, M., Grunden, A. M., Dunn, D. M., Weiss, R. & Adams, M. W. 1998. Characterization of native and recombinant forms of an unusual cobalt-dependent proline dipeptidase (prolidase) from the hyperthermophilic archaeon *Pyrococcus furiosus*. *J Bacteriol,* 180**,** 4781-9.

Gonzales, T. & Robert-Baudouy, J. 1996. Bacterial aminopeptidases: properties and functions. *FEMS Microbiol Rev,* 18**,** 319-44.

Jaakkola, P., Mole, D. R., Tian, Y.-M., Wilson, M. I., Gielbert, J., Gaskell, S. J., Kriegsheim, A. V., Hebestreit, H. F., Mukherji, M., Schofield, C. J., Maxwell, P. H., Pugh, C. W. & Ratcliffe, P. J. 2001. Targeting of HIF-alpha to the von Hippel-Lindau ubiquitylation complex by O2-regulated prolyl hydroxylation. *Science,* 292**,** 468-472.

Jalving, R., Bron, P., Kester, H. C., Visser, J. & Schaap, P. J. 2002. Cloning of a prolidase gene from *Aspergillus nidulans* and characterisation of its product. *Mol Genet Genomics,* 267**,** 218-22.

Janes, K. A., Calvo, P. & Alonso, M. J. 2001. Polysaccharide colloidal particles as delivery systems for macromolecules. *Adv Drug Deliv Rev,* 47**,** 83-97.

Kaleli, S., Akkaya, A., Akdogan, M. & Gultekin, F. 2006. The effects of different treatments on prolidase and antioxidant enzyme activities in patients with bronchial asthma. *Environ Toxicol Pharmacol,* 22**,** 35-9.

Karna, E., Surazynski, A. & Palka, J. 2000. Collagen metabolism disturbances are accompanied by an increase in prolidase activity in lung carcinoma planoepitheliale. *Int J Exp Pathol,* 81**,** 341-7.

Karna, E., Szoka, L. & Palka, J. 2012. Thrombin-dependent modulation of beta1-integrin-mediated signaling up-regulates prolidase and HIF-1alpha through p-FAK in colorectal cancer cells. *Mol Cell Biochem,* 361**,** 235-41.

Kokturk, A., Kaya, T. I., Ikizoglu, G. & Koca, A. 2002. Prolidase deficiency. *Int J Dermatol,* 41**,** 45-48.

Liu, G., Nakayama, K., Awata, S., Tang, S., Kitaoka, N., Manabe, M. & Kodama, H. 2007. Prolidase isoenzymes in the rat: their organ distribution, developmental change and specific inhibitors. *Pediatric Research,* 62**,** 54-59.

Lowther, W. T. & Matthews, B. W. 2002. Metalloaminopeptidases: common functional themes in disparate structural surroundings. *Chem Rev,* 102**,** 4581-608.

Lupi, A., Casado, B., Soli, M., Bertazzoni, M., Annovazzi, L., Viglio, S., Cetta, G. & Iadarola, P. 2002. Therapeutic apheresis exchange in two patients with prolidase deficiency. *Br J Dermatol,* 147**,** 1237-40.

Lupi, A., Della Torre, S., Campari, E., Tenni, R., Cetta, G., Rossi, A. & Forlino, A. 2006. Human recombinant prolidase from eukaryotic and prokaryotic sources: expression, purification, characterization and long-term stability studies. *FEBS J,* 273**,** 5466-78.

Lupi, A., Perugini, P., Genta, I., Modena, T., Conti, B., Casado, B., Cetta, G., Pavanetto, F. & Iadarola, P. 2004. Biodegradable microspheres for prolidase delivery to human cultured fibroblasts. *J Pharm Pharmacol,* 56**,** 597-603.

Lupi, A., Rossi, A., Vaghi, P., Gallanti, A., Cetta, G. & Forlino, A. 2005. N-benzyloxycarbonyl-L-proline: an *in vitro* and *in vivo* inhibitor of prolidase. *Biochim Biophys Acta,* 1744**,** 157-63.

Lupi, A., Tenni, R., Rossi, A., Cetta, G. & Forlino, A. 2008. Human prolidase and prolidase deficiency: an overview on the characterization of the enzyme involved in proline recycling and on the effects of its mutations. *Amino Acids,* 35**,** 739-52.

Maher, M. J., Ghosh, M., Grunden, A. M., Menon, A. L., Adams, M. W., Freeman, H. C. & Guss, J. M. 2004. Structure of the prolidase from *Pyrococcus furiosus*. *Biochemistry,* 43**,** 2771-83.

Miller, C. G. & Green, L. 1983. Degradation of proline peptides in peptidase-deficient strains of *Salmonella typhimurium*. *J Bacteriol,* 153**,** 350-6.

Mitsubuchi, H., Nakamura, K., Matsumoto, S. & Endo, F. 2008. Inborn errors of proline metabolism. *J Nutr,* 138**,** 2016S-2020S.

Mittal, S., Song, X., Vig, B. S. & Amidon, G. L. 2007. Proline prodrug of melphalan targeted to prolidase, a prodrug activating enzyme overexpressed in melanoma. *Pharm Res,* 24**,** 1290-8.

Mittal, S., Song, X., Vig, B. S., Landowski, C. P., Kim, I., Hilfinger, J. M. & Amidon, G. L. 2005. Prolidase, a potential enzyme target for melanoma: design of proline-containing dipeptide-like prodrugs. *Mol Pharm,* 2**,** 37-46.

Morel, F., Frot-Coutaz, J., Aubel, D., Portalier, R. & Atlan, D. 1999. Characterization of a prolidase from *Lactobacillus delbrueckii* subsp. *bulgaricus* CNRZ 397 with an unusual regulation of biosynthesis. *Microbiology,* 145 (Pt 2)**,** 437-46.

Myara, I., Myara, A., Mangeot, M., Fabre, M., Charpentier, C. & Lemonnier, A. 1984. Plasma prolidase activity: a possible index of collagen catabolism in chronic liver disease. *Clin Chem,* 30**,** 211-5.

Namiduru, E. S., Ozdemir, Y., Kutlar, I. & Ersoy, U. 2001. A study of prolidase in mothers, their newborn babies and in non-pregnant controls. *Arch Gynecol Obstet,* 265**,** 73-5.

Nunoshiba, T., Derojas-Walker, T., Wishnok, J. S., Tannenbaum, S. R. & Demple, B. 1993. Activation by nitric oxide of an oxidative-stress response that defends *Escherichia coli* against activated macrophages. *Proc Natl Acad Sci U S A,* 90**,** 9993-7.

O'Cuinn, G. & Fottrell, P. F. 1975. Purification and characterization of an aminoacyl proline hydrolase from guinea-pig intestinal mucosa. *Biochim Biophys Acta,* 391**,** 388-95.

Ohhashi, T., Ohno, T., Arata, J., Sugahara, K. & Kodama, H. 1990. Characterization of prolidase I and II from erythrocytes of a control, a patient with prolidase deficiency and her mother. *Clin Chim Acta,* 187**,** 1-9.

Palka, J., Surazynski, A., Karna, E., Orlowski, K., Puchalski, Z., Pruszynski, K., Laszkiewicz, J. & Dzienis, H. 2002. Prolidase activity disregulation in chronic pancreatitis and pancreatic cancer. *Hepatogastroenterology,* 49**,** 1699-703.

Park, M. S., Hill, C. M., Li, Y., Hardy, R. K., Khanna, H., Khang, Y. H. & Raushel, F. M. 2004. Catalytic properties of the PepQ prolidase from *Escherichia coli*. *Arch Biochem Biophys,* 429**,** 224-30.

Perugini, P., Hassan, K., Genta, I., Modena, T., Pavanetto, F., Cetta, G., Zanone, C., Iadarola, P., Asti, A. & Conti, B. 2005. Intracellular delivery of liposome-encapsulated prolidase in cultured fibroblasts from prolidase-deficient patients. *J Control Release,* 102**,** 181-90.

Petrikovics, I., Cheng, T. C., Papahadjopoulos, D., Hong, K., Yin, R., DeFrank, J. J., Jaing, J., Song, Z. H., Mcguinn, W. D., Sylvester, D., Pei, L., Madec, J., Tamulinas, C., Jaszberenyi, J. C., Barcza, T. & Way, J. L. 2000a. Long circulating liposomes encapsulating organophosphorus acid anhydrolase in diisopropyl fluorophosphate antagonism. *Toxicol Sci,* 57**,** 16-21.

Petrikovics, I., Mcguinn, W. D., Sylvester, D., Yuzapavik, P., Jiang, J., Way, J. L., Papahadjopoulos, D., Hong, K., Yin, R., Cheng, T. C. & DeFrank, J. J. 2000b. *In vitro* studies on sterically stabilized liposomes (SL) as enzyme carriers in organophosphorus (OP) antagonism. *Drug Deliv,* 7**,** 83-9.

Phang, J. M., Donald, S. P., Pandhare, J. & Liu, Y. 2008. The metabolism of proline, a stress substrate, modulates carcinogenic pathways. *Amino Acids,* 35**,** 681-90.

Phang, J. M., Liu, W. & Zabirnyk, O. 2010. Proline metabolism and microenvironmental stress. *Annu Rev Nutr,* 30**,** 441-63.

Savas, M., Yeni, E., Celik, H., Ciftci, H., Utangac, M., Oncel, H., Altunkol, A. & Verit, A. 2010. The association of serum prolidase activity and erectile dysfunction. *J Androl,* 31**,** 146-54.

Selek, S., Altindag, A., Saracoglu, G., Celik, H. & Aksoy, N. 2011. Prolidase activity and its diagnostic performance in bipolar disorder. *J Affect Disord,* 129**,** 84-6.

Sezen, Y., Bas, M., Altiparmak, H., Yildiz, A., Buyukhatipoglu, H., Faruk Dag, O., Kaya, Z. & Aksoy, N. 2010. Serum prolidase activity in idiopathic and ischemic cardiomyopathy patients. *J Clin Lab Anal,* 24**,** 213-8.

Simonian, A. L., Grimsley, J. K., Flounders, A. W., Shoeniger, J. S., Cheng, T.-C., DeFrank, J. J. & Wild, J. R. 2001. Enzyme-based biosensor for the direct detection of fluorine-containing organophosphates. *Analytica Chimica Acta***,** 15 - 23.

Singh, B. K. 2009. Organophosphorus-degrading bacteria: ecology and industrial applications. *Nat Rev Microbiol,* 7**,** 156-64.

Suga, K., Kabashima, T., Ito, K., Tsuru, D., Okamura, H., Kataoka, J. & Yoshimoto, T. 1995. Prolidase from *Xanthomonas maltophilia*: purification and characterization of the enzyme. *Biosci Biotechnol Biochem,* 59**,** 2087-90.

Surazynski, A., Donald, S. P., Cooper, S. K., Whiteside, M. A., Salnikow, K., Liu, Y. & Phang, J. M. 2008a. Extracellular matrix and HIF-1 signaling: the role of prolidase. *Int J Cancer,* 122**,** 1435-40.

Surazynski, A., Liu, Y., Miltyk, W. & Phang, J. M. 2005. Nitric oxide regulates prolidase activity by serine/threonine phosphorylation. *J Cell Biochem,* 96**,** 1086-94.

Surazynski, A., Miltyk, W., Palka, J. & Phang, J. M. 2008b. Prolidase-dependent regulation of collagen biosynthesis. *Amino Acids,* 35**,** 731-8.

Tanoue, A., Endo, F. & Matsuda, I. 1990. Structural organization of the gene for human prolidase (peptidase D) and demonstration of a partial gene deletion in a patient with prolidase deficiency. *J Biol Chem,* 265**,** 11306-11.

Theriot, C. M., Du, X., Tove, S. R. & Grunden, A. M. 2010a. Improving the catalytic activity of hyperthermophilic *Pyrococcus* prolidases for detoxification of organophosphorus nerve agents over a broad range of temperatures. *Appl Microbiol Biotechnol,* 87**,** 1715-26.

Theriot, C. M. & Grunden, A. M. 2011. Hydrolysis of organophosphorus compounds by microbial enzymes. *Appl Microbiol Biotechnol,* 89**,** 35-43.

Theriot, C. M., Semcer, R. L., Shah, S. S. & Grunden, A. M. 2011. Improving the catalytic activity of hyperthermophilic *Pyrococcus horikoshii* prolidase for detoxification of organophosphorus nerve agents over a broad range of temperatures. *Archaea,* 2011**,** 565127.

Theriot, C. M., Tove, S. R., & Grunden, A. M. (2009). Biotechnological applications of recombinant microbial prolidases. *Advances in Applied Microbiology*. http://doi.org/10.1016/S0065-2164(09)01203-9

Theriot, C. M., Tove, S. R. & Grunden, A. M. 2010b. Characterization of two proline dipeptidases (prolidases) from the hyperthermophilic archaeon *Pyrococcus horikoshii*. *Appl Microbiol Biotechnol,* 86**,** 177-88.

Toy, H., Camuzcuoglu, H., Camuzcuoglu, A., Celik, H. & Aksoy, N. 2010. Decreased serum prolidase activity and increased oxidative stress in early pregnancy loss. *Gynecol Obstet Invest,* 69**,** 122-7.

Uramatsu, S., Liu, G., Yang, Q., Uramatsu, M., Chi, H., Lu, J., Yamashita, K. & Kodama, H. 2009. Characterization of prolidase I and II purified from normal human erythrocytes: comparison with prolidase in erythrocytes from a patient with prolidase deficiency. *Amino Acids,* 37**,** 543-51.

Viglio, S., Annovazzi, L., Conti, B., Genta, I., Perugini, P., Zanone, C., Casado, B., Cetta, G. & Iadarola, P. 2006. The role of emerging techniques in the investigation of prolidase deficiency: from diagnosis to the development of a possible therapeutical approach. *J Chromatogr B Analyt Technol Biomed Life Sci,* 832**,** 1-8.

Vural, M., Toy, H., Camuzcuoglu, H. & Aksoy, N. 2011. Comparison of prolidase enzyme activities of maternal serum and placental tissue in patients with early pregnancy failure. *Arch Gynecol Obstet,* 283**,** 953-8.

Vyas, N. K., Nickitenko, A., Rastogi, V. K., Shah, S. S. & Quiocho, F. A. 2010. Structural insights into the dual activities of the nerve agent degrading organophosphate anhydrolase/prolidase. *Biochemistry,* 49**,** 547-59.

Wang, Q., Sun, M., Zhang, H. & Huang, C. 1998. Purification and properties of soman-hydrolyzing enzyme from human liver. *J Biochem Mol Toxicol,* 12**,** 213-7.

Wu, G., Bazer, F. W., Burghardt, R. C., Johnson, G. A., Kim, S. W., Knabe, D. A., Li, P., Li, X., Mcknight, J. R., Satterfield, M. C. & Spencer, T. E. 2011. Proline and hydroxyproline metabolism: implications for animal and human nutrition. *Amino Acids,* 40**,** 1053-63.

Yang, S. I. & Tanaka, T. 2008. Characterization of recombinant prolidase from *Lactococcus lactis*- changes in substrate specificity by metal cations, and allosteric behavior of the peptidase. *FEBS J,* 275**,** 271-80.

Yoshimoto, T., Matsubara, F., Kawano, E. & Tsuru, D. 1983. Prolidase from bovine intestine: purification and characterization. *J Biochem,* 94**,** 1889-96.

Zanaboni, G., Dyne, K. M., Rossi, A., Monafo, V. & Cetta, G. 1994. Prolidase deficiency: biochemical study of erythrocyte and skin fibroblast prolidase activity in Italian patients. *Haematologica,* 79**,** 13-8.

CHAPTER 2

Improving the Catalytic Activity of Hyperthermophilic *Pyrococcus horikoshii* Prolidase for Detoxification of Organophosphorus Nerve Agents Over a Broad Range of Temperatures

Casey M. Theriot, Rebecca L. Kitchener, Saumil S. Shah, and Amy M. Grunden

Citation: Theriot, C.M., Semcer, R.L., Shah, S.S., and Grunden, A.M. (2011). Improving the catalytic activity of hyperthermophilic *Pyrococcus horikoshii* prolidase for detoxification of organophosphorus nerve agents over a broad range of temperatures. *Archaea*, *2011*, Article ID 565127, 9 pages.

Statement of Second Author Contributions

My contributions to this work as second author include column chromatography purification of the four *Pyrococcus horikoshii* prolidase homolog 1 variants discussed in this chapter, purity assessments, and much of their biochemical characterization, along with that of the wild type enzyme. Included in this were the kinetics profiling experiments with the dipeptide leucyl proline at 70°C, as well as temperature profile, substrate specificity, thermostability, and pot-life experiments for these enzymes. I analyzed and interpreted the experimental results for the biochemical characterization, prepared the relevant figures and tables, and reported the findings in the results and discussion section of this paper.

2.1. Abstract

Prolidases hydrolyze Xaa-Pro dipeptides and can also cleave the P-F and P-O bonds found in organophosphorus (OP) compounds, including the nerve agents soman and sarin. *Ph1*prol (PH0974) has previously been isolated and characterized from *Pyrococcus horikoshii* and was shown to have higher catalytic activity over a broader pH range, higher affinity for metal, and increased thermostability compared to *P. furiosus* prolidase, *Pf*prol (PF1343). To obtain a better enzyme for OP nerve agent decontamination and to investigate the structural factors that may influence protein thermostability and thermoactivity, randomly mutated *Ph1*prol enzymes were prepared. Four *Ph1*prol mutants (A195T/G306S-, Y301C/K342N-, E127G/E252D- and E36V-*Ph1*prol) were isolated which had greater thermostability and improved activity over a broader range of temperatures against Xaa-Pro dipeptides and OP nerve agents compared to wildtype *Pyrococcus* prolidases.

2.2. Introduction

Pyrococcus horikoshii and *Pyrococcus furiosus* are both hyperthermophilic archaea, growing optimally at 98-100ºC. They were isolated from a deep hydrothermal vent in the Okinawa Trough in the northeastern Pacific Ocean and from a shallow marine solfatara at Vulcano Island off the coast of Italy, respectively (Fiala et al., 1986; Gonzalez et al., 1998). *Pyrococcus* spp. are some of the most studied hyperthermophilic archaea to date owing in part to their utility for a variety of biotechnological applications (Adams, 1993; Blumer-Schuette et al., 2008; Egorova et al., 2005; Synowiecki et al., 2006; Unsworth et al., 2007). For example, recombinant prolidases from *Pyrococcus* spp. have been studied for their potential use in bio-decontamination applications (Theriot et al., 2009).

Prolidases function *in vivo* to hydrolyze dipeptides with proline in the C-terminus, Xaa-Pro, and a non-polar amino acid in the N-terminus (Lowther et al., 2002). However, studies have demonstrated that prolidases can also hydrolyze and detoxify organophosphate (OP) compounds such as chemical warfare agents (CWA) soman and sarin (Theriot et al., 2009). Two enzymes that have been characterized for potential field detoxification of nerve agents are organophosphorus acid anhydrolase (OPAA) and phosphotriesterase (PTE) (T.-C. Cheng et al., 1998; T. C. Cheng et al., 1999). Recently, the crystal structure of OPAA from *Alteromonas* sp. JD6.5 strain has been solved, and it has been determined to be a prolidase (Vyas et al., 2010). While OPAA does have the capability to degrade OP nerve agents, its activity can be limited by exposure to high temperatures and solvents during use in field situations (T.-C. Cheng et al., 2000; Theriot et al., 2011).

In 2008, the Defense Threat Reduction Agency (DTRA), under the auspices of the Department of Defense, recognized the importance of developing enzyme-based OP nerve agent detoxification systems and created an initiative calling for new enzymes and biocatalysts that are stable over a broad temperature and pH range, in the presence of salts and surfactants, and that do not pose an environmental hazard (Defense Threat Reduction Agency, 2008). In response to the need to develop stable OP nerve agent degrading enzyme systems, thermostable prolidases from *Pyroccocus* spp. were studied (Ghosh et al., 1998; Jeyakanthan et al., 2009; Maher et al., 2004; Theriot, Tove, et al., 2010).

Specifically, *Pyrococcus* prolidases from *P. furiosus* (PF1343 or *Pf*prol) and *P. horikoshii* (PH1149 or *Ph*prol and PH0974 or *Ph1*prol) were characterized both structurally and enzymatically (Jeyakanthan et al., 2009; Maher et al., 2004; Theriot, Tove, et al., 2010). The *Pyrococcus* prolidases were determined to be very similar, with *Pf*prol showing 88% amino acid similarity to *Ph*prol and 55% similarity to *Ph1*prol. Although they have high similarity to each other, the kinetic properties of *Ph1*prol appeared to be more favorable for application purposes than those of *Pf*prol and *Ph*prol. *Ph1*prol has demonstrated higher activity at lower temperatures and over a broader pH range. It has long term stability, higher affinity for substrates and a lower metal requirement for catalysis (Theriot, Tove, et al., 2010). Therefore, it was deemed to be advantageous to use *Ph1*prol in mutagenesis studies in order to develop a better enzyme for OP nerve agent detoxification and to further investigate factors that influence the catalysis of thermophilic metalloenzymes. To this end, a random mutagenesis *Ph1*prol gene library was constructed and screened for production of mutants that showed increased prolidase activity at 30°C compared to wild type *Ph1*prol. Four *Ph1*prol

mutants were isolated and subsequently characterized to determine their substrate catalysis over a broad range of temperatures and their performance against OP nerve agent analogs in comparison to *Ph1* prolidase and the previously characterized *Pf* prolidase.

2.3. Materials and Methods

2.3.1. Bacterial strains, media, and materials.

The *E. coli* K-12 derivative NK5525 (*proA*::Tn*10*) was used to construct the selection strain JD1(λDE3) as described in Theriot, et al. (2010) for screening of cold-adapted *P. horikoshii* prolidase variants. The *P. horikoshii* prolidase expression plasmid pET-*Ph1*prol was previously constructed as described in (Theriot, Tove, et al., 2010). The *E. coli* strains were cultured either in Luria-Bertani (LB) broth or M9 selective minimal medium supplemented with 0.2% glucose, 1 mM MgSO4, 0.05% $VitB_1$, 20 μM IPTG, 20 μM Leu-Pro. Ampicillin (100 μg/ml), kanamycin (50 μg/ml), chloramphenicol (34 μg/ml) and tetracycline (6 μg/ml) were added into the medium when required.

*2.3.2. Construction of a pool of pET-*Ph1*prol plasmids encoding randomly mutated* P. horikoshii *prolidase genes.*

Error-prone PCR mutagenesis using the Genemorph II Random mutagenesis kit (Stratagene, La Jolla, CA) was used to amplify and insert mutations into the *P. horikoshii* prolidase gene (PH0974). PCR amplification was carried out for 30 cycles: (60 sec at 95°C, 60 sec at 55°C, 120 sec at 72°C), with a 10-minute final extension at 72°C. Reactions contained Mutazyme II reaction buffer, 125 ng/μl of each primer, 40 mM dNTP mix, and 2.5 U of

Mutazyme II DNA polymerase. Initial DNA template amounts used were 250 ng and 750 ng in order to select for medium to low mutation rates, respectively. The Genemorph II EZClone (Stratagene, La Jolla, CA) reaction was employed to clone the mutated prolidase gene into the expression vector pET-21b.

The EZClone reaction included EZClone enzyme mix, 50 ng of template plasmid (pET-prol), 500 ng of megaprimer (mutated prolidase PCR product), and EZClone solution. The reactions were amplified for 25 cycles: (50 sec at 95°C, 50 sec at 60°C, 14 min at 68°C). Amplified products were digested with *Dpn I* for 2 hours at 37°C to remove template plasmid. XL1-Gold supercompetent *E. coli* cells were transformed with the mutant plasmid mixture.

2.3.3. Screening for increased activity at low temperature.

pET-Ph1prol plasmids from the mutant P. horikoshii library were transformed into the selective strain JD1(λDE3) and were plated on M9 selective agar plates. Colonies that grew after being incubated for 3-7 d at 20°C were isolated on LB plates and then grown in 10 ml LB medium at 37°C with shaking (200 rpm) until an optical density of 0.6-0.8 was reached. IPTG was then added to the cell culture to a final concentration of 1 mM. The induced culture was shaken at 37°C for 3 h before harvesting the cells. These cell pellets were lysed using 300 μl of B-per buffer (Thermo Scientific, Rockford, IL), and the resulting cell extracts were used for enzyme activity assays conducted at 30°C and at 100°C. Heat-treated soluble protein samples were heated at 80°C for 20 min. Four mutant colonies that exhibited at least 2-3 fold higher activities compared to the cells expressing the wild type *P. horikoshii* prolidase were selected for characterization, and their plasmids were isolated. The prolidase genes present in those

isolated plasmids were sequenced using the T7 promoter and T7 terminator primers (MWG Biotech, Huntsville, AL).

2.3.4. Large-scale expression of recombinant P. horikoshii *prolidase mutants.*

Production of *P. horikoshii* prolidase variants (A195T/G306S-, Y301C/K342N-, E127G/E252D- and E36V-*Ph1*prolidase) was carried out in transformed *E. coli* BL21 (λDE3) cells with the appropriate pET-*Ph1*prol plasmid and pRIL vector. The transformants were grown in 1 L cultures of autoinduction media (Studier, 2005) incubated at 37°C with shaking (200 RPM) overnight.

2.3.5. Purification of recombinant P. horikoshii *prolidase mutants.*

Cell pellets from the four *Ph1*prolidase variants (A195T/G306S-, Y301C/K342N-, E127G/E252D- and E36V-*Ph1*prol) were suspended in 50 mM Tris-HCl, pH 8.0 (3 ml Tris per 1 gram of cell paste), with 1 mM benzamidine and 1 mM DTT. For each variant, diluted cell slurry was passed through a French pressure cell (20,000 lb/in^2) three times. Cell lysates were centrifuged at 38,720 x *g* for 30 min at 4°C, and then the supernatants were heated to 80°C for 30 min anaerobically to denature any proteins not stable at that temperature. Heat treated supernatants were centrifuged at 38,720 x *g* to remove the denatured proteins. Supernatants were sampled both before and after heat treatment for activity analysis. $(NH_4)_2SO_4$ was added gradually to the supernatants to make a final concentration of 1.5 M prior to loading onto a 5 ml Phenyl-Sepharose™ hydrophobic interaction chromatography column (Hi-Trap™ Phenyl HP Column, GE Healthcare Life Sciences, Piscataway, NJ).

Fractions containing the prolidase mutants were pooled and dialyzed overnight into 4 L of 50 mM Tris HCl, pH 8.0 at 4°C, and were further purified on a 5 ml Q Sepharose™ anion exchange chromatography column (Hi-Trap™ Q FF Column, GE Healthcare Life Sciences, Piscataway, NJ). Buffers for both purification steps have been described in (Theriot, Tove, et al., 2010). Fractions from both purification steps were further visualized using SDS-PAGE (12.5% SDS-polyacrylamide gels) and were tested for enzyme activity. Fractions were then pooled based on gel images and enzyme stocks were stored at -80°C. The molecular weights of *Ph1*-prolidase and mutants are approximately 40 kDa. The purity of each *Ph1*-prolidase mutant was estimated to be greater than 95%.

2.3.6. Prolidase enzyme activity assay.

The enzyme activity assay protocol is based on a method previously described by (Ghosh et al., 1998; Theriot, Du, et al., 2010). The reaction mixture (500 µl) contained 50 mM MOPS buffer (3-[*N*-morpholino] propanesulfonic acid) pH 7.0, 200 mM NaCl, water, 5% (vol/vol) glycerol, 100 µg/ml BSA (bovine serum albumin) protein, 0.2 mM $CoCl_2$ and the enzyme. The reaction mixture was heated at 100°C for 5 min allowing time for the metal and enzyme to interact. The reaction was initiated by the addition of substrate (Xaa-Pro, 4 mM final concentration) and allowed to proceed for 10 min at 100°C. The reaction was stopped with 500 µl glacial acetic acid and 500 µl ninhydrin reagent (3% [wt. vol]) and heated again for 10 min at 100°C. The reaction was then cooled to 23°C. Prolidase samples were assayed in triplicate and specific activity was calculated using the absorbance value at 515 nm and an extinction coefficient of 4,570 M^{-1} cm^{-1} for the ninhydrin-proline complex. For assays

evaluating the temperature profile, WT-*Ph1* prolidase and the four prolidase mutants were assayed in triplicate for activity with 4 mM Met-Pro at 10°C, 20°C, 35°C, 50°C, 70°C, and 100°C. Experiments were performed in duplicate.

2.3.7. Substrate specificity and kinetic experiments.

In order to study substrate specificity, the following Xaa-Pro dipeptides were used as substrates (4 mM final concentration) in the enzyme activity assays for WT-*Ph1* prolidase and the four prolidase mutants: Val-Pro, Met-Pro, Phe-Pro, Leu-Pro, Ala-Pro, and Gly-Pro. Prolidase samples were assayed with two additional substrates, Pro-Ala and Val-Leu-Pro, to further illustrate prolidase preference of Xaa-Pro dipeptides (Theriot, Du, et al., 2010). Kinetic parameters of the *Ph1*-prolidase mutants were determined at 70ºC using a range of Leu-Pro (0.25-12 mM).

2.3.8. Thermostability and pot-life experiments.

Thermostability experiments were performed in duplicate on WT-*Ph1*prol and the four mutants. Each enzyme was diluted to a concentration of 0.04 mg/ml in 50 mM MOPS, pH 7.0 and 200 mM NaCl and incubated anaerobically in a sealed vial at 90°C. An initial sample was taken to represent Time = 0 h, and additional samples were taken at 24 h, 48 h, and 72 h. Samples were diluted to 0.4 µg/ml in 50 mM MOPS, pH 7.0 and 200 mM NaCl and were then assayed in triplicate in accordance with the enzyme activity assay protocol described in Section 2.6. In all cases, the substrate used in the activity assay was 4 mM Met-Pro.

Pot-life experiments were also performed in duplicate. Each enzyme was diluted to a concentration of 0.04 mg/ml in 50 mM MOPS, pH 7.0 and 200 mM NaCl and incubated anaerobically in a sealed vial at 70°C. An initial sample was taken to represent Time = 0 days, and additional samples were taken at Time = 1, 7, 14, 16 and 21 days. Samples were diluted to 0.4 µg/ml in 50 mM MOPS, pH 7.0 and 200 mM NaCl and were then assayed in triplicate to determine specific activity.

2.3.9. DSC experiments.

Differential scanning calorimetry (DSC) was performed using a MicroCal VP-DSC scanning calorimeter. The calorimetric samples contained ~1 mg/ml protein in 50 mM MOPS, 200 mM NaCl, 0.2 mM $CoCl_2$, pH 7.0. Protein samples were dialyzed 15 h against this buffer before the experiment. Samples were degassed before loading into the chamber cell. The calorimetric experiment was performed by heating the samples at a scan rate of 100°C/hr.

2.3.10. DFP (diisopropylfluorophosphate) assay.

The hydrolysis of DFP by prolidases was measured by monitoring fluoride release with a fluoride specific electrode as previously described (Hill et al., 2001). Assays were performed at 35°C and 50°C, with continuous stirring in 2.5 ml of buffer (50 mM MOPS, 200 mM NaCl, pH 7.0), 0.2 mM $CoCl_2$ and 3 mM DFP. The enzyme and metal were incubated at the reaction temperature 5 min prior to the start of the reaction. The background of DFP hydrolysis was measured by running a reaction without enzyme present at 35°C and 50°C. The background

hydrolysis of DFP was subtracted from enzymatic hydrolysis to determine specific activity of the enzyme.

2.3.11. p-*Nitrophenyl soman assay (o-pinacolyl* p-*nitrophenyl methylphosphonate activity).*

Prolidase hydrolysis of *p*-nitrophenyl soman was monitored by accumulation of *p*-nitrophenyl (T. C. Cheng et al., 1999; Hill et al., 2001). The p-nitrophenyl soman was synthesized at Edgewood Chemical Biological Center in Aberdeen Proving Ground, MD and contained a racemic mixture of all four stereoisomers. The purity of the soman analog was greater than 90% based on gas chromatography analysis (Vyas et al., 2010). Two milliliter reaction assays contained buffer (50 mM MOPS, 200 mMNaCl, pH 7.0), 0.2 mM $CoCl_2$, and 0.3 mM *p*-nitrophenyl soman. The reactions were conducted at three different temperatures (35°C, 50°C and 70°C). The enzyme and metal were incubated at the specified reaction temperature 5 minutes prior to the start of the reaction. Absorbance of the product *p*-nitrophenylolate was measured at 405 nm over a 5 minute range. To calculate activity, the extinction coefficient for *p*-nitrophenolate of 10,101 M^{-1} cm^{-1} was used.

2.4. Results and Discussion

2.4.1. P. furiosus *and* P. horikoshii *prolidase specific activities with OP nerve agents: DFP and soman analog.*

Previous studies characterizing *P. horikoshii* prolidase homolog 1 (*Ph1*prol, PH0974) demonstrated that it has higher catalytic activity over a broader pH range, higher affinity for metal, and is more thermostable than either *P. furiosus* prolidase, (*Pf*prol, PF1343) or *P.*

horikoshii prolidase (*Ph*prol, PH1149) when assayed with the dipeptide substrate Met-Pro (Theriot, Tove, et al., 2010). Based on these favorable attributes for *Ph1*prol when reacting with its natural substrates, Xaa-Pro dipeptides, there was interest in determining the relative activity of recombinant *Ph1*prol compared to *Pf*prol and *Ph*prol against G-type nerve agent simulants DFP and soman analog, *p*-nitrophenyl soman. As indicated in Figure 2-1, DFP exhibited the greatest hydrolysis with *Ph1*prol. *Ph1*prol had a relative activity that was 843% higher than *Pf*prol and 817% higher than *Ph*prol at 35°C and 1870% higher than both *Pf*prol and *Ph*prol at 50°C (Figure 2-1). In contrast, the trends with the soman analog were very different as shown in Figure 2-2. The relative activity of *Ph1*prol was only 70%, 63% and 68% of the *Pf*prol activity at 35°C, 50°C and 70°C, respectively (Figure 2-2). These results indicate that *Ph1*prol has a preference for DFP and does not exhibit high activity with the soman analog. Differences in the protein structures likely play a role in the substrate preference since *Pf*prol and *Ph1*prol share only 55% amino acid residue similarity (Ghosh et al., 1998). By altering the *Ph1*prol structure further using a random mutagenesis approach, it would be possible to isolate *Ph1*prol variants that show even greater hydrolysis of DFP and/or improved activity against the soman analog.

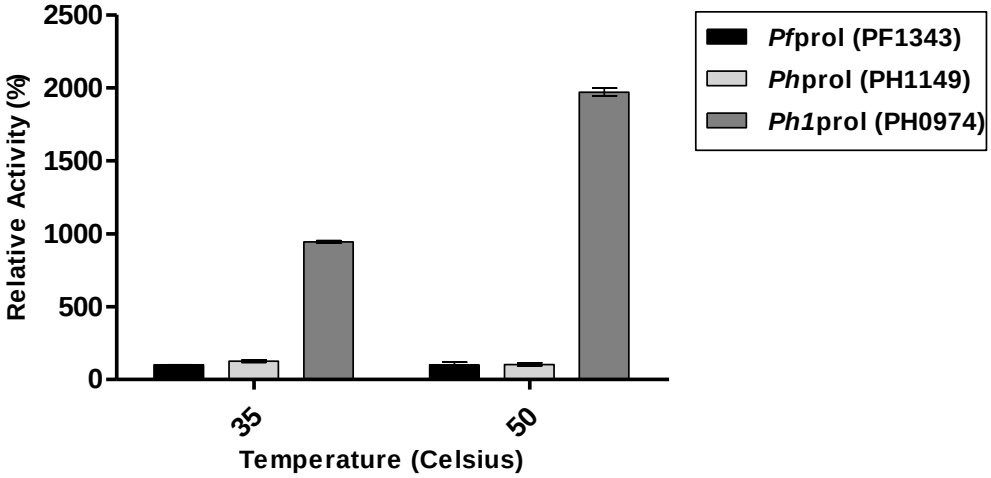

Figure 2-1. Relative activity of WT-*Pf*prol and *P. horikoshii* prolidases with OP nerve agent DFP. All prolidase assays contained 50 mM MOPS, 200 mM NaCl, pH 7.0, 0.2 mM $CoCl_2$, and 3 mM DFP. 100% relative activity corresponds to WT-*Pf*prol specific activity for DFP of 0.42 µmoles product formed/min/mg at 35°C and 0.73 µmoles product formed/min/mg at 50°C.

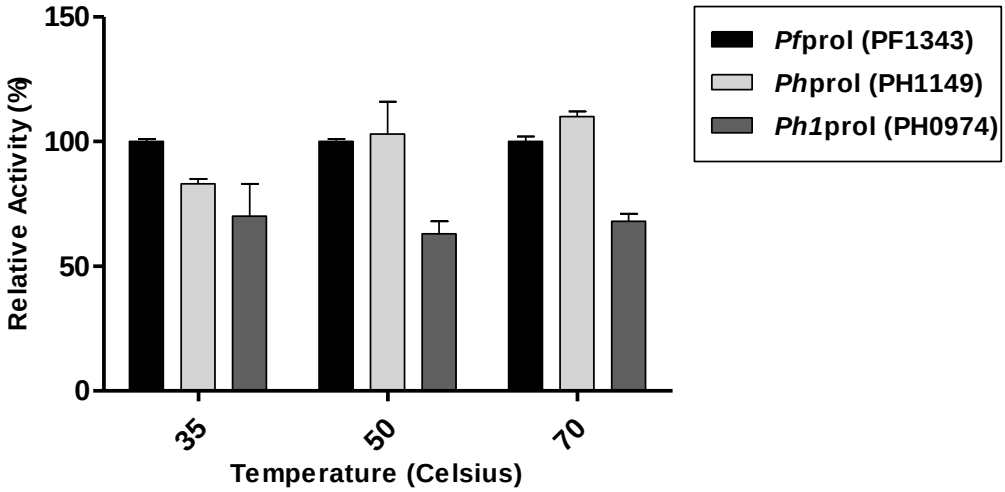

Figure 2-2. Relative activity of WT-*Ph1*prol and prolidase mutants with OP nerve agent analog, *p*-nitrophenyl soman. All prolidase assays contained 50 mM MOPS 200 mM NaCl pH 7.0, 0.2 mM $CoCl_2$, and 3 mM *p*-nitrophenyl soman. 100% relative activity corresponds to WT-*Ph1*prol specific activity for *p*-nitrophenyl soman of 0.26 µmol product formed/min/mg at 35ºC, 0.33 µmol product formed/min/mg at 50ºC, and 0.56 µmol product formed/min/mg at 70ºC.

2.4.2. Screening and isolation of the Ph1*prol mutant population using proline auxotrophic strain JD1 (λDE3).*

Since *Ph1*prol exhibited the most favorable catalytic properties, including higher activity with DFP, it was selected for further mutagenesis using an error prone PCR strategy which employs a mutated polymerase. Transformed *E. coli* JD1 (λDE3) cells were used to select for *Ph1*prol variants on minimal media plates that were supplemented with 20 μM Leu-Pro and grown at 20°C. Colonies that were visible in 3-7 days were plated on minimal and rich (LB) media. *Ph1*prol variants were screened using small-scale expression cultures (10 ml) induced with IPTG. Four *Ph1*prol variants out of over 200 screened were selected for sequencing after showing two-fold higher activity with Leu-Pro at 30°C and somewhat reduced activity at 100°C as compared to wild type. The increased activity at the lower temperature of 30°C and variation at the higher temperature of 100°C is indicative of a mutation in a thermophilic protein, which can compromise activity or stability at higher temperatures but could create more flexibility and increased catalysis at the lower temperatures.

2.4.3. Sequencing of Ph1*prol mutants.*

Prior to sequencing, the four *Ph1*prol mutants were numbered (10, 19, 35 and 72) based solely on the order in which they had been isolated. Sequencing of the variants revealed the locations of the amino acid substitutions for each mutant (Figure 2-3). Mutant no.10 had two mutations: one at position 195 in which there was a change from alanine to threonine (A195T) and the second at amino acid residue 306 in which glycine was changed to serine (G306S). Both of these mutations were located in the C-terminal region of *Ph1*prol. Mutant no.19 had

two mutations: one at position 301 in which there was a change from tyrosine to cysteine (Y301C) and the second at amino acid residue 342 which had a substitution of lysine with an asparagine (K342N). These mutations were in the C-terminal region of the enzyme. Mutant no.35 contained two substitutions; one at residue 127 in the α-helical linker region in which there was a change from glutamate to glycine (E127G), and the second in the C-terminal region at residue 252 with a substitution of glutamate for aspartate (E252D). Variant no.72 contained the only mutation in the N-terminal region at residue 36 with a change from glutamate to valine (E36V) in *Ph1*prol. The mutations were remote from the active site pocket, which is shown in Figure 2-3 as being located between two 3_{10} helices (red helices, residues 191–195 and 281–284). Therefore, the mutations were unlikely to have directly altered the active site chemistry. Rather the mutations such as E36V, E127G, and Y301C may have affected prolidase dimerization as those residues are located along the dimerization interface. Furthermore, the mutations may have affected the conformational dynamics of the enzymes since some the mutations were located in the loop and linker regions. The change in conformational dynamics was likely a contributor to the variants having higher activity over a broader range of temperatures as indicated in section 2.4.4.

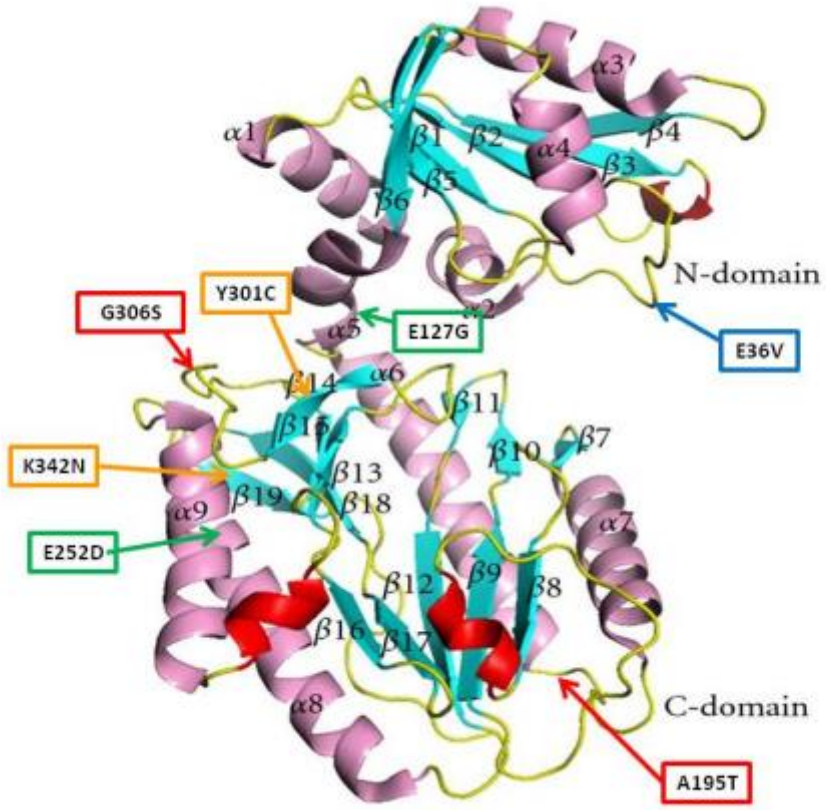

Figure 2-3. Mapping of the mutations in the monomeric structure of *P. horikoshii* prolidase (*Ph1*prol or PH0974). Amino acid substitutions in *Ph1*prol are indicated by colored arrows where red indicates mutations present in variant no.10 (A195T/G306S-*Ph1*prol), orange indicates mutations in variant no.19 (Y301C/K342N), green indicates mutations in variant no.35 (E127G/E252D) and blue indicates mutations in variant no.72 (E36V). The domain structure of *Ph1*prol is presented as a ribbon drawing where the N-terminal (residues 1-120) and C-terminal (131-356) domains are labeled and are connected by a α-helical linker at residues 121-130. The putative active site pocket is located between two 3_{10} helices (two red helices, residues 191–195 and 281–284). Modified from (Jeyakanthan et al., 2009).

2.4.4. Effects of mutagenesis on the temperature profile of P. horikoshii *prolidase variants.*

Both the wild type *Ph1* prolidase and the four variants were most active at 100°C (Figure 2-4). WT-*Ph1*prolidase and E36V-*Ph1*prolidase had very high specific activities (3,955 U/mg and 4094 U/mg, respectively) with 4 mM Met-Pro, both of which are twice as high as that of *Pf* prolidase at 100°C (2,154 U/mg) (Theriot, Du, et al., 2010). A195T/G306S-

and E127G/E252D-*Ph1*prol were slightly less active (2,307 U/mg and 2,831 U/mg, respectively) than WT *Ph1*prol, andY301C/K342N-*Ph1*prol showed the lowest level of activity in comparison to the other mutants at 1,842 U/mg. Activity was reduced by more than half at 70°C for all of the variants; however, WT-*Ph1*prolidase, A195T/G306S- and E36V-*Ph1*prol all had specific activities close to 1,000 U/mg (973 U/mg, 1000 U/mg, and 913 U/mg, respectively), whereas the specific activity of *Pf*prol at 70°C was 806 U/mg (Theriot, Du, et al., 2010). At 50°C, Y301C/K342N-*Ph1*prol had a higher specific activity than any of the other variants and the wild type (450 U/mg) and was roughly three times more active than *Pf*prol at 50°C (Theriot, Du, et al., 2010).

At lower temperatures (e.g., 35°C, 20°C, and 10°C), Y301C/K342N-*Ph1*prol was more active than the other *Ph1*prol variants, the WT-*Ph1*prol, the WT-*Pf*prol and R19G/G39E/K71E/S229T-*Pf*prol (the most active *Pf* prolidase mutant at lower temperatures) (Theriot, Du, et al., 2010). At 35°C, Y301C/K342N-*Ph1*prol (298 U/mg) had relative activity that was 121% that of WT-*Ph1*prol, 489% that of WT-*Pf*prol, and 244% that of R19G/G39E/K71E/S229T-*Pf*prol (246 U/mg, 61 U/mg, and 122 U/mg, respectively). At 20°C, Y301C/K342N-*Ph1*prol (241 U/mg) had a relative activity 184% that of WT-*Ph1*prol, 964% higher than WT-*Pf*prol, and 482% higher than R19G/G39E/K71E/S229T-*Pf*prol (specific activities of 131 U/mg for WT-*Ph1*prol, 25 U/mg for WT-*Pf*prol, and 50 U/mg for R19G/G39E/K71E/S229T-*Pf*prol) (Theriot, Du, et al., 2010). The greatest improvement in catalytic performance for the *Ph1*prol mutants was seen when assayed at 10°C. Y301C/K342N-*Ph1*prol (109 U/mg) had a relative activity that was 166% higher than that of WT-*Ph1*prol, 1,982% higher than that of WT-*Pf*prol, and 396% higher than

R19G/G39E/K71E/S229T-*Pf*prol (specific activities of 66 U/mg for WT-*Ph1*prol, 5.5 U/mg for WT-*Pf*prol, and 27.5 U/mg for R19G/G39E/K71E/S229T-*Pf*prol) (Theriot, Du, et al., 2010).

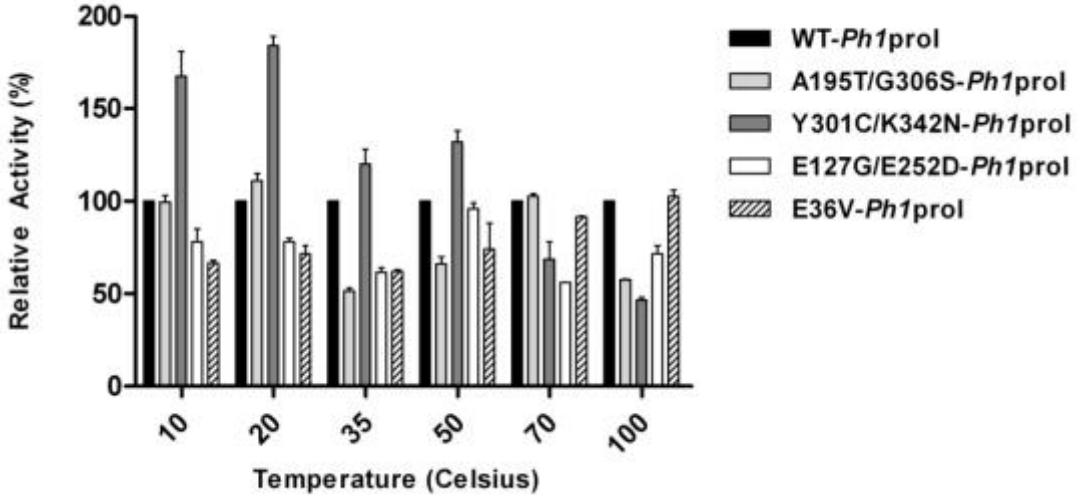

Figure 2-4. Temperature profile of WT-*Ph1* prolidase and the four variants. Relative activities are shown as a percentage of the WT-*Ph1*prol. Prolidase assays were performed in triplicate at 10°C, 20°C, 35°C, 50°C, 70°C and 100°C and contained 0.2 mM $CoCl_2$ and 4 mM Met-Pro. WT-*Ph1*prol specific activity was 66 U/mg at 10°C, 131 U/mg at 20°C, 246 U/mg at 35°C, 340 U/mg at 50°C, 973 U/mg at 70°C, and 3,955 U/mg at 100 °C.

2.4.5. Effects of mutagenesis on substrate specificity and kinetics of P. horikoshii *prolidase variants.*

Substrate specificity of WT-*Ph1* prolidase is shown in Table 2-1 along with the specific activities of A195T/G306S-, Y301C/K342N-, E127G/E252D-, and E36V-*Ph1*prol, which are reported as a percentage relative to the activity of the wild type. WT-*Ph1* prolidase was most active with the dipeptide Val-Pro (4,602 U/mg), while mutants A195T/G306S-,

Y301C/K342N-, E127G/E252D-, and E36V-*Ph1*prol had much lower activity at 33%, 36%, 46% and 56% of the WT *Ph1*prol, respectively. A195T/G306S-*Ph1*prol was most active with Met-Pro at 143% that of the wild type (2,809 U/mg), while Y301C/K342N-, E127G/E252D-, and E36V-Ph1prol had higher affinity for Ala-Pro, with specific activities of 183%, 324% and 556% that of WT-*Ph1* prolidase (1,452 U/mg). WT-*Ph1*prol was more active with very hydrophobic amino acids, while the four variants had the highest activity with a less hydrophobic amino acid in the N-terminal position of the dipeptide substrate. While alanine is hydrophibic, it is less hydrophobic than valine, methionine, phenylalanine and leucine and is most similar in structure to glycine. WT-*Ph1*prol had much lower activity with Gly-Pro than with Ala-Pro (369 compared to 1,452 U/mg). A195T/G306S-, Y301C/K342N-, and E127G/E252D-*Ph1*prol had less or similar activity with Gly-Pro as compared to WT-*Ph1*prol (369 U/mg) while E36V-*Ph1*prol had 444% higher activity.

Specific activities were consistently low with the substrates Pro-Ala and Val-Leu-Pro (2 U/mg, WT-*Ph1*prol) for the wild type *Ph1*prolidase and the four mutants. Due to the nature of the prolidase enzyme and its unique ability to cleave the bond between Xaa-Pro dipeptides, it was expected that the enzyme would not show any notable activity with a Pro-Xaa dipeptide or a tripeptide. While two of the four variants (mutants A195T/G306S- and E36V-*Ph1*prol) show increased activity with Pro-Ala when compared to wild type, it must be noted that specific activity with Pro-Ala for WT-*Ph1*prol was extremely low, at only 14 U/mg. Y301C/K342N-*Ph1*prol had 88% WT activity with Val-Leu-Pro; however, WT-*Ph1*prol specific activity was only 2 U/mg.

Table 2-1. Substrate specificity of recombinant wild-type and variant *P. horikoshii* prolidases with different proline dipeptides and a single proline tripeptide.

Substrate	Relative Activity (%) of WT-*Ph1*prol specific activity				
	WT-*Ph1*prol	A195T/G306S-*Ph1*prol	Y301C/K342N-*Ph1*prol	E127G/E252D-*Ph1*prol	E36V-*Ph1*prol
Val-Pro	100 (4,602)	33	36	46	56
Met-Pro	100 (2,809)	143	33	117	77
Phe-Pro	100 (2,199)	116	53	53	68
Leu-Pro	100 (2,132)	116	36	90	65
Ala-Pro	100 (1,452)	219	183	324	556
Gly-Pro	100 (369)	94	52	107	444
Pro-Ala	100 (14)	137	33	75	332
Val-Leu-Pro	100 (2)	0	88	0	0

Prolidase assays were performed at 100°C and contained 0.2 mM $CoCl_2$ and 4 mM of each substrate. 100% relative activity is reported for WT-*Ph1*prol and correlates to U/mg in parentheses below the relative activity percentage.

The catalytic properties of WT-*Ph1*prol and its mutants were tested at 70ºC with Leu-Pro (Table 2-2). All *Ph1*prol mutants had higher k_{cat} values than the WT-*Ph1*prol suggesting that the amino acid changes in the mutant enzymes did have an effect on structure and ultimately the catalytic activity of the prolidase with the substrate Leu-Pro. Although the k_{cat} values were higher, the overall enzyme turnover rates were not for some of the mutants compared to WT-*Ph1*prol. All of the *Ph1*prol mutants had an increased turnover rate, k_{cat}/K_m, with Leu-Pro except for Y301C/K342N-*Ph1*prol. This could be due to the increase in the K_m of this mutant, which is almost three times higher than WT-*Ph1*prol.

Table 2-2. Kinetic parameters of wild type *Pyrococcus horikoshii* prolidase, *Ph1*prol, and prolidase variants with Leu-Pro at 70°C.

Prolidase	K_m **(mM)**	V_{max} **(∝mol/min/mg)**	k_{cat} **(s^{-1})**	k_{cat}/K_m **($mM^{-1} s^{-1}$)**
WT-*Ph1*prol	0.92 ± 0.16	809 ± 55	1079	1172
A195T/G306S	0.81 ± 0.26	1245 ± 149	1660	2049
Y301C/K342N	2.92 ± 0.40	2146 ± 177	2861	980
E127G/E252D	0.98 ± 0.24	1119 ± 101	1492	1522
E36V	1.6 ± 0.37	1597 ± 174	2129	1331

Enzyme assays were performed using a range of Leu-Pro (0.25-12 mM). Enzyme kinetics were calculated using nonlinear regression (curve fit) and analyzed using the Michaelis-Menten equation in Prism 5 software (GraphPad La Jolla, CA). All *Ph1*prol assays contained 0.2 mM $CoCl_2$.

2.4.6. Effects of amino acid substitutions on the thermostability and pot-life activity of P. horikoshii *prolidase mutants.*

To determine whether the amino acid substitutions in the four *Ph1* prolidase variants had any effect on thermostability, the mutants were incubated in sealed vials at 90°C, anaerobically, for 72 h. Samples were taken every 24 h to measure catalytic activity with Met-Pro (4 mM) as the substrate. In Theriot et al.(2010), it was shown that WT-*Pf* prolidase was more thermostable than the variants and had lost 50% activity with Met-Pro by 21 hours at 90°C (Theriot, Du, et al., 2010). After 40 h at 90°C, WT-*Ph1* prolidase had lost 50% activity. Y301C/K342N-*Ph1*prol and E127G/E252D-*Ph1*prol both demonstrated increased thermostability at 90°C compared to wild type and had lost 50% activity after 58 hours of incubation. A195T/G306S-*Ph1*prol and E36V-*Ph1*prol displayed a 50% loss of activity after 32 and 35 hours at 90°C, respectively. Both WT-*Ph1*prol and the four *Ph1*prol mutants were

stable at 90°C for a significantly longer duration than *Pf*prol and its mutants (Theriot, Du, et al., 2010).

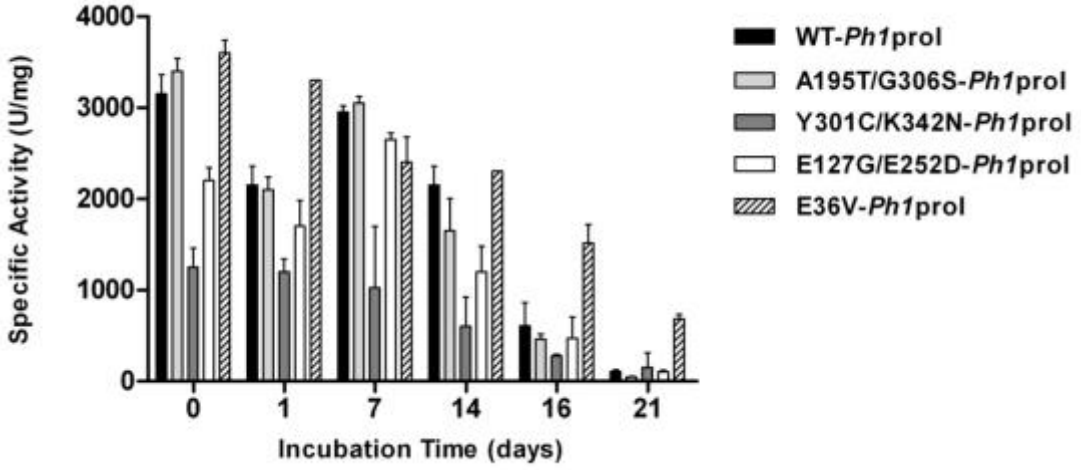

Figure 2-5. Pot-life activity of WT-*Ph1*prol and prolidase mutants incubated anaerobically at 70°C. Pot-life experiments were performed in duplicate and samples were taken at 0, 1, 7, 14, 16 and 21 days to assess reactivity. Prolidase assays were performed in triplicate at 100°C and contained 0.2 mM $CoCl_2$ and 4 mM Met-Pro. Error bars represent standard deviation of specific activity across duplicate runs.

Pot-life activity was monitored over the course of 21 days with samples taken every seven days until day 14 and then again on days 16 and 21 while the samples were incubated anaerobically at 70°C (Figure 2-5). Pot-life experiments with WT-*Pf*prol and its mutants as reported in Theriot et al. (2010) were conducted over a 48 h period at 70°C (Theriot, Du, et al., 2010). In preliminary pot-life experiments with WT-*Ph1*prol and its mutants, the specific activities with Met-Pro were still remarkably high after 48 h (no obvious decrease in specific activity was detected; data not shown), so the experiments were continued until the enzymes were no longer considered active (21 days). Initial specific activities for WT-*Ph1*prol, A195T/G306S-, Y301C/K342N-, E127G/E252D-, and E36V-*Ph1*prol were 3,150 U/mg, 3,400

U/mg, 1,250 U/mg, 2,200 U/mg, and 3,600 U/mg, respectively, with 4 mM Met-Pro as the substrate. WT-*Ph1*prol had lost 50% activity by day 12 of incubation at 70°C. Mutants Y301C/K342N-, E127G/E252D- and E36V-*Ph1*prol had 50% activity remaining by days 12, 13 and 14, respectively. A195T/G306S-*Ph1*prol was at 50% activity after 10 days at 70°C. By 21 days at 70°C, all five prolidases were at or below 25% activity.

As reported in Theriot et al. (2010), the specific activities of WT-*Pf*prol and its three mutants (G39E-, R19G/K71E/S229T-, and R19G/G39E/K71E/S229T-*Pf*prol) were 1,083 U/mg, 599 U/mg, 722 U/mg, and 4,496 U/mg, respectively, with 4 mM Met-Pro after 48 h of incubation at 70°C (Theriot, Du, et al., 2010). In contrast, after 7 days (or 168 h) at 70°C, WT-*Ph1*prol, A195T/G306S-, Y301C/K342N-, E127G/E252D-, and E36V-*Ph1*prol had specific activities of 2,950 U/mg, 3,050 U/mg, 1,230 U/mg, 2,650 U/mg and 2,400 U/mg, respectively, with 4 mM Met-Pro. After 48 h at 70°C, WT-*Pf*prol had a higher specific activity than any of the variants (1,083 U/mg). After 7 days at 70°C, Y301C/K342N-*Ph1*prol showed the lowest specific activity of the *Ph1* prolidases; however, its activity was still 114% that of WT-*Pf*prol at 48 h (Theriot, Du, et al., 2010).

2.4.7. DSC results.

The thermal stability of wild type *Ph1*prol and variants was determined by differential scanning calorimetry (DSC) experiments. Table 2-3 shows the denaturation temperature of the wild type and variant enzymes. The mutations that improved catalytic activity of the *Ph1*prol at lower temperatures did not adversely affect the temperature stability of the enzymes.

Table 2-3. Transition temperature of wild type *Pyrococcus horikoshii* prolidase, *Ph1*prol, and prolidase variants at pH 7.0.

Prolidase	T_m(°C)
WT-*Ph1*prol	114.3 ± 1.1
A195T/G306S[1]	114.4 ± 0.1
Y301C/K342N	113.8 ± 0.6
E127G/E252D	112.2 ± 0.5
E36V	114.9 ± 1.3

T_m is the transition temperatures obtained from the analysis of DSC by using the two-state model. The T_m values are the mean of three independent measurements. [1]The T_m value is from two independent measurements.

2.4.8. Effects of amino acid substitutions on substrate specificity with OP nerve agents DFP and soman analog, p-*nitrophenyl soman.*

Substrate specificity of WT-*Ph1* prolidase with DFP is shown in Figure 2-6 along with the specific activities of A195T/G306S-, Y301C/K342N-, E127G/E252D-, and E36V-*Ph1*prol, which are reported as a percentage relative to the activity of the wild type. WT *Ph1* prolidase was most active with DFP at 35ºC and 50ºC with a specific activity of 4 U/mg and 10 U/mg, respectively. A195T/G306S, Y301C/K342N-, E127G/E252D-, and E36V-*Ph1*prol had significantly lower activity with DFP; even at 50ºC the activity was only 59%, 25%, and 55% of WT-*Ph1*prol activity. However, it should be noted that the *Ph1*prol mutants have 808%, 183%, and 402% (A195T/G306S, Y301C/K342N-, E127G/E252D-, and E36V-*Ph1*prol, respectively) of the DFP activity compared to WT *P. furiosus* prolidase and also compare favorably to the highest DFP activity reported for the R19/G39E/K71E/S229T *Pf*prol mutant, which was shown to have 398% higher activity than WT *Pf*prol (Theriot, Du, et al., 2010).

Figure 2-7 reveals a different trend, where the amino acid substitutions in *Ph1*prol increased the specific activity with the soman analog, *p*-nitrophenyl soman at lower temperatures. WT-*Ph1*prol showed the highest activity with the soman analog at 70ºC, with a specific activity of 0.56 U/mg. A195T/G306S-*Ph1*prol had a similar specific activity to WT-*Ph1*prol when incubated at 35ºC, 50ºC, and 70ºC. Y301C/K342N-, E127G/E252D-, and E36V-*Ph1*prol showed increased activity with the soman analog over WT-*Ph1*prol at each assay temperature. The most notable specific activities with the soman analog were seen with Y301C/K342N-, E127G/E252D- and E36V-*Ph1*prol at 70ºC, which correlated to 125%, 186% and 157% increase over WT-*Ph1*prol. Furthermore, the activities for the *Ph1*prol mutants against *p*-nitrophenyl soman (0.7, 1.0 and 0.9 U/mg for Y301C/K342N-, E127G/E252D- and E36V-*Ph1*prol, respectively) compare favorably to the improved activities with soman analog reported for the *P. furiosus* prolidase mutants (0.86, 1.02, and 1.7 U/mg for G39E-, R19G/K71E/S229T-, and R19G/G39E/K71E/S229T-*Pf*prol, respectively) (Theriot, Du, et al., 2010). When looking at the substrate specificity of the WT-*Ph1*prol and variants with proline dipeptides, it was noticed that there was a shift in preference from more hydrophobic to less hydrophobic amino acids among the mutants. This is also seen with the OP nerve agents, where there is a shift in substrate specificity from DFP to the soman analog. The WT-*Ph1*prol prefers DFP as a substrate over the soman analog, while the *Ph1*prol variants show decreased activity with DFP and increased activity with the soman analog.

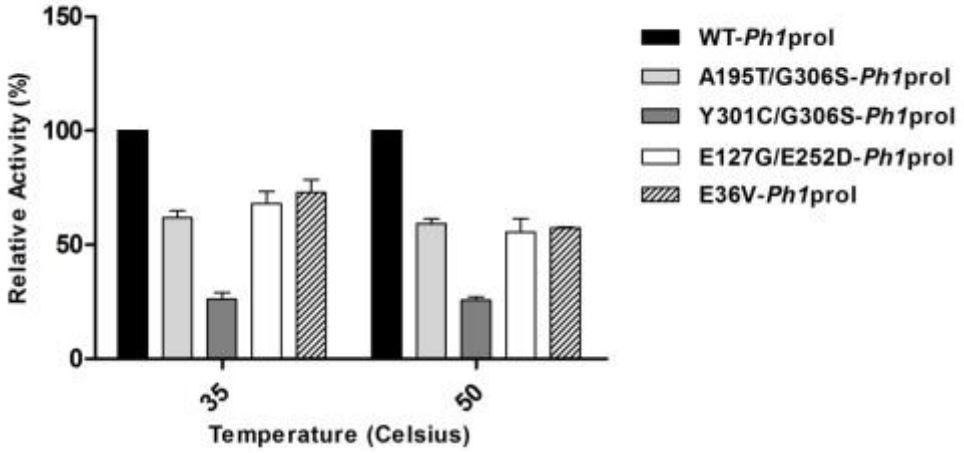

Figure 2-6. Relative activity of WT-*Ph1*prol and prolidase mutants with OP nerve agent DFP. All prolidase assays contained 50 mM MOPS, 200 mM NaCl, pH 7.0, 0.2 mM $CoCl_2$, and 3 mM DFP. 100% relative activity corresponds to WT-*Ph1*prol specific activity for DFP of 4 µmol product formed per minute per milligram at 35ºC and 10 µmol of product formed per minute per milligram at 50ºC.

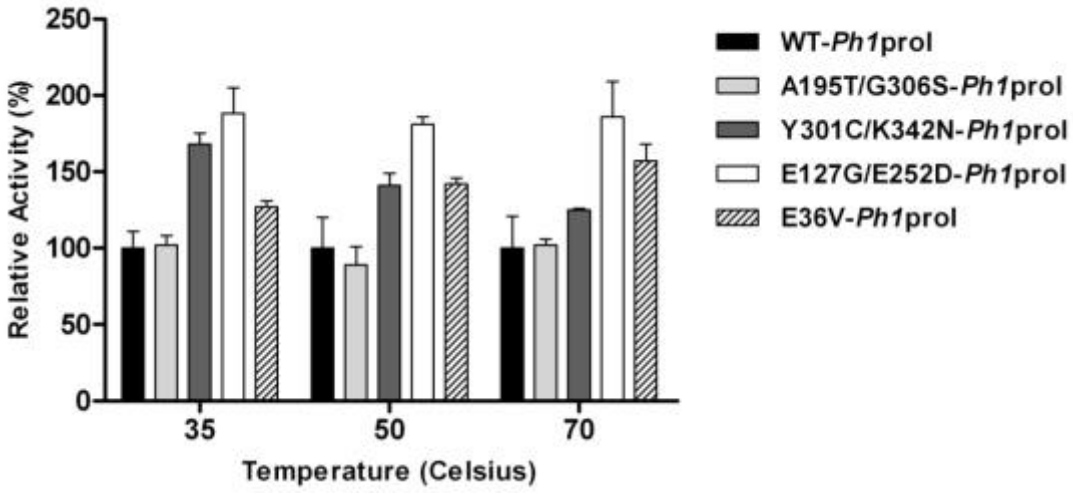

Figure 2-7. Relative activity of WT-*Ph1*prol and prolidase mutants with OP nerve agent analog, *p*-nitrophenyl soman. All prolidase assays contained 50 mM MOPS, 200 mM NaCl, pH 7.0, 0.2 mM $CoCl_2$, and 3 mM *p*-nitrophenyl soman. 100% relative activity corresponds to WT-*Ph1*prol specific activity for *p*-nitrophenyl soman of 0.26 µmol product formed per minute per milligram at 35ºC, 0.33 µmol product formed per minute per milligram at 50ºC, and 0.56 µmol product formed per minute per milligram at 70ºC.

2.5. Conclusion

Current biodecontamination formulations for degradation of OP nerve agents that incorporate *Alteromonas* prolidases (OPAA) and PTE have limitations when used in the field (Vyas et al., 2010). Long-term stability of the enzyme is not attainable in a formulation mixture that includes other solvents and denaturing solutions, and the need to add excess metal to reach maximum activity poses further complications for an enzyme-based detoxification system. A highly active enzyme that is stable over the long term and requires very little metal addition would be best suited for this application. The wild type and mutant prolidases characterized from *P. horikoshii* had favorable enzymatic properties that made them potential candidates for future optimization studies for OP nerve agent degradation. Compared to *Pf*prol, *Ph1*prol and the four *Ph1*prol variants had higher activity, increased affinity for the substrate, and significantly lower metal requirement for catalysis. Two of the variants, Y301C/K342N- and E127G/E252D-*Ph1*prol were thermostable nearly three-fold as long as *Pf*prol and double the time of *Ph1*prol. A195T/G306S-*Ph1*prol has 808% of the DFP activity compared to wild type *P. furiosus* prolidase and wa superior to any of the improved *P. furiosus* prolidase mutants (Theriot, Du, et al., 2010). Furthermore, Y301C/K342N-, E127G/E252D-, and E36V-*Ph1*prol all have improved activities against *p*-nitrophenyl soman relative to WT *Ph1*prol and also compared favorably to the most active *P. furiosus* prolidase mutants (Theriot, Du, et al., 2010). The *Ph1* prolidase variants have the potential to significantly improve upon current biodecontamination strategies. Their increased thermostability and pot-life and activities against OP nerve agent analogs warrant further study into large-scale production and purification of these prolidases.

Acknowledgements

The authors would like to thank Dr. Sherry Tove for her helpful comments on the manuscript and to acknowledge Dr. Nathaniel Hentz and Jessica Bridges Weaver at the NCSU Biomanufacturing Training and Education Center (BTEC) for contributing their time and expertise to the purification and characterization of the prolidases. We would like to thank Dr. James Carney and Patricia Buckley for performing the DSC experiment. Support for this study was provided by the Army Research Office (contract number 44258LSSR).

References

Adams, M. W. (1993). Enzymes and proteins from organisms that grow near and above 100 degrees C. *Annual Review of Microbiology*, *47*, 627–58.

Blumer-Schuette, S. E., Kataeva, I., Westpheling, J., Adams, M. W., & Kelly, R. M. (2008). Extremely thermophilic microorganisms for biomass conversion: status and prospects. *Current Opinion in Biotechnology*, *19*(3), 210-217.

Cheng, T.-C., & Defrank, J. J. (2000). Hydrolysis of organophosphorus compounds by bacterial prolidases. In *Enzymes in Action: Green Solutions for Chemical Problems* (pp. 243–261). Dordrecht: Springer Netherlands.

Cheng, T.-C., Rastogi, V. K., DeFrank, J. J., & Sawiris, G. P. (1998). G-type nerve agent decontamination by *Alteromonas* prolidase. *Annals of the New York Academy of Sciences*, *864*(1), 253–258.

Cheng, T. C., DeFrank, J. J., & Rastogi, V. K. (1999). *Alteromonas* prolidase for organophosphorus G-agent decontamination. In *Chemico-Biological Interactions* (Vol. 119–120, pp. 455–462).

Defense Threat Reduction Agency. (2008). *Joint Science and Technology Office for Chemical and Biological Defense FY10/11 - New Initiatives*.

Egorova, K., & Antranikian, G. (2005). Industrial relevance of thermophilic Archaea. *Current Opinion in Microbiology*, *8*(6), 649-655.

Fiala, G., & Stetter, K. O. (1986). *Pyrococcus furiosus* sp. nov. represents a novel genus of marine heterotrophic archaebacteria growing optimally at 100 degrees C. *Archives of Microbiology*, *145*(1), 56–61.

Ghosh, M., Grunden, A. M., Dunn, D. M., Weiss, R., & Adams, M. W. (1998). Characterization of native and recombinant forms of an unusual cobalt-dependent proline dipeptidase (prolidase) from the hyperthermophilic archaeon *Pyrococcus furiosus*. *J Bacteriol*, *180*(18), 4781–4789.

Gonzalez, J. M., Masuchi, Y., Robb, F. T., Ammerman, J. W., Maeder, D. L., Yanagibayashi, M., … Kato, C. (1998). *Pyrococcus horikoshii* sp. nov., a hyperthermophilic archaeon isolated from a hydrothermal vent at the Okinawa Trough. *Extremophiles*, *2*(2), 123–130.

Hill, C. M., Li, W. S., Cheng, T. C., DeFrank, J. J., & Raushel, F. M. (2001). Stereochemical specificity of organophosphorus acid anhydrolase toward p-nitrophenyl analogs of soman and sarin. *Bioorganic Chemistry*, *29*(1), 27–35.

Jeyakanthan, J., Takada, K., Sawano, M., Ogasahara, K., Mizutani, H., Kunishima, N., … Yutani, K. (2009). Crystal structural and functional analysis of the putative dipeptidase from *Pyrococcus horikoshii* OT3. *Journal of Biophysics* (Hindawi Publishing Corporation: Online*), 2009*, 434038.

Lowther, W. T., & Matthews, B. W. (2002). Metalloaminopeptidases: common functional themes in disparate structural surroundings. *Chemical Reviews*, *102*(12), 4581–4608.

Maher, M. J., Ghosh, M., Grunden, A. M., Menon, A. L., Adams, M. W. W., Freeman, H. C., & Guss, J. M. (2004). Structure of the prolidase from *Pyrococcus furiosus*. *Biochemistry*, *43*(10), 2771–2783.

Studier, F. W. (2005). Protein production by auto-induction in high-density shaking cultures. *Protein Expression and Purification*, *41*(1), 207–234.

Synowiecki, J., Grzybowska, B., & Zdziebło, A. (2006). Sources, properties and suitability of new thermostable enzymes in food processing. *Critical Reviews in Food Science and Nutrition*, *46*, 197–205.

Theriot, C. M., Du, X., Tove, S. R., & Grunden, A. M. (2010). Improving the catalytic activity of hyperthermophilic *Pyrococcus* prolidases for detoxification of organophosphorus nerve agents over a broad range of temperatures. *Applied Microbiology and Biotechnology*, *87*(5), 1715–1726.

Theriot, C. M., & Grunden, A. M. (2011). Hydrolysis of organophosphorus compounds by microbial enzymes. *Applied Microbiology and Biotechnology*.

Theriot, C. M., Tove, S. R., & Grunden, A. M. (2009). Biotechnological applications of recombinant microbial prolidases. *Advances in Applied Microbiology*.

Theriot, C. M., Tove, S. R., & Grunden, A. M. (2010). Characterization of two proline dipeptidases (prolidases) from the hyperthermophilic archaeon *Pyrococcus horikoshii*. *Applied Microbiology and Biotechnology*, *86*(1), 177–188.

Unsworth, L. D., van der Oost, J., & Koutsopoulos, S. (2007). Hyperthermophilic enzymes - stability, activity and implementation strategies for high temperature applications. *The FEBS Journal*, *274*(16), 4044–56.

Vyas, N. K., Nickitenko, A., Rastogi, V. K., Shah, S. S., & Quiocho, F. A. (2010). Structural insights into the dual activities of the nerve agent degrading organophosphate anhydrolase/prolidase. *Biochemistry*, *49*(3), 547–559.

CHAPTER 3.

Methods for Enhancing Cyanobacterial Stress Tolerance to Enable Improved Production of Biofuels and Industrially Relevant Chemicals

Rebecca L. Kitchener and Amy M. Grunden

Submitted for publication August 2017;

3.1. Abstract

Cyanobacteria are photosynthetic prokaryotes that can fix atmospheric CO_2 and can be engineered to produce industrially important compounds such as alcohols, free fatty acids, and alkanes used in next-generation biofuels, and commodity chemicals such as ethylene or farnesene. They can be easily genetically manipulated, have minimal nutrient requirements, and are quite tolerant to abiotic stress making them an appealing alternative to other biofuel-producing microbes which require additional carbon sources, as well as plants which compete with food crops for arable land. Many of the compounds produced in cyanobacteria are toxic as titers increase which can slow growth, reduce production, and decrease overall biomass. Additionally, many factors associated with outdoor culturing of cyanobacteria such as UV exposure and fluctuations in temperature can also limit the production potential of cyanobacteria. For cyanobacteria to be utilized successfully as biofactories, tolerance to these stressors must be increased and ameliorating stress responses must be enhanced. Genetic manipulation, directed evolution, and supplementation of culture media with antioxidants are all viable strategies for designing more robust cyanobacteria strains that have the potential to meet industrial production goals.

3.2. Introduction

The need for mankind to reduce reliance on fossil fuels and seek out more sustainable alternatives is becoming increasingly more apparent. Atmospheric buildup of CO_2, depletion of the protective ozone layer, and climate change have all been directly correlated to over-use of fossil fuels (Patel et al. 2005; Solomon et al. 2009; Wilcox, 2014). Cyanobacteria represent

a promising sustainable avenue for fuel production because they are capable of fixing atmospheric CO_2 to produce next-generation biofuels and commodity chemicals (Gronenberg et al. 2013). As prokaryotic autotrophs capable of oxygenic photosynthesis (utilizing both photosystems I and II), cyanobacterial metabolism is similar to that of plants, yet they can be successfully cultivated with minimal nutritional requirements - natural or artificial light, CO_2, water, nitrogen, and mineral salts – and have almost no requirement for additional carbon sources (Brasil et al. 2017; Singh et al., 2013; Zhou and Li, 2010). Genetic manipulation of cyanobacteria is relatively straightforward, and they can produce biomass much more rapidly than higher plants without competing with food crops for arable land (Case and Atsumi 2016; Cassier-Chauvat and Chauvat 2015; Golden and Canales, 2003). Cyanobacteria exhibit remarkable tolerance to abiotic stress and are found in all light-exposed ecosystems on Earth (Pade and Hagemann, 2014). Some of the products that can be made using cyanobacterial strains include ethanol, isopropanol, butanol, isobutanol, ethylene, isoprene, farnesene, 2,3-butanediol, acetone, sucrose, lactic acid, and several free fatty acids (Case and Atsumi 2016; Gao et al. 2012; Gronenberg et al. 2013; Hirokawa et al. 2015; Kusakabe et al. 2013; Machado and Atsumi 2012). The utility of cyanobacteria extends well beyond the chemical and biofuel industries into pharmaceuticals, bioremediation, and agriculture, to name a few (Sarma et al. 2016). In addition, cyanobacteria represent a potentially valuable resource as producers of industrial enzymes such as proteases and lipases, and the fact that many strains do not produce endotoxin makes them promising hosts for production of biotherapeutics (Brasil et al. 2017; Su et al. 2011).

While chemical production in cyanobacteria represents an advantageous avenue for sustainable replacement of fossil fuels, several technical hurdles must first be overcome. As with other prokaryotic producers of industrially important chemicals, many of these products are also toxic to the organisms making them which can slow overall biomass accumulation by directing carbon flux away from metabolism which in turn lowers potential product yield (Angermayr et al. 2009; Dexter and Fu 2009; Dunlop et al. 2011; Nicolaou et al. 2010; Oliver et al. 2014). Additionally, ideal culture conditions for sustainable growth include outdoor ponds or photobioreactors and would use seawater so as not to compete with food crops for arable land and fresh water (Ruffing, 2014; Su et al. 2017). Culturing cyanobacteria under these conditions, in which both temperature fluctuations, high intensity light/UV radiation, and salinity can all negatively impact cyanobacterial growth presents another set of challenges in which abiotic stress tolerance must be maximized for large-scale chemical production in cyanobacteria to become a reality (Ruffing, 2014).

Several recent review papers have thoroughly discussed stress responses in cyanobacteria and other chemical-producing bacteria, as well as the pathways (both naturally-occurring and synthetic) in which prokaryotes can be manipulated to produce commodity chemicals and biofuels (Abed et al. 2009; Case and Atsumi 2016; Dunlop et al. 2011; Dutta et al. 2005; Nicolaou et al. 2010; Sarma et al. 2016). This review instead aims primarily to highlight current research, in cyanobacteria specifically, in which efforts are being made to overcome stress responses stemming from growth conditions and chemical production by both improving stress tolerance and augmenting endogenous stress responses. Similar to strategies for increasing production titers in cyanobacteria, several avenues for stress mitigation in

cyanobacteria have been examined including genetic engineering targeting both metabolic processes and stress response genes, directed evolution, and enriching culture conditions with additives that improve stress tolerance by being taken up into the cells (Gombos et al. 1992; He and Häder 2002; M. Singh et al. 2013; Su et al. 2017; Zhou and Li 2010). The benefits of improving cyanobacterial stress tolerance are two-fold: first, it represents a strategy for maximizing production of next-generation biofuels by taking advantage of the photosynthetic properties of cyanobacteria. Secondly, the ease with which cyanobacteria can be genetically manipulated, and their similarity to plant chloroplasts provides a model system for testing of stress mitigation hypotheses, with the potential for scaling up successful strategies to be employed in higher plants (Singh et al. 2013).

Table 3-1. Chemicals produced in cyanobacteria: synthesis pathways and industrial applications.

Chemical Family	Chemical Name	Production Pathway	Applications	References
Alcohols & Fatty alcohols	Ethanol	1. Heterologous ethanol biosynthesis pathway 2. Overexpression of alcohol dehydrogenase genes 3. Re-routing carbon flux 4. Overexpression of RuBisCO	Biofuel Fuel additive	(Dexter, Armshaw, Sheahan, & Pembroke, 2015; Dexter & Fu, 2009; Gao et al., 2012; J. Zhou & Li, 2010)
	Isopropanol	1. Synthetic metabolic pathway 2. Altered culture conditions	Can be converted to plastics: propylene/polypropylene Biodiesel production	(Hanai, Atsumi, & Liao, 2007; Hirokawa et al., 2015; Kusakabe et al., 2013)
	1-butanol, isobutanol	1. Rerouting CoA pathway via malonyl CoA 2. Synthetic isobutanol pathway 3. Overexpression of RuBisCO	Chemical precursor Fuel additive Advanced biofuel alternative	(Anfelt et al., 2013; Hanai et al., 2007; Kämäräinen et al., 2012; Kusakabe et al., 2013; Wang, Wang, Zhang, & Meldrum, 2012; J. Zhou & Li, 2010)
	2-methyl-1-butanol	Heterologous gene expression: citramalate pathway enzymes	Solvent, manufacture of chemicals	(Shen et al., 2012; Yao, Qi, Tan, & Lu, 2014)
	2,3-butanediol	Synthetic pathway	Carbon feedstock for plastics/solvents/fuel	(Ji, Huang, & Ouyang, 2011; Kanno, Carroll, & Atsumi, 2017; Oliver, Machado, Yoneda, & Atsumi, 2013)
	Hexadecanol Octadecanol	1. Reduction of fatty acyl-CoA or acyl-ACP to fatty alcohol using heterologous enzymes 2. Inactivation of aldehyde-deformylation oxygenase gene	Industrial chemicals, biofuel additives, petrochemical substitutes, lubricants, detergents, cosmetics, pharmaceuticals, fragrance, flavorings	(Mudge, 2005; Noweck & Grafahrend, 2006; Yao et al., 2014; Y. J. Zhou et al., 2016)
Fatty acids	Palmitic acid, palmitoleic acid, heptadecanoic acid, stearic acid, oleic acid, linoleic acid, linolenic acid	1. Exogenous gene expression: *E. coli* thioesterase (*tes*A), algal RuBisCO 2. Overexpression of exogenous RuBisCO 3. Gene knockout (inactivate acyl-ACP synthetase gene, *aas*, to prevent FFA recycling) 4. Using strong promoters 5. Using tolerant strains 6. Weakening cell wall to increase FFA diffusion from cytoplasm	Feedstocks for renewable energy production	(Kato et al., 2017; Liu, Sheng, & Curtiss, 2011; Machado & Atsumi, 2012; Ruffing, 2014; Yao et al., 2014)
Hydrocarbons	Ethylene	Heterologous ethylene forming enzyme (EFE)	Polyethylene precursor, jet fuel, polyvinylchloride (PVC), ethanol, gasoline	(Ungerer et al., 2012)
	Heptadecane/heptadecene	Co-expression of two cyanobacterial alkane synthesis pathways	Biofuels	(Wang et al., 2012; Yoshino et al., 2015)
	Isoprenoids/terpenoids: □ Hemiterpenes (C5): isoprene, limonene □ Monoterpenes (C10) □ Sesquiterpenes (C15): Farnesene □ Diterpenes (C20): Tolypodiol □ Tripterpenes (C30): Squalene, hopanoids □ Tetraterpenes (C40): Carotenoids	1. Endogenous methylerythritol phosphate pathway (MEP) 2. Modified MEP pathway with heterologous genes (ex. plant isoprene synthase gene with light-dependent promoter, farnesene synthase gene)	Biofuels, aviation fuels, fuel additives, pharmaceuticals, medical equipment, rubber industry (toys, tires, textiles), neutraceuticals, cosmetics, disinfectants, food colorants, agrichemicals, flavorings, nutrition, animal feed supplements	(George, Alonso-Gutierrez, Keasling, & Lee, 2015; Halfmann, Gu, Gibbons, & Zhou, 2014; Lindberg, Park, & Melis, 2010; Machado & Atsumi, 2012; Pattanaik & Lindberg, 2015)
Compatible solutes	Sucrose	1. Natural accumulation of sucrose under high-salt conditions 2. Heterologous expression of sucrose exporter genes which steer flux away from glycogen production	Sugar feedstock for other fermentative organisms (replaces sugarcane)	(Case & Atsumi, 2016; Du, Liang, Duan, Tan, & Lu, 2013)
	Glucosylglycerol	1. Endogenous synthesis pathway driven by salt 2. Interruption of glycogen synthesis pathway to favor GG by introducing deletions	Cosmetics, pharmaceuticals, stabilizer for commercial proteins	(Ferjani et al., 2003; Pade & Hagemann, 2014; Tan, Luo, & Lu, 2016)
Industrial enzymes	Cellulases, amylolytic enzymes, galactosidases, proteases, lipases, phytases, laccases, antioxidant enzymes, carbohydrate accumulation enzymes	1. Expression/overexpression of endogenous and heterologous genes 2. Media supplementation to drive gene expression	Bioremediation, biofuel production, animal feed, textiles, food industry (colorants, brewing, flavorants, preservatives), pulp and paper industry, detergents, cosmetics, medical	(Brasil et al., 2017)
Other	Lactic acid	Exogenous L-lactate dehydrogenase gene (*Bacillus*)	Chemical feedstock for bioplastic production	(Angermayr, Paszota, & Hellingwerf, 2012)
	Hydrogen	Drive electron flux toward H_2 biosynthesis via native hydrogenases and nitrogenases	Fossil fuel alternative	(Dutta et al., 2005)

3.3. Chemical production in cyanobacteria

The ability of cyanobacteria to use atmospheric CO_2 to produce industrially important chemicals such as next generation biofuels is beneficial for several reasons. First, cyanobacteria represent a sustainable, renewable option for production of fossil fuel replacements. By using atmospheric CO_2 as their carbon source, fuel production by cyanobacteria could either reduce or slow buildup of CO_2 in the atmosphere. The chemicals can also be produced in ways that do not emit more CO_2 – for example the traditional method of ethylene production is currently the largest CO_2-emitting process in the chemical industry, while ethylene production in cyanobacteria does not emit CO_2 (Ungerer et al. 2012). Table 3-1 highlights important classes of chemicals that have been synthesized in cyanobacteria, the various strategies that have been employed to produce them, and their industrial applications. In addition to fuel production, cyanobacteria are also able to synthesize compatible solutes, and industrially-relevant enzymes.

3.4. Technical roadblocks to production

One of the main advantages of cyanobacterial or microalgal-based chemical production platforms is that these organisms can be cultured outdoors in photobioreactors or open ponds, thereby eliminating the need for facilities in which to house them and ensuring no competition with food crops for land. Culturing outdoors presents several challenges that must be addressed. Photobioreactors and open ponds are susceptible to fluctuations in temperature (both high and low), high irradiance, and microbial contamination (Su et al. 2017). Both psychrophilic and thermophilic cyanobacteria do exist; however, most species that have been

used for chemical production grow optimally between 25-35 °C, while temperatures in outdoor photobioreactors can reach 40 °C in subtropical zones (Lürling et al. 2013; Ong et al. 2010; Sarma et al. 2016). Culturing in elevated temperatures can be beneficial as well, as it is an effective way to reduce the potential for microbial contamination. Sunlight outside the spectrum of photosynthetically active radiation (PAR, 400-700 nm) is not used during photosynthesis and creates heat - another avenue for potential temperature fluctuations (Nozzi et al. 2013). While sunlight is a driver of photosynthetic processes, UV radiation (UVR) can be detrimental to culture growth when it enters the cell and interacts with molecular oxygen and organic compounds (Singh et al. 2010). Both UV-B (280 - 315 nm) and UV-A (315-400 nm) have been shown to damage DNA (either directly or indirectly) and UV-B specifically damages proteins, lipids, and can even inhibit photosynthesis by inducing formation and buildup of reactive oxygen species (ROS) within the cell and by inhibiting ribulose-1,5-bisphosphate carboxylase/oxygenase function (RuBisCO; the enzyme involved in the first step of carbon fixation), and the reactions of the Calvin cycle (He and Häder 2002; Singh et al. 2010; Zeeshan and Prasad 2009). Prolonged exposure to UVR and/or high intensity light causes photoinhibition by directly damaging photosystem II (PSII) (Murata et al. 2007). Additionally, when sunlight serves as the sole light source for cyanobacterial growth, production is limited to a diurnal cycle. Development of strains that continue to produce in the dark is more beneficial than using additional light sources (Nozzi et al. 2013). Cyanobacteria employ the following strategies to protect themselves from damaging UVR and high irradiance: avoidance, non-enzymatic and enzymatic antioxidants, production of UV-

absorbing compounds such as micosporine-like amino acids (MAAs), and repair and resynthesis of damaged macromolecules (Singh et al. 2010; Sinha et al. 2001).

Exposure to low temperatures causes several adverse effects to cyanobacteria such as decreasing membrane fluidity, inhibiting the necessary continuous repair of PSII by the D1 protein, increasing ROS production, and decreasing Calvin cycle activity (Murata et al. 2007; Thomas et al. 1999). Genes associated with cold stress in cyanobacteria can be categorized by function, including temperature-sensing and signal transduction (Hik proteins), transcription/translation (sigma factors), membrane fluidity (fatty acid desaturases), and maintaining photosynthesis and respiration (Sinetova and Los 2016). Heat exposure (10-15 ºC above ambient temperature) directly damages the light harvesting activity of cyanobacterial PSII by dissociating the phycobilisomes from the PSII reaction centers and degrading phycobilins, the pigments responsible for capturing light energy (Wen et al. 2005). Elevated temperature can also inhibit repair of PSII, disrupt photosynthesis by inactivating the heat-sensitive activase enzyme for RuBisCO and cause ROS buildup within the cell (Murata et al. 2007). Photobleaching and slowed growth or cell death are all results of prolonged exposure to high temperatures in cyanobacteria (Červený et al. 2015). In response to elevated temperatures, expression of heat shock proteins (Hsps) is induced. Some of the main proteins making up the cyanobacterial heat shock response (HSR) include HspA, GroEL1&2, GroES, HtpG, DnaK, DnaJ, and ClpB. Their functions include protection of proteins and enzymes, protection of photosynthetic apparatus, preventing photosynthetic inhibition, thylakoid membrane stabilization, and targeting proteins for folding (Rajaram et al. 2014).

Large scale cultivation of these organisms requires high volumes of water to produce ample biomass, but the impact of this is decreased when cyanobacteria can be successfully cultured in sea water. Culturing in sea water (or even waste water) eliminates use of fresh water and reduces restrictions on water quality as well as cost, and increased salinity can also reduce the potential for contamination and associated economic losses (Kämäräinen et al. 2012; Pade and Hagemann 2014; Su et al. 2017). Using wastewater or agricultural runoff in growth media also alleviates any competition with plants for nutrients such as nitrogen and phosphorus, and reduces risk of contamination (Nozzi et al. 2013). A drawback to sea water is that physiological salt tolerance must be improved in the target organisms in order for them to thrive in growth media that is highly saline such as those containing sea water (Su et al. 2017). Exposure to high concentrations of salt in the growth media can cause ionic and osmotic stress to the cell by lowering water availability and increasing intracellular ion concentrations (Pade and Hagemann 2014; Singh et al. 2013). In addition to water loss, increased salt concentrations in the growth media can inhibit metabolic processes such as nitrogen fixation, photosynthesis (by inhibiting repair of PSII), and transcription/translation (Murata et al. 2007; Pade and Hagemann 2014). Salt stress in cyanobacteria elicits a response similar to that of the previously-discussed stress conditions. Heat shock genes (*hspA*, *htpG*, *dnaK2*, *dnaJ*, *groEL2*), proteases (*clpB1* and *htrA*), and antioxidant genes are strongly upregulated in the presence of high salt concentrations. Cyanobacteria also express a small number of genes that are specific to salt response and are involved with synthesis of compatible solutes such as glucosylglycerol which function as osmoprotectants and help to stabilize enzymes (Castielli et al. 2009; Sleator and Hill, 2002).

While cost effectiveness of cyanobacterial biofactories is contingent upon maximizing solvent titers, it is also necessary to study tolerance of these organisms to these products as they accumulate within the cell or the growth media. Many fuels and fuel components are known to have antimicrobial activity, and product toxicity is a common problem across all strain engineering applications (Dunlop et al. 2011). Solvents and biofuel-related compounds can affect cells by damaging macromolecules through denaturation or imparting oxidative damage, or by altering cellular membrane stability and function (Anfelt et al. 2013). Organic solvents such as alcohols inhibit membrane function by accumulating in the phospholipid bilayer and disrupting energy maintenance, inhibiting the overall function of the membrane, displacing proteins, and altering membrane permeability leaving the cell incapable of maintaining homeostasis (Nicolaou et al. 2010). In general, longer chain alcohols are more toxic to cells than short chain, and increased solvent hydrophobicity is more damaging (Dunlop et al. 2011; Kämäräinen et al. 2012). Alkanes have been shown to be less toxic to cyanobacteria than alcohols, aldehydes, or fatty acids (Kämäräinen et al. 2012). Free fatty acid (FFA) production decreases viability in cyanobacteria by causing detrimental membrane modifications, increasing ROS production and altering photosynthesis by reducing photosynthetic yield and altering pigments (Ruffing, 2014).

During normal aerobic metabolism, reactive oxygen species (ROS) such as superoxide (O_2^-), singlet oxygen ($^1O_2$), hydrogen peroxide (H_2O_2), and the hydroxyl radical ($\cdot OH$) are produced at low levels as by-products of oxidative metabolism. They serve primarily as signaling molecules which can regulate not only responses to abiotic stress, but also overall cell growth (Pinto et al. 2003; Shi et al. 2017). In photosynthetic organisms, O_2^- is generated

by the reaction center of photosystem I (PSI) (Mittler and Tel-Or 1991). Excessive buildup of ROS, which occurs during exposure to high irradiance, UV-B, salt stress, solvent exposure, or temperature fluctuations can directly affect cells by damaging proteins (degradation and enzymatic inactivation), lipids (peroxidation), and DNA (strand breaks). ROS can adversely affect photosynthetic organisms by inhibiting PSII repair by suppressing synthesis of the D1 protein, disrupting electron flow through PSI, or degrading chlorophyll thereby reducing overall photosynthetic efficiency (Mittler et al. 2011; Schieber and Chandel, 2014).

Cyanobacteria have many strategies in place for maintaining ROS homeostasis. Energy dissipation (or quenching) is carried out by carotenoid pigments, or specialized proteins such as high light-inducible proteins (HLIPs) or CP43'(Latifi et al. 2009). Aside from carotenoids, additional non-enzymatic antioxidants which are produced in cyanobacteria include compatible solutes or osmoprotectants such as glycine betaine (GB), ascorbate, tocopherols, reduced glutathione, or the free amino acid, proline (Gabbay-Azaria et al. 1988; Matysik et al. 2002). As a second line of defense, cyanobacteria will increase expression of scavenger antioxidant enzymes beyond basal levels needed to maintain oxidative homeostasis when ROS accumulation occurs. Superoxide dismutase (SOD) detoxifies superoxide via disproportionation to form H_2O_2 and free oxygen. H_2O_2 is then further detoxified to form oxygen and water by catalases and peroxidases. Glutathione peroxidase, peroxiredoxin, ruberythrin, and DNA-binding protein (Dps) have also been found in cyanobacterial species and are capable of detoxifying H_2O_2 (Latifi et al. 2009; Mittler and Tel-Or 1991; Perelman et al. 2003).

3.5. Industrial stress mitigation strategies in cyanobacteria

Nozzi, et al. (2013) discussed in detail the challenges facing cyanobacterial biofactories and some current strategies for maximizing biochemical titers in cyanobacteria (Nozzi et al. 2013). Many of the genetic manipulation strategies for titer maximization can also be employed to decrease the effects of abiotic or oxidative stress or to improve endogenous stress responses. Additional strategies include utilization of strains with increased tolerance to light, heat, salt, and/or solvents; as well as performing directed evolution, supplementing media with additives that can be taken up into cells to improve stress tolerance, or continuously removing the product (if secreted) from the growth media (He and Häder 2002; Kato et al. 2017; Ruffing, 2014). Table 3-2 lists the strategies for stress mitigation that have been successfully used in cyanobacteria thus far.

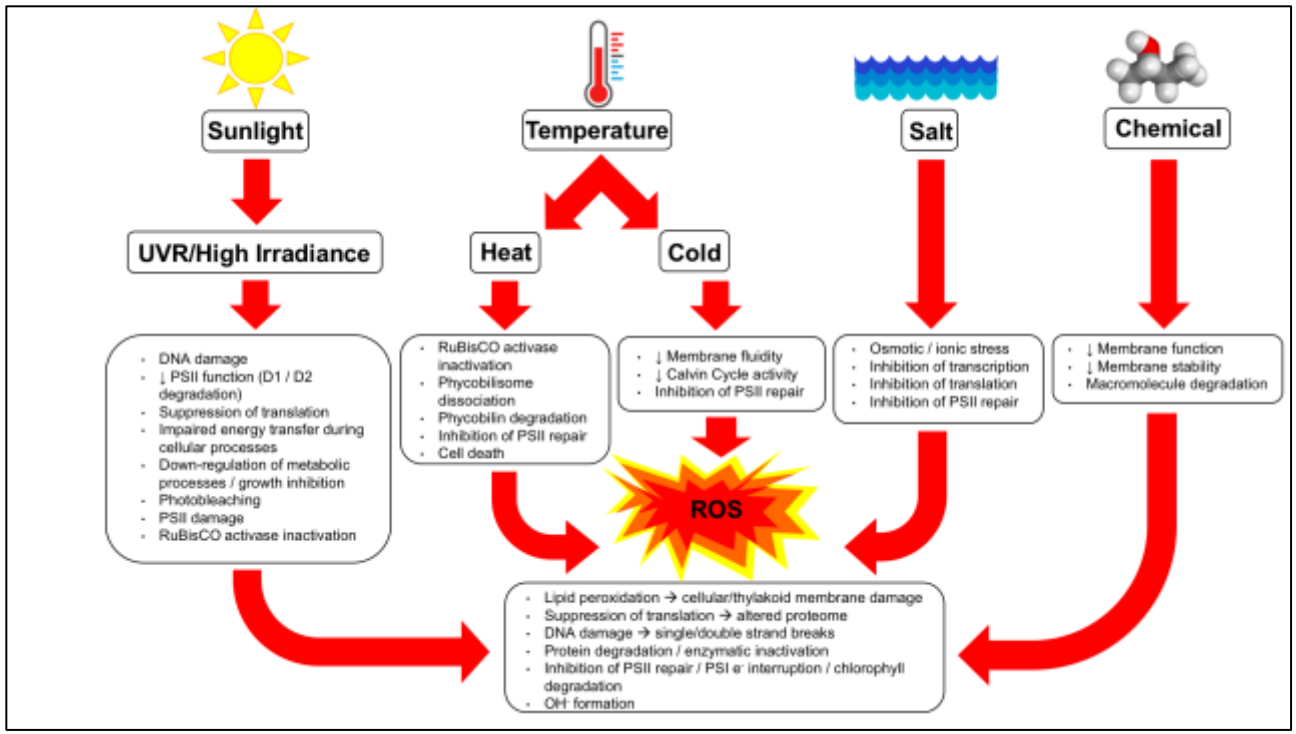

Figure 3-1. Potential sources of abiotic stress arising from culturing cyanobacteria in outdoor photobioreactors and their effects on cellular function.

Table 3-2. Potential sources of abiotic stress arising from outdoor photobioreactors for culturing cyanobacteria, and some successful strategies for stress mitigation.

	Stress conditions associated with outdoor photobioreactors					
Stress mitigation strategies	**UVR**	**Temp**	**Salt**	**Chemical or Solvent**	**ROS**	**References**
Identify tolerant strains	✓	✓	✓	✓		(Anfelt et al., 2013; Ruffing, 2014)
Directed evolution to select for tolerant strains				✓		(Johnson, Halfmann, Zahler, Zhou, & Gibbons, 2016)
Overexpress HSPs (endogenous and exogenous)	✓	✓	✓	✓		(Anfelt et al., 2013; Chaurasia & Apte, 2009; Su et al., 2017)
Express antioxidant enzymes (exogenous)	✓	✓	✓	✓	✓	(Kitchener, 2017)
Desaturate membrane lipids	✓	✓	✓			(Gombos et al., 1992; S. C. Singh, Sinha, & Häder, 2002)
Increase osmolyte synthesis			✓			(M. Singh et al., 2013)
Pre-treat with sub-lethal heat	✓					(Mishra, Chaurasia, & Rai, 2009)
Supplement growth medium with ROS-scavenging compounds					✓	(He & Häder, 2002)
Remove toxic products from growth medium				✓		(Kato et al., 2017)
Slowly increase exposure to stressor to build tolerance				✓		(Anfelt et al., 2013)

3.6. Endogenous gene expression to improve stress tolerance

Anfelt, et al. (2013) found that transcriptome sequencing could be used to assess genes involved in cellular response to short-term butanol exposure in order to target genes for overexpression during butanol shock, and they were able to design a mutant strain with increased tolerance (Anfelt et al. 2013). Ruffing (2014) coupled genetic manipulation and strain tolerance by employing *Synechococcus* sp. PCC 7002, a marine cyanobacterium that exhibits tolerance to salt, heat, and high irradiance that had been modified to overexpress RuBisCO which in turn enhanced CO_2 fixation (Ruffing, 2014). The resulting phenotype was a three-fold increase in FFA production compared to titers previously obtained in the freshwater strain *Synechococcus elongatus* sp. PCC 7942.

Chaurasia and Apte (2009) increased both heat and salt tolerance in *Anabaena* sp. strain PCC7120 by expressing an extra copy of the native *groESL* operon under control of a constitutive promoter. The *groESL* operon encodes genes for two co-chaperonin proteins, GroEL and GroES, that are responsible for solubilizing, folding, aggregating, or degrading damaged proteins during heat shock or other abiotic stress. The recombinant strain exhibited more robust growth, increased photosynthetic pigments, and improved nitrogen fixation compared to the wild type strain under optimal growth conditions. Under both salt and heat stress, the recombinant strain had less stress-mediated protein aggregation, as well as improved photosynthetic efficiency and nitrogen fixation when compared to the stressed wild type (Chaurasia and Apte, 2009).

3.7. Heterologous gene expression to improve stress tolerance

Gombos et al. (1992) showed that enhancing capabilities for desaturation of fatty acids of membrane lipids improves adaptation to cold stress by expressing *des*A, a Δ^{12} desaturase gene that creates a double bond at the C12 position from *Synechocystis* PCC6803 alongside the endogenous Δ^{9} desaturase gene in *Synechococcus elongatus* PCC 7942 (Gombos et al. 1992). Subsequent studies have shown that increasing unsaturation in membrane lipids confers increased tolerance to high intensity light and salt stress as well (Allakhverdiev et al. 2001; Gombos et al. 1992; Singh et al. 2002). Singh, et al. (2013) were able to improve salt tolerance (and ultimately create a halophilic strain) in salt-sensitive freshwater species *Anabaena doliolum* by transforming with N-methyltransferase genes from a halophilic cyanobacterium in order to increase synthesis of the osmolyte glycine betaine (GB) which confers salt tolerance (Singh et al. 2013).

Su et al. (2017) expressed two heterologous stress response proteins in *S. elongatus* PCC 7942: HspA, a heat shock chaperone protein from a thermotolerant cyanobacterium and osmotin, a stress-response plant protein that protects against both decreased and elevated temperature, salt, and drought. They found that both the HspA strain and the osmotin strain had increased growth and photosynthetic rates compared to the control strain when grown with increased light intensity, temperature, and salt. Ultimately, both strains were able to grow in seawater in an outdoor photobioreactor while the control strain could not, although the HspA strain's growth surpassed the osmotin strain (Su et al. 2017).

Our lab has approached improvement of stress tolerance by focusing on direct enhancement of ROS detoxification. By constitutively expressing an archaeal superoxide reductase (SOR) gene from the hyperthermophile *Pyrococcus furiosus* in *S. elongatus* PCC 7942, we have demonstrated improved growth, increased protection of PSII (higher F_v/F_m ratio indicating less photoinhibition), and decreased lipid peroxidation and free proline (biomarkers indicative of oxidative stress) when compared to the empty vector control strain in the presence of methyl viologen (Kitchener, 2017). Methyl viologen directly induces ROS formation (specifically O_2^-, the superoxide anion) within the cytosol (Hassett et al. 1987). The endogenous superoxide dismutase (SOD) enzyme detoxifies O_2^- effectively, but its expression is tightly regulated, and the products it forms – H_2O_2 and ultimately free oxygen – are prone to spontaneously reacting to form additional ROS, including more O_2^- and the toxic hydroxyl radical (Hassett et al. 1987; Im et al. 2009; Thomas et al. 1998). SOR catalyzes the reduction of O_2^- to form water and H_2O_2, but no free oxygen (Jenney et al. 1999). Expression of SOR has been shown to improve tolerance to abiotic stress such as heat and drought in plant cell culture and higher plants (Im et al. 2005, Geng et al. 2016; Im et al. 2010; Im et al., 2009). In addition to improved tolerance to direct ROS formation within the cell, our SOR strain has increased tolerance to and recovery from high-intensity light, UV-B exposure, prolonged heat stress, and solvent exposure (Kitchener, 2017).

3.8. Additional strategies for enhancing stress tolerance

In addition to genetic manipulation, other strategies for enhancing stress tolerance in cyanobacteria include adaptation/directed evolution, media supplementation, and in the case

of product toxicity, removing the product from the culture media to drive further production. Mishra, et al. (2009) found that exposing *A. doliolum* cultures to a 1-hour heat treatment at an elevated, but sub-lethal, temperature increased tolerance to UV-B exposure. The short heat treatment prior to UV-B exposure initiated expression of several HSR proteins involved in ROS scavenging, signaling, maintenance of redox balance, and maintenance of photosynthetic processes which are also necessary for UV-B tolerance (Mishra et al. 2009). Johnson et al. (2016) aimed to improve cyanobacterial biofuel tolerance by employing a directed evolution strategy. Three species of cyanobacteria were grown in the presence of increasing concentrations of next-generation biofuels in order to select for increased tolerance and create a library of tolerant mutants which could then be engineered to theoretically produce the higher titers of toxic hydrocarbons (Johnson et al. 2016). He and Häder (2002) found that adding ROS scavengers to growth media offers a protective effect against ROS production during UV-A and UV-B exposure when taken up into the cells. When ascorbic acid or *N*-acetyl-L-cysteine (NAC) were added to the cyanobacterial culture medium prior to UV exposure, increased survival rates and decreased lipid peroxidation, chlorophyll bleaching, and DNA strand breaks were observed (He and Häder, 2002).

In an effort to improve cyanobacterial lipid production and circumvent toxicity of intracellular free fatty acid (FFA) buildup, Kato et al. (2017) examined the effects of continuously removing secreted FFA from the culture medium on FFA titers and cell survival. Using a two-phase aqueous-organic culturing system, the continuous removal of FFA led to improved secretion of FFA from cells, more than three-fold increased production of FFA compared to what had been achieved in cyanobacteria previously, and decreased overall effects

of FFA toxicity on culture viability (Kato et al., 2017). Other strategies of developing tolerant phenotypes in non-cyanobacterial model industrial organisms have been described in detail in a review by Nicolau, et al. (2010). Many of the strategies for improving cyanobacterial stress tolerance have also been used successfully in other industrial microbes such as *Escherichia coli*, *Clostridium* sp., and *Saccharomyces cerevisiae* to improve production titers and decrease solvent toxicity (Nicolaou et al., 2010). Additional avenues, such as heterologous expression of solvent-specific efflux pumps to prevent toxic buildup within the cell, genomic approaches such as deletion libraries or whole-genome shuffling, or integrating multiple stress tolerance strategies in concert, could potentially be used in cyanobacterial model systems as well.

In conclusion, the ability of cyanobacteria to convert solar energy into industrially valuable chemicals using minimal nutrients makes them an attractive candidate for many biotechnological applications, including production of next-generation biofuels, aviation fuels, commodity chemicals, and industrial enzymes. The similarities between cyanobacteria and plant chloroplasts allow for an experimental model for testing stress responses in higher plants, and for exploring modes of improving plant stress tolerance (Singh et al. 2013). Genetic manipulation of cyanobacteria is relatively uncomplicated compared to eukaryotic biofuel producers, and they are able to produce biomass at a much quicker rate. The prevalence of cyanobacteria in varied aqueous ecosystems and their ability to adapt to sub-optimal growth conditions allows for their potential cultivation in outdoor photobioreactors utilizing seawater or wastewater, and prevents any competition with plants for arable land. Outdoor culturing creates technical hurdles associated with abiotic stress that must be overcome in order for cyanobacterial biofactories to become a reality. Responses to heat stress, cold stress, UV

exposure, high irradiance, salt stress, solvent toxicity, and the inevitable buildup of ROS associated with the aforementioned stressors must be improved to create more robust cyanobacterial production strains. Genetic manipulation, selection of tolerant strains, directed evolution, media supplementation, and continuous product removal are some of the avenues being pursued to improve cyanobacterial stress tolerance and production capabilities.

References

Abed, R. M. M., Dobretsov, S., & Sudesh, K. (2009). Applications of cyanobacteria in biotechnology. *Journal of Applied Microbiology*, *106*(1), 1–12.

Allakhverdiev, S. I., Kinoshita, M., Inaba, M., Suzuki, I., & Murata, N. (2001). Unsaturated fatty acids in membrane lipids protect the photosynthetic machinery against salt-induced damage in *Synechococcus*. *Plant Physiology*, *125*(4).

Anfelt, J., Hallström, B., Nielsen, J., Uhlén, M., & Hudson, E. P. (2013). Using transcriptomics to improve butanol tolerance of *Synechocystis* sp. strain PCC 6803. *Applied and Environmental Microbiology*, *79*(23), 7419–27.

Angermayr, S. A., Hellingwerf, K. J., & Teixeira de Mattos, M. J. (2009). Energy biotechnology with cyanobacteria. *Current Opinion in Biotechnology*, *20*(3), 257–263.

Angermayr, S. A., Paszota, M., & Hellingwerf, K. J. (2012). Engineering a cyanobacterial cell factory for production of lactic acid. *Applied and Environmental Microbiology*, *78*(19), 7098–106.

Brasil, B. dos S. A. F., de Siqueira, F. G., Salum, T. F. C., Zanette, C. M., & Spier, M. R. (2017). Microalgae and cyanobacteria as enzyme biofactories. *Algal Research*, *25*, 76–89.

Case, A. E., & Atsumi, S. (2016). Cyanobacterial chemical production. *Journal of Biotechnology*, *231*, 106–114.

Cassier-Chauvat, C., & Chauvat, F. (2015). Responses to oxidative and heavy metal stresses in cyanobacteria: Recent advances. *International Journal of Molecular Sciences*, *16*(1), 871–886.

Castielli, O., De la Cerda, B., Navarro, J. A., Hervás, M., & De la Rosa, M. A. (2009). Proteomic analyses of the response of cyanobacteria to different stress conditions. *FEBS Letters*, *583*(11), 1753–1758.

Červený, J., Sinetova, M. A., Zavřel, T., & Los, D. A. (2015). Mechanisms of high temperature resistance of *Synechocystis* sp. PCC 6803: an impact of histidine kinase 34. *Life*, *5*(1), 676–699.

Chaurasia, A. K., & Apte, S. K. (2009). Overexpression of the groESL operon enhances the heat and salinity stress tolerance of the nitrogen-fixing cyanobacterium *Anabaena* sp. strain PCC7120. *Applied and Environmental Microbiology*, *75*(18), 6008–6012.

Dexter, J., Armshaw, P., Sheahan, C., & Pembroke, J. T. (2015). The state of autotrophic ethanol production in cyanobacteria. *Journal of Applied Microbiology*, *119*(1), 11–24.

Dexter, J., & Fu, P. C. (2009). Metabolic engineering of cyanobacteria for ethanol production. *Energ Environ Sci*, *2*.

Du, W., Liang, F., Duan, Y., Tan, X., & Lu, X. (2013). Exploring the photosynthetic production capacity of sucrose by cyanobacteria. *Metabolic Engineering*, *19*, 17–25.

Dunlop, M. J., Dossani, Z. Y., Szmidt, H. L., Chu, H. C., Lee, T. S., Keasling, J. D., … Mukhopadhyay, A. (2011). Engineering microbial biofuel tolerance and export using efflux pumps. *Molecular Systems Biology*, *7*(487), 487.

Dutta, D., De, D., Chaudhuri, S., & Bhattacharya, S. K. (2005). Hydrogen production by cyanobacteria. *Microbial Cell Factories*, *4*, 36.

Ferjani, A., Mustardy, L., Sulpice, R., Marin, K., Suzuki, I., Hagemann, M., & Murata, N. (2003). Glucosylglycerol, a compatible solute, sustains cell division under salt stress. *Plant Physiology*, *131*(4), 1628–1637.

Gabbay-Azaria, R., Tel-Or, E., & Schönfeld, M. (1988). Glycinebetaine as an osmoregulant and compatible solute in the marine cyanobacterium Spirulina subsalsa. *Archives of Biochemistry and Biophysics*, *264*(1), 333–9.

Gao, Z., Zhao, H., Li, Z., Tan, X., & Lu, X. (2012). Photosynthetic production of ethanol from carbon dioxide in genetically engineered cyanobacteria. *Energy Environ. Sci.*, *5*(12), 9857–9865.

Geng, X.-M., Liu, X., Ji, M., Hoffmann, W. A., Grunden, A. M., & Xiang, Q.-Y. J. (2016). Enhancing heat tolerance of the little dogwood *Cornus canadensis* L. f. with introduction of a superoxide reductase gene from the hyperthermophilic archaeon *Pyrococcus furiosus*. *Frontiers in Plant Science*, *7*, 26.

George, K. W., Alonso-Gutierrez, J., Keasling, J. D., & Lee, T. S. (2015). Isoprenoid drugs, biofuels, and chemicals—artemisinin, farnesene, and beyond. In *Advances in biochemical engineering/biotechnology* (Vol. 148, pp. 355–389).

Golden, S. S., & Canales, S. R. (2003). Cyanobacterial circadian clocks--timing is everything. *Nature Reviews. Microbiology*, *1*(3), 191–9.

Gombos, Z., Wada, H., & Murata, N. (1992). Unsaturation of fatty acids in membrane lipids enhances tolerance of the cyanobacterium *Synechocystis* PCC6803 to low-temperature photoinhibition. *Proceedings of the National Academy of Sciences of the United States of America*, *89*(20), 9959–9963.

Gronenberg, L. S., Marcheschi, R. J., & Liao, J. C. (2013). Next generation biofuel engineering in prokaryotes. *Current Opinion in Chemical Biology*, *17*(3), 462–471.

Halfmann, C., Gu, L., Gibbons, W., & Zhou, R. (2014). Genetically engineering cyanobacteria to convert CO2, water, and light into the long-chain hydrocarbon farnesene. *Applied Microbiology and Biotechnology*, *98*(23), 9869–9877.

Hanai, T., Atsumi, S., & Liao, J. C. (2007). Engineered synthetic pathway for isopropanol production in *Escherichia coli*. *Applied and Environmental Microbiology*, *73*(24), 7814–7818.

Hassett, D. J., Britigan, B. E., Svendsen, T., Rosen, G. M., & Cohen, M. S. (1987). Bacteria form intracellular free radicals in response to paraquat and streptonigrin: demonstration of the potency of hydroxyl radical. *The Journal of Biological Chemistry*, *262*(28), 13404–13408.

He, Y.-Y., & Häder, D.-P. (2002). UV-B-induced formation of reactive oxygen species and oxidative damage of the cyanobacterium *Anabaena* sp.: protective effects of ascorbic acid and N-acetyl-l-cysteine. *Journal of Photochemistry and Photobiology B: Biology*, *66*(2), 115–124.

Hirokawa, Y., Suzuki, I., & Hanai, T. (2015). Optimization of isopropanol production by engineered cyanobacteria with a synthetic metabolic pathway. *Journal of Bioscience and Bioengineering*, *119*(5), 585–590.

Im, Y. J., Ji, M., Lee, A. M., Killens, R., Grunden, A. M., & Boss, W. F. (2009). Expression of *Pyrococcus furiosus* superoxide reductase in Arabidopsis enhances heat tolerance. *Plant Physiology*, *151*(2), 893–904.

Jenney, F. E., Verhagen, M. F., Cui, X., & Adams, M. W. (1999). Anaerobic microbes: oxygen detoxification without superoxide dismutase. *Science*, *286*(5438).

Ji, X.-J., Huang, H., & Ouyang, P.-K. (2011). Microbial 2,3-butanediol production: A state-of-the-art review. *Biotechnology Advances*, *29*(3), 351–364.

Johnson, T. J., Halfmann, C., Zahler, J. D., Zhou, R., & Gibbons, W. R. (2016). Increasing the tolerance of filamentous cyanobacteria to next-generation biofuels via directed evolution. *Algal Research*, *18*, 250–256.

Kämäräinen, J., Knoop, H., Stanford, N. J., Guerrero, F., Akhtar, M. K., Aro, E. M., … Jones, P. R. (2012). Physiological tolerance and stoichiometric potential of cyanobacteria for hydrocarbon fuel production. *Journal of Biotechnology*, *162*(1), 67–74.

Kanno, M., Carroll, A. L., & Atsumi, S. (2017). Global metabolic rewiring for improved CO_2 fixation and chemical production in cyanobacteria. *Nature Communications*, *8*, 14724.

Kato, A., Takatani, N., Ikeda, K., Maeda, S., & Omata, T. (2017). Removal of the product from the culture medium strongly enhances free fatty acid production by genetically engineered *Synechococcus elongatus*. *Biotechnology for Biofuels*, *10*(1), 141.

Kitchener, R.L. (2017). Superoxide reductase from the thermophilic archaeon *Pyrococcus furiosus* improves tolerance to abiotic stress in the cyanobacterium *Synechococcus elongatus* PCC 7942. Unpublished.

Kusakabe, T., Tatsuke, T., Tsuruno, K., Hirokawa, Y., Atsumi, S., Liao, J. C., & Hanai, T. (2013). Engineering a synthetic pathway in cyanobacteria for isopropanol production directly from carbon dioxide and light. *Metabolic Engineering*, *20*, 101–108.

Latifi, A., Ruiz, M., & Zhang, C. C. (2009). Oxidative stress in cyanobacteria. *FEMS Microbiology Reviews*, *33*(2), 258–278.

Lindberg, P., Park, S., & Melis, A. (2010). Engineering a platform for photosynthetic isoprene production in cyanobacteria, using *Synechocystis* as the model organism. *Metab Eng*, *12*.

Liu, X., Sheng, J., & Curtiss, R. (2011). Fatty acid production in genetically modified cyanobacteria. *Proceedings of the National Academy of Sciences of the United States of America*, *108*(17), 6899–904.

Lürling, M., Eshetu, F., Faassen, E. J., Kosten, S. & Huszar, V. L. M. (2013). Comparison of cyanobacterial and green algal growth rates at different temperatures. *Freshwater Biology*, *58*(3), 552–559.

Machado, I. M. P., & Atsumi, S. (2012). Cyanobacterial biofuel production. *Journal of Biotechnology*, *162*(1), 50–56.

Matysik, J., Alia, Bhalu, B., & Mohanty, P. (n.d.). Molecular mechanisms of quenching of reactive oxygen species by proline under stress in plants. *Current Science*, *82*, 525–532.

Mishra, Y., Chaurasia, N., & Rai, L. C. (2009). Heat pretreatment alleviates UV-B toxicity in the cyanobacterium *Anabaena doliolum*: a proteomic analysis of cross tolerance. *Photochemistry and Photobiology*, *85*(3), 824–833.

Mittler, R., & Tel-Or, E. (1991). Oxidative stress responses in the unicellular cyanobacterium *Synechococcus* PCC 7942. *Free Radical Research Communications*, *12–13 Pt 2*(October), 845–50.

Mittler, R., Vanderauwera, S., Suzuki, N., Miller, G., Tognetti, V. B., Vandepoele, K., … Van Breusegem, F. (2011). ROS signaling: The new wave? *Trends in Plant Science*, *16*(6), 300–309.

Mudge, S. M. (2005). Fatty Alcohols – a review of their natural synthesis and environmental distribution. *The Soap and Detergent Association*, *132*, 1–141.

Murata, N., Takahashi, S., Nishiyama, Y., & Allakhverdiev, S. I. (2007). Photoinhibition of photosystem II under environmental stress. *Biochimica et Biophysica Acta (BBA) - Bioenergetics*, *1767*(6), 414–421.

Nicolaou, S. A., Gaida, S. M., & Papoutsakis, E. T. (2010). A comparative view of metabolite and substrate stress and tolerance in microbial bioprocessing: From biofuels and chemicals, to biocatalysis and bioremediation. *Metabolic Engineering*, *12*(4), 307–331.

Noweck, K., & Grafahrend, W. (2006). Fatty alcohols. In *Ullmann's Encyclopedia of Industrial Chemistry*. Weinheim, Germany: Wiley-VCH Verlag GmbH & Co. KGaA.

Nozzi, N. E., Oliver, J. W. K., & Atsumi, S. (2013). Cyanobacteria as a platform for biofuel production. *Frontiers in Bioengineering and Biotechnology*, *1*, 7.

Oliver, J. W. K., Machado, I. M. P., Yoneda, H., & Atsumi, S. (2013). Cyanobacterial conversion of carbon dioxide to 2,3-butanediol. *Proceedings of the National Academy of Sciences of the United States of America*, *110*(4), 1249–54.

Oliver, J. W. K., Machado, I. M. P., Yoneda, H., & Atsumi, S. (2014). Combinatorial optimization of cyanobacterial 2,3-butanediol production. *Metabolic Engineering*, *22*, 76–82.

Ong, S.-C., Kao, C.-Y., Chiu, S.-Y., Tsai, M.-T., & Lin, C.-S. (2010). Characterization of the thermal-tolerant mutants of *Chlorella* sp. with high growth rate and application in outdoor photobioreactor cultivation. *Bioresource Technology*, *101*(8), 2880–2883.

Pade, N., & Hagemann, M. (2014). Salt acclimation of cyanobacteria and their application in biotechnology. *Life (Basel, Switzerland)*, *5*(1), 25–49.

Patel, M., Neelis, M., Gielen, D., Olivier, J., Simmons, T., Theunis, J., … Edenhofer, O. (2005). Carbon dioxide emissions from non-energy use of fossil fuels: summary of key issues and conclusions from the country analyses. *Resources, Conservation and Recycling*, *45*(3), 195–209.

Pattanaik, B., & Lindberg, P. (2015). Terpenoids and their biosynthesis in cyanobacteria. *Life (Basel, Switzerland)*, *5*(1), 269–93.

Perelman, A., Uzan, A., Hacohen, D., & Schwarz, R. (2003). Oxidative stress in *Synechococcus* sp. strain PCC 7942: various mechanisms for H_2O_2 detoxification with different physiological roles. *Journal of Bacteriology*, *185*(12), 3654–60.

Pinto, E., Sigaud- Kutner, T. C. S., Leitao, M. A. S., & Okamoto, O. K. (2003). Heavy metal-induced oxidative stress in algae. *J. Phycol.*, *39*, 1008–1018.

Rajaram, H., Chaurasia, A. K., & Apte, S. K. (2014). Cyanobacterial heat-shock response: role and regulation of molecular chaperones. *Microbiology*, *160*(Pt_4), 647–658.

Ruffing, A. M. (2014). Improved free fatty acid production in cyanobacteria with *Synechococcus* sp. PCC 7002 as host. *Frontiers in Bioengineering and Biotechnology*, *2*, 17.

Sarma, M. K., Kaushik, S., & Goswami, P. (2016). Cyanobacteria: A metabolic power house for harvesting solar energy to produce bio-electricity and biofuels. *Biomass and Bioenergy*, *90*, 187–201.

Schieber, M., & Chandel, N. S. (2014). ROS function in redox signaling and oxidative stress. *Current Biology*, *24*(10).

Shen, C. R., Liao, J. C., Shelton, J., Lebedeva, N. V., Yarrow, J., Min, H., … Cho, K. M. (2012). Photosynthetic production of 2-methyl-1-butanol from CO2 in cyanobacterium *Synechococcus elongatus* PCC7942 and characterization of the native acetohydroxyacid synthase. *Energy & Environmental Science*, *5*(11), 9574.

Shi, K., Gao, Z., Shi, T.-Q., Song, P., Ren, L.-J., Huang, H., & Ji, X.-J. (2017). Reactive oxygen species-mediated cellular stress response and lipid accumulation in oleaginous microorganisms: the state of the art and future perspectives. *Frontiers in Microbiology*, *8*, 793.

Sinetova, M. A., & Los, D. A. (2016). New insights in cyanobacterial cold stress responses: genes, sensors, and molecular triggers. *Biochimica et Biophysica Acta (BBA) - General Subjects*, *1860*(11), 2391–2403.

Singh, M., Sharma, N. K., Prasad, S. B., Yadav, S. S., Narayan, G., & Rai, A. K. (2013). The freshwater cyanobacterium *Anabaena doliolum* transformed with ApGSMT-DMT exhibited enhanced salt tolerance and protection to nitrogenase activity, but became halophilic. *Microbiology*, *159*(Pt_3), 641–648.

Singh, S. C., Sinha, R. P., & Häder, D.-P. (2002). Role of lipids and fatty acids in stress tolerance in cyanobacteria. *Acta Protozool*, *41*, 297–308.

Singh, S. P., Häder, D.-P., & Sinha, R. P. (2010). Cyanobacteria and ultraviolet radiation (UVR) stress: Mitigation strategies. *Ageing Research Reviews*, *9*(2), 79–90.

Sinha, R. P., Klisch, M., Gröniger, A., & Häder, D.-P. (2001). Responses of aquatic algae and cyanobacteria to solar UV-B. *Plant Ecology*, *154*(1–2), 221–236.

Sleator, R. D., & Hill, C. (2002). Bacterial osmoadaptation: the role of osmolytes in bacterial stress and virulence. *FEMS Microbiology Reviews*, *26*(1), 49–71.

Solomon, S., Plattner, G.-K., Knutti, R., & Friedlingstein, P. (2009). Irreversible climate change due to carbon dioxide emissions. *Proceedings of the National Academy of Sciences*, *106*(6), 1704–1709.

Su, H.-Y., Chou, H.-H., Chow, T.-J., Lee, T.-M., Chang, J.-S., Huang, W.-L., & Chen, H.-J. (2017). Improvement of outdoor culture efficiency of cyanobacteria by over-expression of stress tolerance genes and its implication as bio-refinery feedstock. *Bioresource Technology*.

Su, H.-Y., Lee, T.-M., Huang, Y.-L., Chou, S.-H., Wang, J.-B., Lin, L.-F., & Chow, T.-J. (2011). Increased cellulose production by heterologous expression of cellulose synthase genes in a filamentous heterocystous cyanobacterium with a modification in photosynthesis performance and growth ability. *Botanical Studies*, *52*(3), 265–275.

Tan, X., Luo, Q., & Lu, X. (2016). Biosynthesis, biotechnological production, and applications of glucosylglycerols. *Applied Microbiology and Biotechnology*, *100*(14), 6131–6139.

Thomas, D. J., Avenson, T. J., Thomas, J. B., & Herbert, S. K. (1998). A cyanobacterium lacking iron superoxide dismutase is sensitized to oxidative stress induced with methyl viologen but is not sensitized to oxidative stress induced with norflurazon. *Plant Physiology*, *116*(4), 1593–602.

Thomas, D. J., Thomas, J. B., Prier, S. D., Nasso, N. E., & Herbert, S. K. (1999). Iron superoxide dismutase protects against chilling damage in the cyanobacterium *Synechococcus* species PCC7942. *Plant Physiology*, *120*, 275–82.

Ungerer, J., Tao, L., Davis, M., Ghirardi, M., Maness, P.-C., Yu, J., & Ogawa, T. (2012). Sustained photosynthetic conversion of CO2 to ethylene in recombinant cyanobacterium *Synechocystis* 6803. *Energy & Environmental Science*, *5*(10), 8998.

Wang, B., Wang, J., Zhang, W., & Meldrum, D. R. (2012). Application of synthetic biology in cyanobacteria and algae. *Frontiers in Microbiology*, *3*, 344.

Wen, X., Gong, H., & Lu, C. (2005). Heat stress induces an inhibition of excitation energy transfer from phycobilisomes to photosystem II but not to photosystem I in a cyanobacterium *Spirulina platensis*. *Plant Physiology and Biochemistry*, *43*(4), 389–395.

Wilcox, J. (2014). Grand challenges in advanced fossil fuel technologies. *Frontiers in Energy Research*, *2*, 47.

Yao, L., Qi, F., Tan, X., & Lu, X. (2014). Improved production of fatty alcohols in cyanobacteria by metabolic engineering. *Biotechnology for Biofuels*, *7*(1), 94.

Yoshino, T., Liang, Y., Arai, D., Maeda, Y., Honda, T., Muto, M., … Tanaka, T. (2015). Alkane production by the marine cyanobacterium *Synechococcus* sp. NKBG15041c possessing the α-olefin biosynthesis pathway. *Applied Microbiology and Biotechnology*, *99*(3), 1521–1529.

Zeeshan, M., & Prasad, S. M. (2009). Differential response of growth, photosynthesis, antioxidant enzymes and lipid peroxidation to UV-B radiation in three cyanobacteria. *South African Journal of Botany*, *75*(3), 466–474.

Zhou, J., & Li, Y. (2010). Engineering cyanobacteria for fuels and chemicals production. *Protein & Cell*, *1*(3), 207–210.

Zhou, Y. J., Buijs, N. A., Zhu, Z., Qin, J., Siewers, V., & Nielsen, J. (2016). Production of fatty acid-derived oleochemicals and biofuels by synthetic yeast cell factories. *Nature Communications*, *7*, 11709.

CHAPTER 4.

Superoxide Reductase from Thermophilic Archaeon *Pyrococcus furiosus* Improves Tolerance to Abiotic Stress in the Cyanobacterium *Synechococcus elongatus* PCC 7942

Rebecca L. Kitchener

4.1 Abstract

Chemical production in cyanobacteria represents a promising avenue for sustainable replacement of a diminishing fossil fuel supply. Cyanobacteria have been engineered to produce a variety of industrial chemicals and fuel components. They can utilize atmospheric CO_2 as their sole carbon source (potentially reducing harmful greenhouse gases) and have minimal nutrient requirements compared to other biofuel-producing microbes. The economic impact of cyanobacterial bio-production systems can be maximized while minimizing environmental impact by culturing the organisms in outdoor photobioreactors with seawater or waste water as the growth medium. A potential technical roadblock to outdoor culturing is abiotic stress, since these organisms are potentially exposed to temperature fluctuations, UV radiation, high irradiance and high salinity. In addition, many of the chemicals produced in cyanobacteria have anti-microbial qualities and can damage the host cells as concentrations increase. Exposure to these stress conditions cause detrimental effects to not only cellular growth and function, but can significantly limit production titers. One potential solution to this issue is to increase cyanobacterial tolerance to abiotic stress. A common consequence across all sources of abiotic stress is intracellular accumulation of reactive oxygen species, which can damage cell structures and disrupt metabolism. By expressing an antioxidant enzyme (superoxide reductase, or SOR) from thermophilic *Pyrococcus furiosus*, in *Synechococcus elongatus* PCC 7942, we have shown that tolerance to several abiotic stressors can be improved by augmenting ROS scavenging capabilities. This research expands on a novel strategy for stress mitigation, already successful at improving stress tolerance in plants, that could increase potential yield from cyanobacterial biofactories.

4.2. Introduction

Cyanobacteria are photosynthetic prokaryotes capable of utilizing carbon dioxide (CO_2) as a nutrient source. They are easily genetically manipulated to become producers of industrial chemicals, next-generation biofuels, and aviation fuels (Dunlop, 2011). This avenue of chemical production simultaneously offers a source of sustainable replacements for diminishing fossil fuel reserves, and a way to reduce harmful greenhouse gas emissions (Nozzi et al., 2013). The benefits of chemical production in cyanobacteria stand to be maximized if they can be cultivated using seawater or waste water in outdoor photobioreactors located in hot, dry climates as this eliminates competition for fresh water or arable land needed for food crops and decreases overhead costs of maintaining facilities in which to house growth systems (Su et al., 2017). For this production platform to become a reality, cyanobacteria must demonstrate enhanced tolerance to temperature fluctuations, high intensity light, UV radiation, high salinity and, if they are to be producers of commodity chemicals, solvents (Kitchener et al., 2017). Each of these abiotic stressors can negatively impact cellular growth and function, and induce formation of reactive oxygen species (ROS) through a variety of pathways within the cell (Mittler et al., 1991).

During normal metabolism, reactive oxygen species (ROS) such as superoxide ($O_2^{\bullet -}$), singlet oxygen ($^1O_2$), hydrogen peroxide (H_2O_2), and the hydroxyl radical ($\bullet OH$), are produced at low levels as redox by-products and serve primarily as signaling molecules inducing the antioxidant ROS mitigation response (He & Häder, 2002). In photosynthetic organisms, molecular oxygen is constantly reduced to singlet oxygen and superoxide as by-products of oxygenic photosynthesis, specifically by the Mehler reaction, in photosystem I (PSI) (Pinto et

al., 2003). Basal ROS levels are strictly regulated by a delicate balance of ROS production and ROS scavenging by both enzymatic and non-enzymatic systems. Antioxidant enzymes such as superoxide dismutases (SODs), catalase, and peroxidase work in concert with non-enzymatic antioxidant compounds including ascorbate, glutathione, compatible solutes such as free proline or glucosylglycerol, and accessory pigments such as carotenoids to prevent and manage deleterious effects of ROS buildup (Latifi et al., 2009).

Abiotic stress such as fluctuations in temperature or light intensity, UV-B exposure, increased salinity, intracellular solvent buildup, heavy metal exposure, or any combination of these can lead to production and accumulation of ROS in the cell which subsequently induces cellular antioxidant response. If stress conditions persist, ROS can reach toxic levels that can overwhelm stress response systems and ultimately lead to cell death. ROS can directly affect cells by damaging proteins (e.g., degradation and enzymatic inactivation), lipids (e.g., peroxidation), and DNA (e.g., lesions and strand breaks), and can indirectly adversely affect photosynthetic organisms by inhibiting photosystem II (PSII) repair, disrupting electron flow through PSI, or degrading chlorophyll thereby reducing overall photosynthetic efficiency (He, Häder, et al., 2002; Murata et al., 2007).

Superoxide is a strong oxidizing agent. It contains an unpaired electron making it highly reactive, and can disrupt iron-sulfur clusters necessary for cellular enzyme function. This process renders these iron-sulfur containing enzymes inactive, disrupting cellular metabolic processes and releasing free iron into the cell which can undergo Fenton chemistry and generate the extremely toxic hydroxyl radical (Imlay, 2003). The superoxide dismutase enzyme in aerobes catalyzes the simultaneous reduction and oxidation of superoxide and

hydrogen peroxide into O_2 and water. While no external reducing equivalents are needed for this reaction, the molecular oxygen produced can easily be reduced to form more superoxide (Sheng et al., 2014). Another enzyme capable of detoxifying superoxide is superoxide reductase (SOR). SOR was initially thought to have evolved in anaerobic organisms because it reduces superoxide to H_2O_2 without forming molecular oxygen. SOR has since been found to be present in both anaerobes and aerobes, and across all three domains of life. Following reduction of superoxide, SOR must be re-reduced in order to be reactivated, and therefore was thought to be co-expressed *in vivo* with rubredoxin, a known electron donor to SOR. SOR has been shown to be able to utilize electrons from other sources, making it possible for it to be heterologously expressed utilizing basic cloning strategies (Sheng et al., 2014).

Expression of SOR from *P. furiosus* in Arabidopsis and ornamental dogwood has been shown to improve tolerance to heat (Geng et al., 2016; Im et al., 2005). When expressed heterologously, SOR forms a complex with ferrocyanide in which superoxide can be reduced completely to water without accumulation of H_2O_2 (Molina-Heredia et al., 2006). *P. furiosus* SOR is extremely thermostable, with a functional temperature range of 4°C to 100°C, and is catalytically superior to SOD in that it has a higher affinity for superoxide (Jenney et al., 1999).

In this research, we have expressed *P. furiosus* SOR in the model cyanobacterium *S. elongatus* PCC 7942 with the goal of augmenting its abiotic stress tolerance. We hypothesized that constitutive expression of SOR would provide protection against environmental stressors by limiting basal ROS levels and dampening detrimental effects of ROS accumulation. Successful ROS control by SOR establishes it as a viable option for improving stress tolerance

in biofuel- or chemical-producing cyanobacteria, and in addition could support diversified culturing conditions for bio-production applications.

4.3. Materials and Methods

4.3.1. Bacterial strains and media

Cyanobacterial species *Synechococcus elongatus* PCC 7942 and the pSyn_6 expression vector were supplied in the GeneArt™ *Synechococcus* Protein Expression Kit by Life Technologies (Carlsbad, CA, USA). Cloning and vector construction were initially carried out in *E. coli* TOP10 cells from Invitrogen, grown in Luria-Bertani (LB) media or plated on LB agar supplemented with 100 µg/ml spectinomycin. All cyanobacterial cultures were grown in 1X BG-11 media from Life Technologies supplemented with 25 mM sodium bicarbonate ($NaHCO_3$) and 10 µM $FeSO_4$ in addition to atmospheric CO_2, and 10 µg/ml spectinomycin for selection.

The *egfp:sor* construct was originally created for expression in *Nicotiana tabacum* (NT1) cells by amplifying the coding region of *sor* from *P. furiosus*, cloning it into a pENTR Gateway entry vector (Invitrogen/Life Technologies, Carlsbad, CA, USA) and ultimately into the pK7FWG2 destination vector where the 389 bp *sor* gene became fused to a 720 bp *egfp* N-terminal fluorescent tag for expression in plants (Im et al., 2005).

4.3.2. Construction of the modified pSyn_6 (mod_pSyn_6) cyanobacterial expression vector

To maximize expression of the *sor* and *egfp*:*sor* genes in *S. elongatus* PCC 7942, some modifications were made to the pSyn_6 expression vector. A 51-bp region flanked by

recognition sites for the restriction enzymes *Nde*I and *Hin*dIII was excised by restriction digest in order to increase the proximity of the *egfp:sor* gene to a ribosome binding site sequence located at the 3' end of the *psb*A1 promoter region in order to ensure efficient mRNA translation. In order to circularize the vector prior to insertion of the *egfp:sor* gene, blunt ends were created from the 5' overhangs left behind following digestion with *Nde*I and *Hin*dIII using the Large (Klenow) Fragment of DNA Polymerase I from NEB which has 3'-5' exonuclease activity. The vector was ligated and then subsequently digested with *Eco*RI and *Kpn*I to allow for directional cloning of the *egfp:sor* gene.

The modified pSyn_6 vector was then used to transform both *E. coli* TOP10 (for plasmid propagation and storage) and PCC7942 (for all cyanobacterial stress experiments). The presence and sequence fidelity of the *egfp:sor* transgene in both *E. coli* and PCC7942 were confirmed in purified plasmid (*E. coli*) or genomic (PCC7942) DNA using classical PCR with primers specific for the *egfp:sor* gene (forward primer: 5'-TTTTGAATTCATGGTGAGCAAGGGCGAGGA-3', and reverse primer: 5'-TTTTGGTACCTCACTCTAAAGTGACTTCGTTTTCCC-3'), restriction mapping, and DNA sequencing using a forward primer that bound the pSyn_6 vector upstream (5') of the insert (5'-TTTACAACCTCGAAGGAGCG-3'). Sanger sequencing revealed no mutations in the gene aside from a known nucleotide substitution (thymine to guanine) at position 328, which results in a tyrosine to aspartic acid substitution in the enzyme. This missense mutation originally occurred spontaneously in the lab strain of *P. furiosus* that served as the source of the transgenic SOR and was not known to cause any deleterious effects in enzyme function (Im et al. 2009).

4.3.3. Confirmation of expression and function of EGFP:SOR

To prepare the insoluble and soluble fractions for SDS-PAGE and Western blot analysis, 10 ml cultures of the four initial cell lines (WT *S. elongatus* PCC 7942, PCC 7942 transgenic lines containing either empty mod pSyn_6 vector as a true negative control, SOR alone, or EGFP:SOR fusion protein) were grown under optimal conditions and allowed to reach mid-logarithmic growth phase. The cultures were then diluted to an optical density of 0.5 (as measured by absorbance at 750 nm), pelleted by centrifugation, and re-suspended in phosphate-buffered saline, pH 7.4. Half of the cell slurry was dissolved with a sample buffer of 2X Laemmli buffer containing SDS and ß-mercaptoethanol and boiled for 10 min to prepare the insoluble fraction. To prepare the soluble fraction, the remaining half of the cell slurry was lysed by further dilution with B-PER™ (Thermo Scientific, Waltham, MA, USA) followed by vortex mixing with 0.1 mm glass beads for three minutes. The lysate was then centrifuged to remove cell debris, 2X sample buffer was added, and the sample was boiled for 10 min. Purified SOR was run as a positive control for antibody recognition. Both soluble and insoluble extracts for all three strains and the positive control were electrophoresed through 12% TGX polyacrylamide gels from Bio-Rad (Hercules, CA, USA) and subsequently transferred to a PVDF membrane using the TransBlot® Turbo™ semi-dry blotting system also from Bio-Rad.

The membrane was then blocked in a solution of tris-buffered saline with Tween 20 (TBS-T) and 5% solution of non-fat milk. The membrane was probed first with antibodies raised against SOR in rabbits (Cocalico Biologicals, Inc., Reamstown, PA, USA) at a 1:10,000 dilution in TBS-T/milk, and then a conjugated secondary antibody (goat anti-rabbit conjugated

with horseradish peroxidase, Thermo Fisher Scientific, Waltham, MA, USA) at a 1:15,000 dilution in TBS-T. The blot was visualized using Clarity Western ECL Substrate from Bio-Rad and imaged by exposure to X-Ray film for 1 min.

EGFP:SOR (hereafter referred to as SOR) activity was determined by a standard indirect activity assay for superoxide dismutase by which superoxide is generated in the assay mix by the reaction of xanthine oxidase with xanthine. Superoxide reduces cytochrome *c* which yields a colorimetric product that absorbs light at 550 nm. Cytochrome *c* in the assay mix competes with the enzyme (either SOD, SOR, or both) for superoxide causing a quantifiable decrease in reduction of cytochrome *c* by O_2^- which can then be measured spectrophotometrically (McCord et al., 1969). 5 ml cultures of each strain growing logarithmically (day 4 or 5) under optimal conditions were pelleted by centrifugation, re-suspended in 1.5 ml B-PER™, and mixed by vortex for three min. The lysate was centrifuged to remove cellular debris, and the supernatant was diafiltered into the assay buffer (0.05 M potassium phosphate buffer, pH 7.8 containing 0.1 mM EDTA) using Amicon® Ultra Centrifugal Filters from Millipore (4 ml volume, 3K MWCO) at 4 °C to remove any contaminating detergent and metal (Im et al., 2009).

The assay mix consisted of 10 µM ferricytochrome *c* from horse heart, 50 µM xanthine, and enough xanthine oxidase (all from Sigma-Aldrich, St. Louis, MO, USA) to produce a rate of reduction of cytochrome *c* of 0.025 absorbance units per min, measured on a UV-2401PC UV-Vis Recording Spectrophotometer (Shimadzu, Kyoto, Kyoto Prefecture, JP) at 25°C. Lysates containing SOR and/or endogenous SOD were added to the reaction mix until a 50% decrease in the rate of formation of reduced cytochrome *c* was observed (a rate of 0.0125 ±

0.0025 absorbance units per min). One unit of SOR/SOD activity was defined as the amount of enzyme (units per mg of protein) that inhibits the rate of cytochrome *c* reduction by 50% (A_{550} measured over 120 s). In our strains, SOR was co-expressed with the endogenous SOD meaning there was no way to specifically pinpoint SOR activity independent of SOD without heat treating the lysates which would have denatured the EGFP, damaged the integrity of the fusion protein, or potentially altered the conformation of the active site. Because of this, both wild-type PCC 7942 and the empty vector control were run as assay controls to determine endogenous SOD activity assumed to be at basal levels since cultures were grown under optimal conditions, had reached mid-log phase, and had not been exposed to any environmental stressors. Any increase in SOR/SOD activity beyond basal levels was attributed to a functional SOR in the transgenic lines. Total protein concentrations of all extracts were determined using the Bicinchoninic Acid (BCA) Protein Assay Kit from Pierce (Waltham, MA, USA) with a 7-point bovine serum albumin (BSA) standard curve.

4.3.4. Establishment of optimal growth conditions and parameters for monitoring culture growth

Liquid cultures of PCC 7942 have been shown to grow optimally at 33 ℃ in BG-11 media with agitation under constant cool fluorescent light at anywhere between 50-120 µmol photons m^{-2} s^{-1} with either atmospheric or added carbon (in the form of CO_2 gas or bicarbonate supplementation in growth media) (Invitrogen by Life Technologies, 2013; Kuan et al., 2015;). Unless otherwise stated, the cultures used for these experiments were grown on orbital shakers in a Precision Plant Growth Chamber from Thermo Scientific™ at 33 ℃ under constant cool

fluorescent light provided by two 48-inch T12 fluorescent tubes (from GE) providing approximately 50-100 µmol photons m^{-2} s^{-1} as measured with a MultiSpeQ beta instrument (Kuhlgert et al., 2016). All cultures used in the study were grown in plastic cell culture flasks (25 cm^2) with vented caps to maximize light exposure and minimize evaporation.

4.3.5. Parameters for monitoring culture growth

Culture densities were determined under optimal growth conditions by measuring absorbance at 750 nm (optical density, OD_{750}) of the cultures using an Eon 96-well plate reader (BioTek Instruments, Inc; Winooski, VT). To validate optical density against cell counts, WT cultures were grown for 7 days under optimal conditions (n=4); each day, OD_{750} was measured, and cells were counted in a Neubauer Improved hemocytometer. Average cell densities were plotted against OD_{750}, and the resulting linear equation was applied to OD values as a correction factor to calculate cells/ml in all cultures.

Chlorophyll a content was measured using a modified protocol from Meeks and Castenholz (1971). In this method, methanol was used to extract chlorophyll a from pelleted cells followed by quantitation of absorbance at 665 nm. An extinction coefficient of 79.95 $L \cdot g^{-1} \cdot cm^{-1}$ for chlorophyll a in methanol was used to calculate concentration (Meeks et al., 1971; Porra et al., 1989). Briefly, 250 µl aliquots were taken from each culture at designated time points, pelleted by centrifugation, and the supernatant discarded. Pellets were re-suspended in 250 µl methanol, heated for 5 min at 65°C in the dark, and then incubated in the dark for another 5 min at room temperature. Samples were again pelleted by centrifugation, 200 µl of supernatant was loaded into a 96-well UV microplate, and absorbance was read at 665 nm

using an Eon 96-well plate reader (BioTek Instruments, Inc; Winooski, VT). After subtracting background absorbance from a methanol blank, and multiplying by a correction factor of 1.8 (determined independently to account for the difference in pathlength for methanol versus water), the corrected A_{665} value was divided by the converted extinction coefficient of 12.5 $ml \bullet \mu g^{-1} \bullet cm^{-1}$ and the number of cells per ml. Chlorophyll a was calculated in µg/cell, and then reported as $ng/10^6$ cells.

To fully characterize PCC 7942 growth under these conditions, growth studies were carried out for 28 days. Generation times (in h) were determined using linear regression analysis in GraphPad Prism software to determine the slope of the linear portion of logarithmic growth phase, and then dividing the natural log of 2 by the slope (or growth rate, k) (ln 2/k).

4.3.6. Growth inhibition studies

To determine the effects of oxidative stress on the overall growth of our PCC7942 strains, abiotic stress conditions were generated in the cultures in several ways. Superoxide was produced in the cytosol by the addition of paraquat at varying concentrations (0.25 µM up to 1.0 µM). To confirm localized expression of SOR in the cytosol, cultures were exposed to norflurazon, another herbicide, at concentrations of 0.1 µM – 5.0 µM. Cultures were exposed to UVB radiation by suspending a low-intensity UVB lamp (18-inch, T8 fluorescent bulb, approximately 100 Microwatts UVB, from Zilla®; Franklin, WI) directly over the flasks for the duration of the study. To examine salt tolerance, NaCl was added to cultures at 2%, 3%, or 3.5% w/v. Solvent tolerance was assessed with both isopropanol (1 g/L, 2.5 g/L, 5 g/L, and 7.5

g/L) and 2-butanol (1 g/L, 2.5 g/L, and 5 g/L) added to the growth media. Heat exposure studies were carried out at both 42°C and 45°C.

In all cases, cultures were grown to mid-log phase (OD_{750} of 0.75 – 1.2) and were then diluted in growth media to an OD_{750} representative of early log phase (0.5 ± 0.05) and aliquoted into three or four identical replicates prior to stress induction. Samples were taken immediately prior to stress induction (t = 0 h) and then at 6 h, 12 h, 24 h, and 48 h following exposure, unless otherwise stated. Aside from the stressor, cultures were grown under otherwise optimal conditions. In all cases, with the exception of heat exposure, unstressed cultures were included in each study for comparison. For all sample time points, culture densities and chlorophyll a content were measured. Generation times were calculated as described previously.

4.3.7. Measurement of PSII photoinhibition

To quantify photoinhibition of PSII in both strains due to oxidative stress, maximum photosynthetic efficiency of PSII was measured using a PAM2000 Chlorophyll Fluorometer (Heinz Walz GmbH, Effeltrich, DE). The maximum quantum efficiency of PSII was measured at designated time points during both paraquat and UVB exposure by loading 200 µl of each culture into a black 96-well microplate (n = 5 for each culture), covering the plate with an aluminum plate seal, and allowing the samples to equilibrate to darkness for 15 min. A pipette tip was used to puncture the foil over each well at the time of the reading. A dark-adapted read was taken first (F_0) which measures the chlorophyll fluorescence when all PSII reaction centers are fully open and there is no non-photochemical quenching (NPQ) taking place (Murchie et al., 2013). Following this, a saturating pulse of actinic light was delivered causing the reaction

centers to close and giving a maximum fluorescence value (F_m). The ratio of the change in fluorescence ($F_m - F_0$, or variable fluorescence, F_v) to F_m itself is indicative of the maximum quantum yield of PSII and can reveal decreased yield due to damage or quenching.

4.3.8. Quantitation of oxidative stress biomarkers

4.3.8.1. Intracellular ROS content (DCFH-DA assay)

A method modified from Hakkila et al. (2014) in which 2', 7'-dichlorodihydrofluorescein diacetate (DCFH-DA) - a cell-permeant fluorogenic dye - was used to estimate cellular ROS content. Upon diffusion into the cell, DCFH-DA is deacetylated by cellular esterases and becomes non-fluorescent DCFH. DCFH is then oxidized by intracellular ROS and peroxides into the highly fluorescent 2', 7'-dichlorofluorescein (Hakkila et al., 2014; Rastogi et al., 2010). In our assay, 1 ml culture aliquots were taken at each time point, pelleted by centrifugation, and re-suspended in 50 mM sodium phosphate buffer, pH 7.2. 500 µl of re-suspended cells were transferred to amber tubes and 2 mM DCFH-DA (Sigma Aldrich, ST. Louis, MO, USA) in ethanol was added to a working concentration of 25 µM. Both 500 µl aliquots (stained and unstained) were incubated in the dark at 37°C for 45 min.

The unstained cells were loaded directly into a black 96-well fluorescence microplate in duplicate (200 µl per well). The stained cells were pelleted by centrifugation, re-suspended in 500 µl fresh phosphate buffer to remove any free dye left in solution, and loaded into the same microplate in duplicate (200 µl per well). The plate was then read using a SynergyHT fluorescence plate reader (BioTek Instruments, Inc., Winooski, VT, USA). To detect DCF signal and background from the unstained cells, the wells were exposed to an excitation

wavelength of 485 nm and the emission signal was recorded at 535 nm in relative fluorescence units (RFU).

To account for interference from chlorophyll fluorescence (autofluorescence), the wells were again exposed to an excitation wavelength of 485 nm but emission (in RFU) was instead recorded at 680 nm. Stained and unstained RFU values were normalized against autofluorescence, then unstained background signal was subtracted from stained signal and the replicates were averaged. Finally, that value was divided by the number of cells/ml in the culture to report estimated intracellular ROS content in RFU per million (10^6) cells.

4.3.8.2. Quantitation of intracellular free proline via UPLC™

Intracellular free proline, a known ROS scavenger, was quantified using ultra performance liquid chromatography (UPLC™) and the AccQ-Tag™ Ultra pre-column derivatization method (Fiechter et al., 2011; Waters Corporation, 2014). At each time point, 10 ml culture aliquots were pelleted by centrifugation and re-suspended in 1.5 ml of 100 mM borate buffer, pH 8.8. Cells were lysed with a Mini-Bead Beater-16 from BioSpec Products (Bartlesville, OK, USA) and 0.1 mm silica beads. 80 µl of clarified lysate was then added to 20 µl of derivatizing reagent (6-aminoquinolyl-N-hydroxysuccinimidyl carbamate, AQC) in glass Total Recovery Vials (Waters Corporation, Milford, MA, USA), and the samples were heated for 10 min at 55°C to label the amine functional group on the amino acids with a chromophore which enabled UV detection at 260 nm. A 7-point standard curve was prepared using Amino Acid Hydrolysate Standard (Waters Corporation, Milford, MA, USA; P/N

WAT088122), a mixture of 21 amino acids ranging from 12.5 pmol/µl to 0.195 pmol/µl that was derivatized as described above.

Separation of free amino acids was performed using reversed phase chromatography on an AccQ-Tag Ultra C18, 1.7 µm, 2.1 mm x 100 mm column heated to 53.5°C and an Acquity UPLC™ system (both from Waters Corporation, Milford, MA, USA). Single injections (1.0 µl) from multiple experimental replicates (n=3) were performed over 30 min runs. Proline data were collected in Empower® software based on an expected retention time of 5.5 – 6 min for proline, and analyzed against the standard curve in Microsoft Excel. Results were reported in ng free proline per million (10^6) cells. For one run, seven additional amino acids (lysine, threonine, alanine, valine, isoleucine, leucine, and tryptophan) were quantified as well to examine if there were any trends in overall intracellular free amino acid concentrations.

Table 4-1. Mobile phase composition for amino acid analysis on the Acquity UPLC™ System (Waters Corp., Milford, MA, USA)

Mobile Phase	Reagent Name	Formulation
A	Waters AccQ-Tag Ultra Eluent A	Acetonitrile (ACN)/formic acid (proprietary formulation), diluted 1:10 in DI H_2O
B	Waters AccQ-Tag Ultra Eluent B	Acetonitrile (proprietary formulation)

Table 4-2. Gradient used for separation of free amino acids on the Acquity UPLC™ System (Waters Corp., Milford, MA, USA). From (Waters Corporation, 2014).

Time (min)	% Mobile Phase B	Flow Rate (ml/min)
0.00	0.1	0.7
0.54	0.1	0.7
5.74	9.1	0.7
7.74	21.2	0.7
8.04	59.6	0.7
8.05	90.0	0.7
8.64	90.0	0.7
8.73	0.1	0.7
9.50	0.1	0.7

4.3.8.3. Analysis of lipid peroxidation (TBARS assay)

Lipid peroxidation was determined using a method for quantifying thiobarbituric acid reactive substances (TBARS) modified from (Buege et al., 1978). Malondialdehyde (MDA) is a degradant of polyunsaturated fatty acids that reacts with thiobarbituric acid (TBA). The reaction forms a colorimetric product that can be detected spectrophotometrically by reading absorbance at 535 nm.

20 ml culture aliquots were taken at each time point and pelleted by centrifugation. Cell pellets were lysed in 1 ml of 150 mM KCl using the Mini-Bead Beater-16 from BioSpec Products (Bartlesville, OK, USA). The reaction mixture consisted of 500 µl of clarified supernatant and 1 ml of detection reagent (0.375% TBA, 7.5% trichloroacetic acid, 0.25 N HCl). A 7-point standard curve (50 µM – 0.78 µM) was prepared by diluting MDA standard (Cayman Chemical, Ann Arbor, MI, USA) in 150 mM KCl, and mixing 500 µl of each standard

with 1 ml of detection reagent. A reagent blank containing only 150 mM KCl and detection reagent was also prepared. Samples and standards were boiled for 15 min, centrifuged for 10 min at 10,000 x g, and the supernatant was then loaded into a 96-well UV microplate in triplicate (200 µl per well) and absorbance at 535 nm was read on a Synergy4 plate reader (BioTek Instruments, Inc., Winooski, VT, USA). Protein concentrations were assessed using the Micro-Bicinchoninic Acid Assay (Micro BCA Assay) with a 7-point standard BSA standard curve from Pierce (Waltham, MA, USA). Lipid peroxidation was ultimately reported as nmol MDA per milligram of protein.

4.4. Results & Discussion

4.4.1. Functional EGFP:SOR is expressed in transgenic S. elongatus PCC 7942.

The pSyn_6 vector offers several features which made it favorable to use for these experiments. Figure 4-1 shows a map of the modified pSyn_6 vector that was created to maximize SOR expression in PCC 7942. Prior to the insertion of the *egfp:sor* gene, a 51 bp region of the multiple cloning site was excised, and the vector was repaired via blunt-end ligation. The purpose of the modification was to maximize the potential for translation by positioning the *egfp:sor* gene, flanked by restriction enzyme recognition sequences for E*co*RI (5'-GAATTC-3') and *Kpn*I (5'-GGTACC-3'), so that the start ATG for *egfp:sor* was as near as possible (24 bp) to the ribosome binding site nucleotide sequence (5'-GAAGGAG-3') in the expression vector. The pUC origin of replication allowed for high copy number replication of the plasmid when expressed in *E. coli*. Per kit recommendations, the pSyn_6-*egfpsor* construct was used to transform *E. coli* TOP10 cells, which are *rec*A and *end*A deficient

making them appropriate for long-term vector storage. The presence of a spectinomycin resistance gene and promoter allowed for selection of positive clones and ensured presence of the *egfp:sor* gene in both *E. coli* and PCC7942 when plated on or grown in media containing spectinomycin (100 µg/ml for *E. coli* and 10 µg/ml for PCC 7942). Additionally, the pSyn_6 plasmid is unable to replicate in PCC7942, so selecting for antibiotic resistance ensures a successful recombination event.

Like many cyanobacteria, PCC 7942 is naturally competent, meaning it can take up foreign DNA from its surrounding environment and incorporate it into its genome provided the DNA is flanked by neutral sites that share homology with the genome (Shestakov et al., 1970). When incubated together, the neutral sites (NS1a and NS1b) on pSyn_6 allowed for both the *egfp:sor* gene and the spectinomycin resistance gene to homologously recombine with the PCC 7942 genome. The *psbA* promoter from *S. elongatus* PCC 7942 encodes the D1 protein responsible for continuous repair of PSII photodamage and is activated by light exposure (Nair et al., 2001). Growing transgenic cultures under constant light (instead of a diurnal cycle) ensured consistent, high level expression of *egfp:sor*.

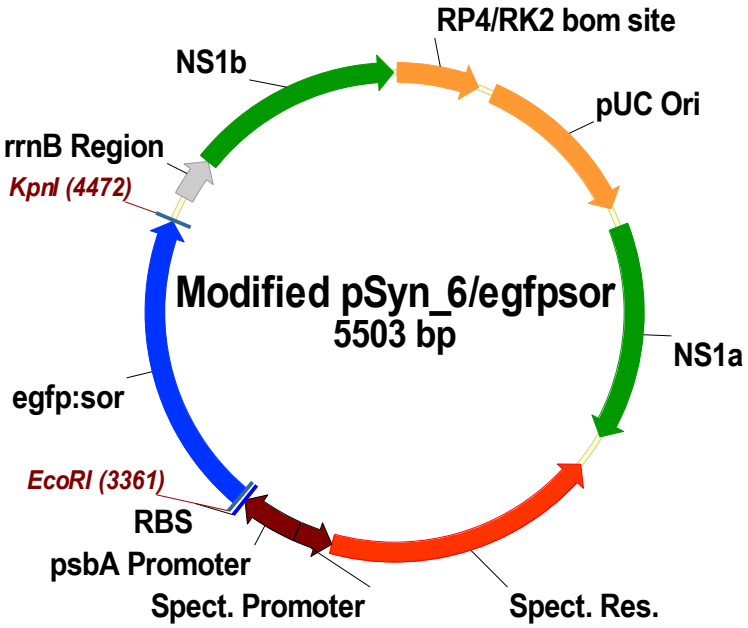

Figure 4-1. Map of the 5,503 bp modified pSyn_6 vector. The vector was designed to maximize SOR translation by increasing proximity of the *egfp:sor* gene to the ribosome binding site sequence. Modified from Life Technologies *Synechococcus* Protein Expression kit instructions (Invitrogen by Life Technologies, 2013).

Presence and integrity of the *egfp:sor* transgene was confirmed by PCR screening, restriction mapping, and Sanger sequencing. Figure 4-2a shows the expected 1.1 kb PCR product generated in the SOR-producing strain, which is absent from the wild type and empty vector control strains when purified genomic DNA was amplified with primers specific for *egfp:sor*. Lane 1 contains the GeneRuler 1 kb Plus DNA Ladder (Thermo Scientific, Waltham, MA, USA). Lane 2 is the no-template control containing only water, PCR master mix and primers. Lane 3 is the *egfp:sor* positive control with a single visible band at 1.1 kb. Lanes 4 and 5 contain WT PCC 7942 and PCC 7942 transformed with empty mod_pSyn_6 vector, respectively. Lane 6 contains PCC 7942 transformed with *egfp:sor* in mod_pSyn_6 also displaying a single band at 1.1 kb.

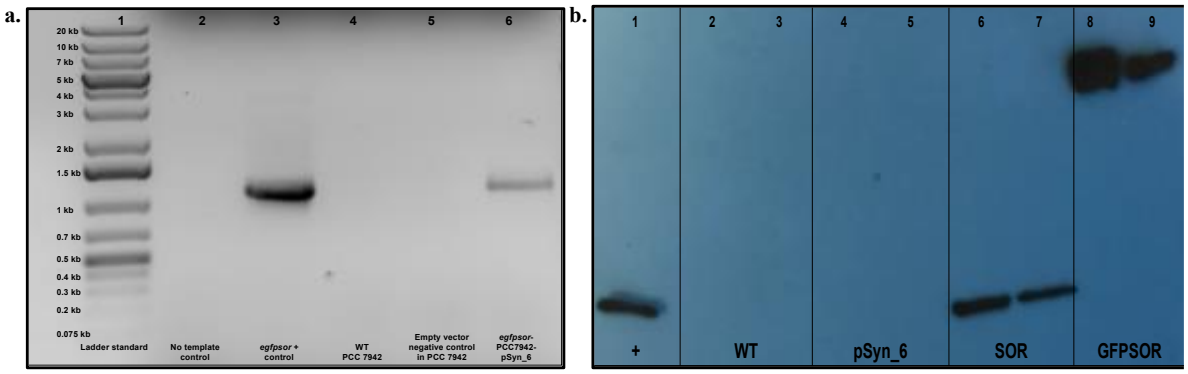

Figure 4.2. Confirmatory gel images of the *egfp:sor* PCR product and EGFPSOR fusion protein. **a)** Image of 1% agarose gel containing PCR products generated with *egfp:sor* primers. **b)** Immunoblot (Western blot) analysis of PCC 7942 extracts probed with monoclonal antibody raised in rabbit against SOR.

The immunoblot results presented in Figure 4-2b confirm the presence of the SOR protein in the transgenic cellular extracts. Lane 1 contains a positive control for antibody specificity (purified SOR, not fused to EGFP, at 1.5 µg/ml) displaying a band of the expected size, 14 kDa (ladder not shown, actual band size was determined by overlaying exposed X-ray film on top of the PVDF membrane which contained a pre-stained molecular weight ladder standard). Lanes 2 and 3 contain the insoluble and soluble fractions from wild type *S. elongatus* PCC 7942. Lanes 4 and 5 contain the insoluble and soluble fractions from PCC 7942 transformed with empty mod_pSyn_6 vector, referred to as the empty vector control. Lanes 6 and 7 contain the insoluble and soluble fractions from PCC 7942 expressing SOR (not fused with EGFP), and display bands identical to the positive control at the expected size, 14 kDa. Lanes 8 and 9 contain the insoluble and soluble fractions from PCC 7942 expressing SOR (fused with EGFP) where clear bands are visible at the expected molecular weight for the fusion protein, 42 kDa.

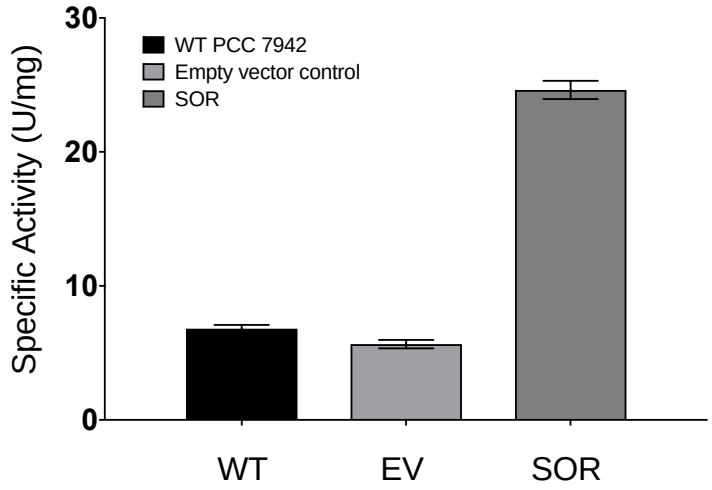

Figure 4-3. SOD/SOR activity in WT and transgenic PCC 7942. Specific activities (in units/mg) of endogenous superoxide dismutase (SOD) in wild type PCC 7942 and the empty vector negative control, as well as activities of SOD and putative SOR co-expressed in the transgenic lines. Average specific activities were: 6.82 ± 0.96 U/mg (wild type PCC 7942), 5.66 ± 1.10 U/mg (empty vector control), and 24.62 ± 2.38 U/mg (SOR). Error bars represent standard error of the mean and assay was run over three separate days for a total of 12 replicates.

Figure 4-3 shows enzyme activity assay results used to confirm functional SOR expression in cyanobacterial lysates. Since both SOD and SOR enzymes act on the same substrate (superoxide) there is no way to selectively assay SOR alone unless: 1) the endogenous *sod* gene has been deleted or 2) the extracts are exposed to a high temperature heat treatment (85°C) prior to the assay. In this study, the goal was to co-express both antioxidant enzymes with the hypothesis that SOR would enhance endogenous ROS detoxification capabilities. While SOR is thermostable and will retain activity following a heat treatment, EGFP will not. A 15-min heat treatment at 85°C causes a 100% loss of activity from the fusion protein, likely due heat-induced aggregation of EGFP altering the conformation of the SOR active site or causing the fusion protein to precipitate from the solution altogether. We therefore

reasoned, due to confirmed presence of the gene in the PCC 7942 genome, confirmed expression of the SOR protein in the soluble and insoluble cellular extracts, and observed phenotype (to be discussed subsequently) that the increased specific activity when SOR is expressed is due to the presence of functional SOR.

It is unknown to what degree the presence of EGFP on the N-terminus of SOR effects the catalytic properties of the enzyme. *P. furiosus* SOR is a 14.4 kDa Class II SOR, meaning that it contains one iron cation in its active site near the C-terminus, and exists *in vivo* as a homotetramer. The active site is surrounded by positively-charged residues to attract or draw-in superoxide. The four SOR monomers are positioned in a cube-like structure with the C-termini and catalytic centers oriented on the outside at each corner which maximizes exposure to and interaction with superoxide in the cytosol (Sheng et al., 2014). We hypothesize that the presence of 27 kDa EGFP on the N-terminus prevents formation of this tetrameric structure, however, whether or not this impacts the kinetic profile of the enzyme remains to be studied.

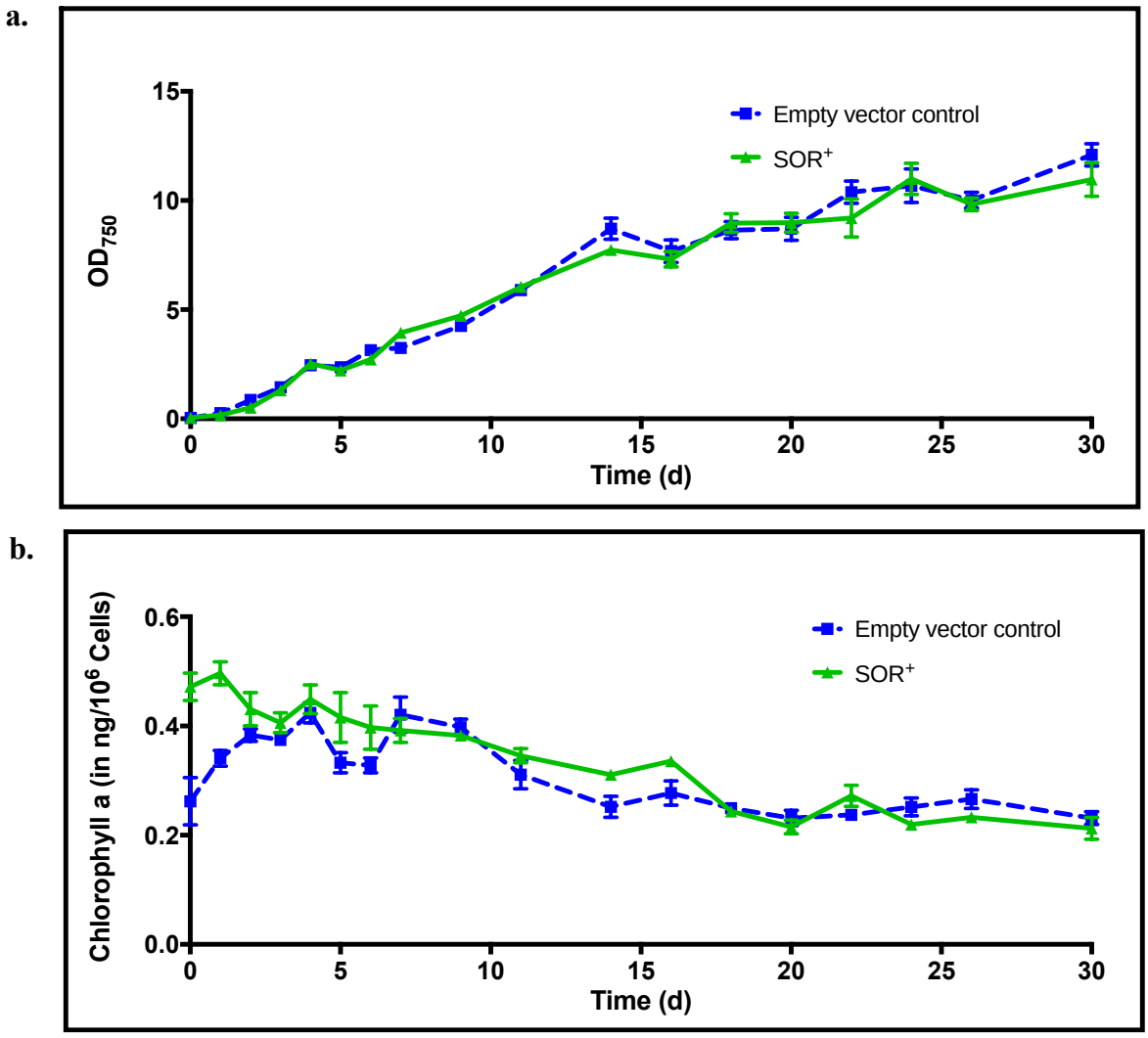

Figure 4-4. 30-day growth curve data for 120 ml cultures of both the empty vector negative control and the SOR^+ cell lines grown under optimal conditions. Optimal conditions were: BG-11 media (with 25 mM $NaHCO_3$ and 10 µM $FeSO_4$), 33°C, constant illumination with cool fluorescent light between 50-120 µmol photons m^{-2} s^{-1}, gentle shaking on orbital rotator. **a)** Culture growth, measured by optical density at 750 nm, and **b)** chlorophyll a content (in ng per one million cells). Error bars represent standard error of the mean, n=4.

Culture densities were measured spectrophotometrically by recording absorbance at 750 nm. Typically, culture density for photosynthetic microorganisms is measured at 750 nm

(near-IR range) instead of the 600 nm used for bacteria so that turbidity, or light scatter, can be assessed without interference from chlorophylls or accessory pigments (Rodrigues et al., 2011). Morphologically, both cell lines appeared identical under a microscope – the cells were smaller during logarithmic growth phase and grow larger as the cultures transition into stationary phase (data not shown). When cultured under optimal conditions, there were no significant differences in growth trends for the empty vector control and the SOR-expressing strains, as seen in Figure 4-4a. SOR expression does not appear to enhance growth, which is consistent with previous SOR experiments performed *in planta* (Im et al., 2009). For both cell lines, logarithmic growth phase occurs during days 1-5 ($OD_{750} \approx 2.0 – 3.0$), after which the cultures enter stationary phase. Although the optical densities for both continue to increase from days 6-30, the growth becomes linear rather than exponential. The addition of 25 mM sodium bicarbonate to the growth medium as an additional carbon source reduced the generation time by nearly 65% as seen in Figure 4-5.

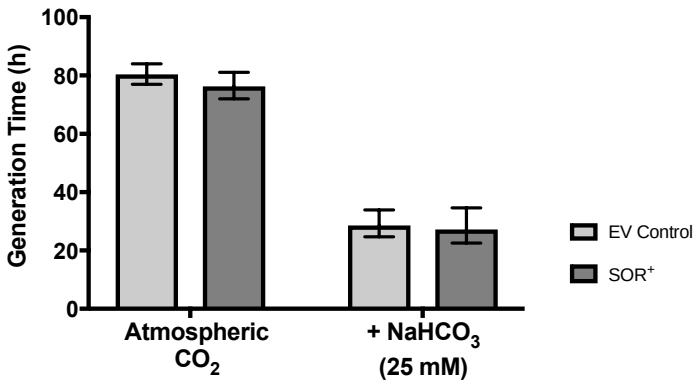

Figure 4-5. Generation times with and without bicarbonate. Empty vector and SOR^+ cultures were grown under optimal conditions with either atmospheric CO_2 as a carbon source, or 25 mM sodium bicarbonate. Actual generation times were: 80.4 h and 28.6 h for empty vector without and with added bicarbonate respectively, and 76.3 h and 27.2 h for SOR^+ without and with added bicarbonate, respectively. Error bars represent standard error of the mean for transformed data, n=4.

The addition of 10 µM $FeSO_4$ to the growth medium did not cause any notable changes in growth rate (data not shown); however, it allowed for a more pronounced SOR phenotype in subsequent stress studies. This is because all known superoxide reductase enzymes contain Fe^{2+} ions in their catalytic sites which become oxidized as superoxide is reduced. When SOR is expressed in a recombinant system without iron supplied in the growth medium, the active site will incorporate Zn^{2+} instead of Fe^{2+} rendering the enzyme inactive (Sheng et al., 2014). While BG-11 contains a small amount of iron in the form of ferric ammonium sulfate (Thermo Fisher Scientific, n.d.), adding 10 µM $FeSO_4$ ensured that the SOR catalytic centers were loaded with the proper metal cation.

A notable phenotype that was observed during this growth study and all subsequent studies is that the SOR line contains more chlorophyll a than the empty vector control during early logarithmic growth (Figure 4.4b). In some studies performed in our lab, the amount of

chlorophyll a per cell was nearly double that of the empty vector line. It is not yet known whether the presence of more chlorophyll increases the photosynthetic efficiency of these cells. No differences were observed in growth patterns for the two strains, and there were no differences in cell size when observed under a microscope, at this time it cannot be inferred that excess chlorophyll in the SOR line confers any obvious advantage. It is possible that the presence of SOR slows or prevents chlorophyll turnover or degradation due to ROS accumulation, but whether this then allows for higher throughput in the photosynthetic electron transport chain, ultimately rendering more reduced NADP (NADPH) available for CO_2, fixation, requires further study. It is also not known whether the cells contain an elevated concentration of accessory pigments compared to the empty vector control as well. Since phycobilins function as light harvesting antennae, absorbing light energy and shuttling it to the chlorophyll in PSI and II, it is possible that the presence of more phycobilins in addition to chlorophyll could indicate higher photosynthetic efficiency. Further analysis of photosynthetic output or carbon fixation (by O_2 probe or radio-labeled carbon, $^{14}CO_2$, respectively); and/or quantitation of accessory pigments such as phycobilins or carotenoids (either spectrophotometrically or via analytical techniques such as HPLC) are necessary to further our understanding of this phenotype.

4.4.2. SOR expression in the cytosol enhances tolerance to chemically-induced ROS in S. elongatus.

In order to confirm that SOR was expressed cytosolically in PCC 7942 as it is in plants, both cell lines were exposed to the herbicide norflurazon (Im et al., 2005). Norflurazon inhibits

carotenoid synthesis in the thylakoid membrane which leads to chlorophyll depletion and then inhibition of photosynthesis (Breitenbach et al., 2001). Ultimately, norflurazon exposure culminates in superoxide formation in the thylakoid membrane from molecular oxygen in the chlorophyll antenna. Since superoxide is negatively charged, it cannot permeate the phospholipid bilayer and cross into the cytosol. If our SOR was indeed present in the cytosol, we did not expect to see resistance to norflurazon exposure in either the empty vector control or the SOR line (Thomas et al., 1998). As expected, norflurazon exposure (at 0.1 µM, 1 µM, and 5 µM for 24 h) led to decreased growth, loss of chlorophyll, and eventual photobleaching in both the empty vector control and the SOR-expressing cell lines (data not shown), therefore we could conclude that SOR expression was limited to the cytosol.

To assess the ROS scavenging capabilities of SOR in PCC 7942 and its protective effects under oxidative stress conditions, the cultures were treated with paraquat at 0.25 µM, 0.5 µM, and 1.0 µM for 48 h. Paraquat is an herbicide that catalyzes the formation of superoxide in the cytosol at sites of electron transfer in PSI, leading to diversion of electrons from the PSI cyclic pathway as it becomes oxidized by molecular oxygen (Fujii et al., 1990). It intercepts PSI electrons, diverting them from reduction of NADP and transfers them to molecular oxygen, reducing it to superoxide. In this study, the empty vector control and SOR lines were grown to mid-log phase (OD_{750} of 1.0 – 1.5) under optimal conditions, then diluted to an OD_{750} of 0.5 ± 0.05 (representative of early log phase) and aliquoted into 15 ml replicates. Samples were taken immediately before paraquat addition to represent time = 0 h, and after exposure at time = 6 h, 12 h, 24 h, and 48 h. By 48 h exposure, a clear phenotype was visible (Figure 4-6). At all concentrations of paraquat (including 0 µM), the SOR cultures exhibited a

bright greenish-blue appearance, while the empty vector control became more photobleached (or photoinhibited) with increasing severity as paraquat concentrations increased.

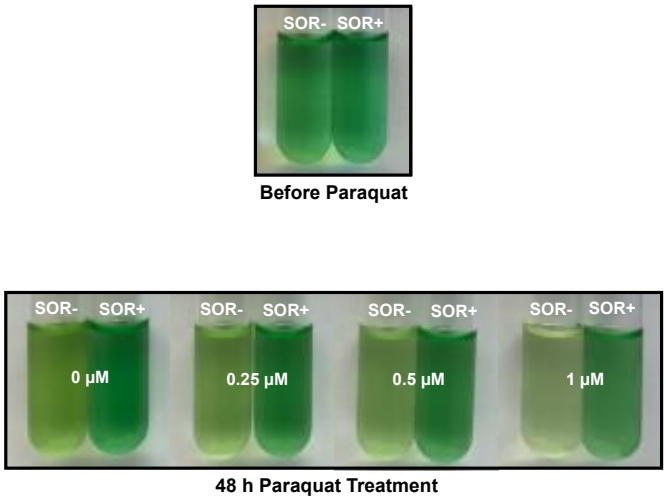

Figure 4-6. Effect of paraquat on culture appearance following 48 h treatment. Empty vector control and SOR cultures are pictured before paraquat exposure (top) and after (bottom) the 48 h treatment. In this image, all 48 h cultures were diluted to an OD_{750} of 0.5 to allow for comparison to the cultures before exposure, and to rule out culture density as a contributing factor to appearance.

Figure 4-7a shows the growth of the two lines over the 48 h treatment with four concentrations of paraquat. In the absence of paraquat, both cultures had more than doubled in density, and both cultures reached a similar OD_{750} (≈1.25). Growth inhibition increased (for both strains) directly in correlation with increasing paraquat concentrations, and neither strain doubled its culture density within 48 h when exposed to 1 µM paraquat. At 0, 0.25, and 0.5 µM paraquat, generation times for both the empty vector control and SOR^+ were similar to each other (data not shown); however, at 1 µM paraquat, the generation time for SOR^+ was notably lower than that of the empty vector control (87.3 h for SOR^+ and 150.3 h for empty

vector line). While neither cell line doubled its density over the 48-h treatment with 1 µM paraquat, the lower generation time for SOR^+ indicates that culture density would eventually double well before the empty vector line.

ROS levels in both lines were estimated by incubating the cells with DCFH-DA (Figure 4-7b). DCFH-DA is a membrane-permeant derivative of fluorescein that displays quenched fluorescence upon entering the cell, but its degradation in the presence of ROS leads to enhanced fluorescence. At all time points designated with a star, the ROS content was higher in the empty vector control than in the SOR^+ line. The fact that this trend was present for all time points in the absence of paraquat indicates that SOR was effectively reducing basal ROS levels. There was an increase in ROS levels at the 12 h time point in all treated cultures, but from 12 h to 48 h, ROS decreased in the empty vector line, likely due to the endogenous antioxidant response. ROS levels for SOR^+ remained stable from 12 h to 48 h, neither increasing nor decreasing, which was indicative of dampened ROS signaling due to SOR activity which ultimately led to a weaker induction of the antioxidant stress response.

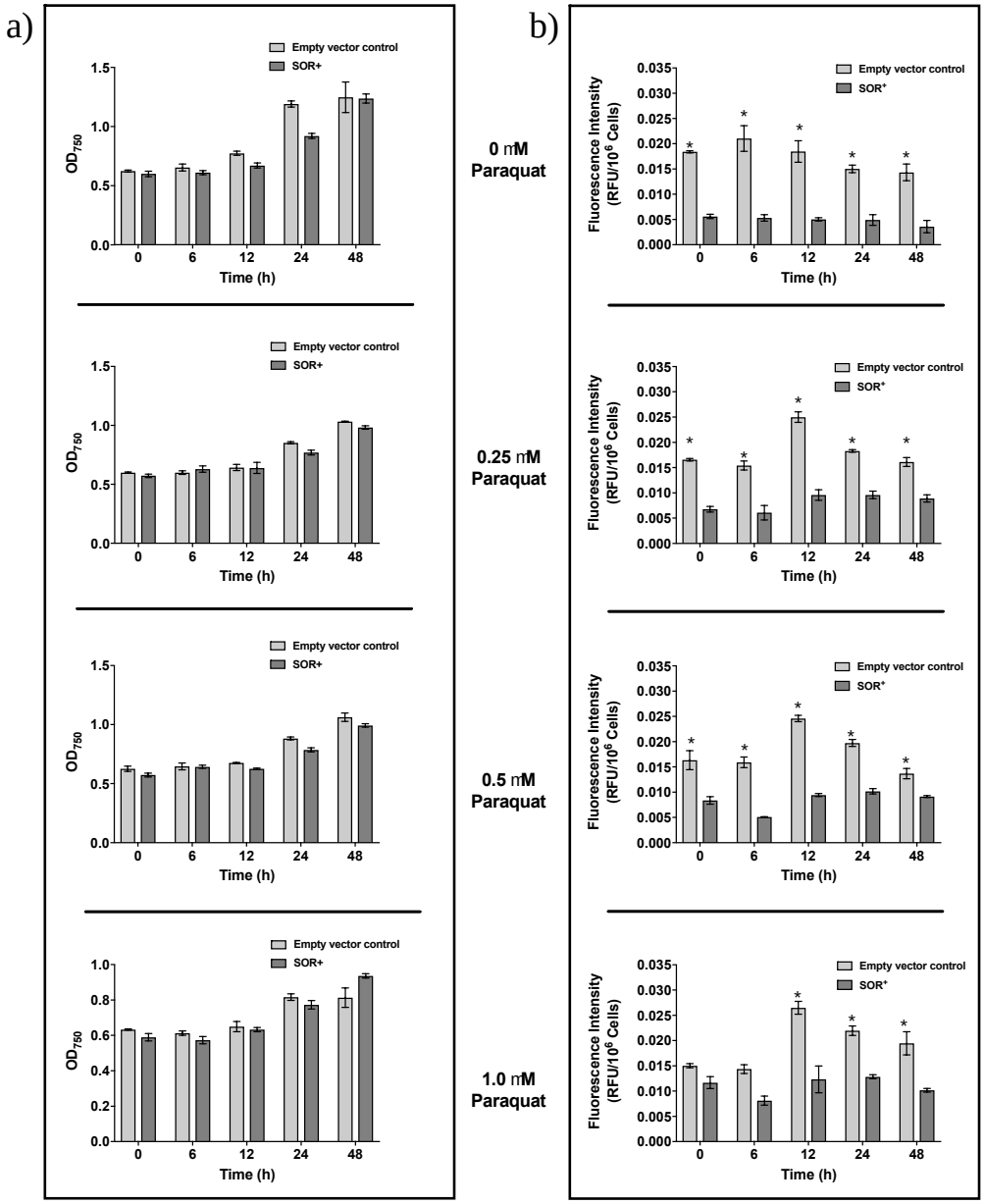

Figure 4-7. Effects of paraquat on culture density and ROS content. **a)** Culture densities and, **b)** relative intracellular ROS content were assayed in the empty vector negative control and SOR^+ over 48 h exposure to varying concentrations of paraquat (0 µM, 0.25 µM, 0.5 µM, and 1.0 µM). Error bars represent standard error of the mean, n = 3. The difference in ROS content between the two lines is statistically significant ($P < 0.05$) at all data points designated with a star (*). Two-way ANOVA was performed in Prism software from GraphPad to determine statistical significance, and the Šidák method was applied to correct for multiple comparisons.

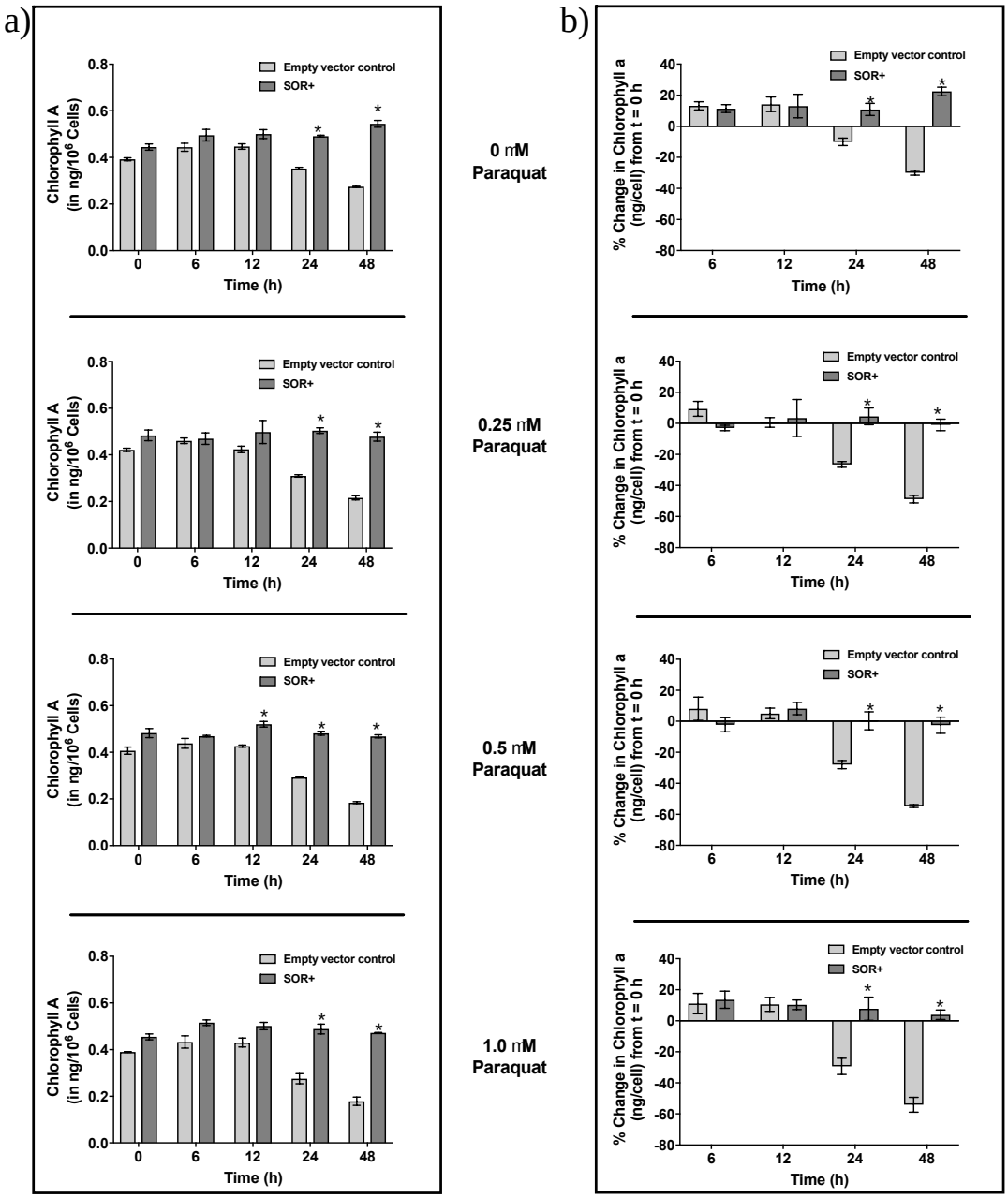

Figure 4-8. Effect of paraquat on chlorophyll a concentration. **a)** Chlorophyll a content (in ng/10^6 cells) and, **b)** the percent change from the starting chlorophyll a content (at t = 0 h) gained or lost over 48 h exposure to varying concentrations of paraquat. In both cases, error bars represent standard error of the mean, n = 3. In both representations of these data, a star (*) denotes data points where the difference between the two strains is statistically significant ($P < 0.05$). Two-way ANOVA was performed in Prism software from GraphPad to determine statistical significance, and the Šidák method was applied to correct for multiple comparisons.

The results of methanol extraction of chlorophyll a from cultures exposed to varying concentrations of paraquat at all time points are represented in Figure 4-8a. For all paraquat concentrations, the same trend in chlorophyll a described under optimal growth conditions was seen: as the cultures entered what would ordinarily be logarithmic growth phase (after 24 and 48 h of growth), the SOR^+ cultures contained significantly more chlorophyll a than the empty vector controls. This trend became even more evident at higher paraquat concentrations (0.5 µM and 1.0 µM), where by t = 48 h the SOR^+ samples contained more than twice as much chlorophyll a per cell as the empty vector control. Figure 4-8b shows that in all cases, even in the absence of paraquat, the empty vector line actually lost chlorophyll a by 24 and 48 h of growth, while SOR^+ either accumulated more chlorophyll or enhanced stability and retention of existing chlorophyll. Evidence of chlorophyll retention and biosynthesis had been exhibited previously when SOR was expressed in Arabidopsis plants exposed to heat stress (Im et al., 2009). Retention of chlorophyll in SOR^+ signifies a functional photosynthetic apparatus and decreased ROS damage, both indicative of increased tolerance to ROS.

This decreased chlorophyll a concentration in the empty vector line is visible in Figure 4-6, where the cultures became more yellow with increasing paraquat concentrations. Photoinhibition occurs when the equilibrium between photodamage to PSII and repair of PSII becomes imbalanced and the rate of damage exceeds the rate of repair (Hsieh et al., 2014). ROS accumulation can cause this to happen several ways: by causing oxidative damage to the D1 protein responsible for the continuous repair of PSII or proteins associated with PSII function, by disrupting electron transfer at photosynthetic reaction sites, by damaging DNA

or RNA affecting transcription or translation and potentially altering the proteome, or by degrading chlorophyll directly, reducing its ability to funnel energy into the light reactions of photosynthesis (Schieber et al., 2014).

4.4.3. SOR enhances tolerance to other ROS-inducing stress conditions.

4.4.3.1. UV-B

In cyanobacteria, exposure to UV-B radiation is extremely detrimental. It inhibits growth, causes photobleaching of photosynthetic pigments, and down-regulates important photosynthetic processes such as CO_2 uptake, RuBisCO (ribulose-1,5 bisphosphate carboxylase/oxygenase) activity, photosystem II repair (by degrading the D1 and D2 proteins necessary for repair) and nitrogen fixation. Translation in general is inhibited during UV-B exposure, subsequently altering the entire proteome. DNA can be damaged directly by absorption of UV-B resulting in lesions, and also indirectly by UV-B induced ROS production. Lipids are damaged by peroxidation of polyunsaturated fatty acids (PUFA) in cellular membranes, also initiated by UV-B induced ROS accumulation (He & Häder, 2002; S. P. Singh et al., 2010).

When exposed to continuous UV-B radiation, culture growth was inhibited somewhat in both cell lines as seen in Figure 4-9a, where both cultures should have doubled in density after 24 h, but instead had just barely doubled after 48 h. After 12 h exposure to UV-B, optical density for the SOR^+ line had increased enough for the difference between the two lines to be statistically significant ($P < 0.05$). At every time point the SOR^+ line contained more chlorophyll a per cell than the empty vector control ($P < 0.05$) for all sampling times), even

though by 48 h both lines had lost chlorophyll (Figure 4-9b). ROS content remained significantly lower in SOR^+ than in the empty vector control ($P < 0.05$) through 12 h exposure. The fact that SOR^+ was able to increase culture density after 12 h exposure, and had lower ROS content than the empty vector control up to 12 h indicated some SOR-mediated tolerance to UV-B occurs early-on during exposure, and metabolic processes, while inhibited in both lines, are less impacted than the empty vector line (Figure 4-9c). The notable increase in ROS content seen at 48 h in both cell lines is likely due to the fact that photosynthetic pigments act as photosensitizers. They are capable of absorbing UV-B light energy and transferring it to other molecules in the form of electrons. In increased irradiance, as molecular oxygen builds up in the cell due to ROS detoxification by antioxidants, excess electrons are transferred to molecular oxygen forming singlet oxygen and superoxide anion. In this case, higher chlorophyll content (as seen in SOR^+) might not be beneficial, as it would indicate more chlorophyll is available to absorb UV-B energy, increasing electron transfer to O_2 and subsequent ROS formation, potentially overwhelming the cell.

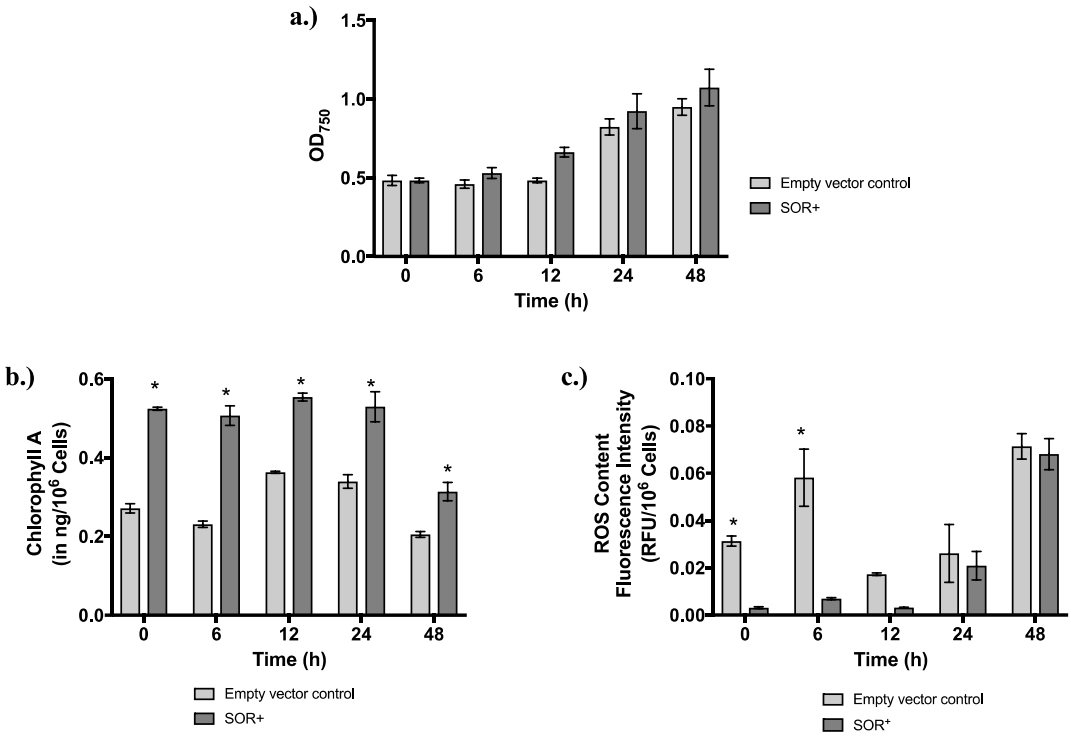

Figure 4-9. Effect of continuous UV-B exposure on culture density, chlorophyll a concentration, and ROS content. **a)** Optical density (A_{750}), **b)** chlorophyll a content, and **c)** ROS content of the empty vector control and SOR^+ exposed to continuous UV-B for 48 h. Error bars indicate standard error of the mean, n = 3. Two-way ANOVA was performed in Prism software from GraphPad to determine statistical significance ($P < 0.05$), and the Šidák method was applied to correct for multiple comparisons. Data points in which the difference between the two strains was statistically significant are designated with a star (*).

4.4.3.2. NaCl

Salt acclimation and enhanced salt tolerance in cyanobacteria is necessary if cultures are to be grown in seawater (Hagemann, 2011). Growth in salt water eliminates the requirement for fresh water and also increases the potential for axenic growth, maximizing target biomass and production titers by minimizing potential for microbial contamination (Su et al., 2017). Additionally, salt stress is one strategy for increasing production of lipids or solvents through the process of sodium stress cycling (Carrieri et al., 2010). To compare effects

of NaCl on growth of our PCC 7942 cultures with the findings of a similar study by Su et al. (2017) in which exogenous heat shock proteins were overexpressed in PCC 7942 and then evaluated for heat and salt tolerance, we exposed our cultures to the same NaCl concentrations (2%, 3%, and 3.5% w/v, with 3.5% NaCl representative of the average salinity of seawater (Millero et al., 2008). We saw a similar trend in growth to what was previously displayed in their Kan_r empty vector control for PCC 7942, where at 2% NaCl both of our cell lines were able to increase culture density over 48 h, albeit without doubling (data not shown). At 3% and 3.5% NaCl, both cell lines increased culture density very slightly over 48 h (from 0.5 to ≈0.65), which was also in keeping with what seen by Su et al. (2017) (data not shown).

There was very little difference in ROS content between the two cell lines with the exception of the 48 h time points for 2% and 3% NaCl, as seen in Figure 4-10a. With 2% NaCl, 48-h ROS content for the empty vector line increased while ROS content in the SOR^+ strain remained stable over 48 h following an initial decrease from t = 0 h. With 3% NaCl, ROS content for both lines had increased slightly by 24 h and more than doubled by t = 48 h. For all NaCl concentrations, a decrease in ROS was seen for both lines between t = 0 h and t = 6 h, and ROS concentrations remained low through t = 12 h. The trends for chlorophyll a (concentration and % gain/loss) were similar to ROS content: both lines maintained or slightly increased their chlorophyll a per cell through 12 h, followed by a decline in chlorophyll a concentration through 24 and 48 h, respectively (Figure 4-10b and c). The SOR^+ line, however, lost significantly ($P < 0.05$) less chlorophyll than the empty vector line during these time points.

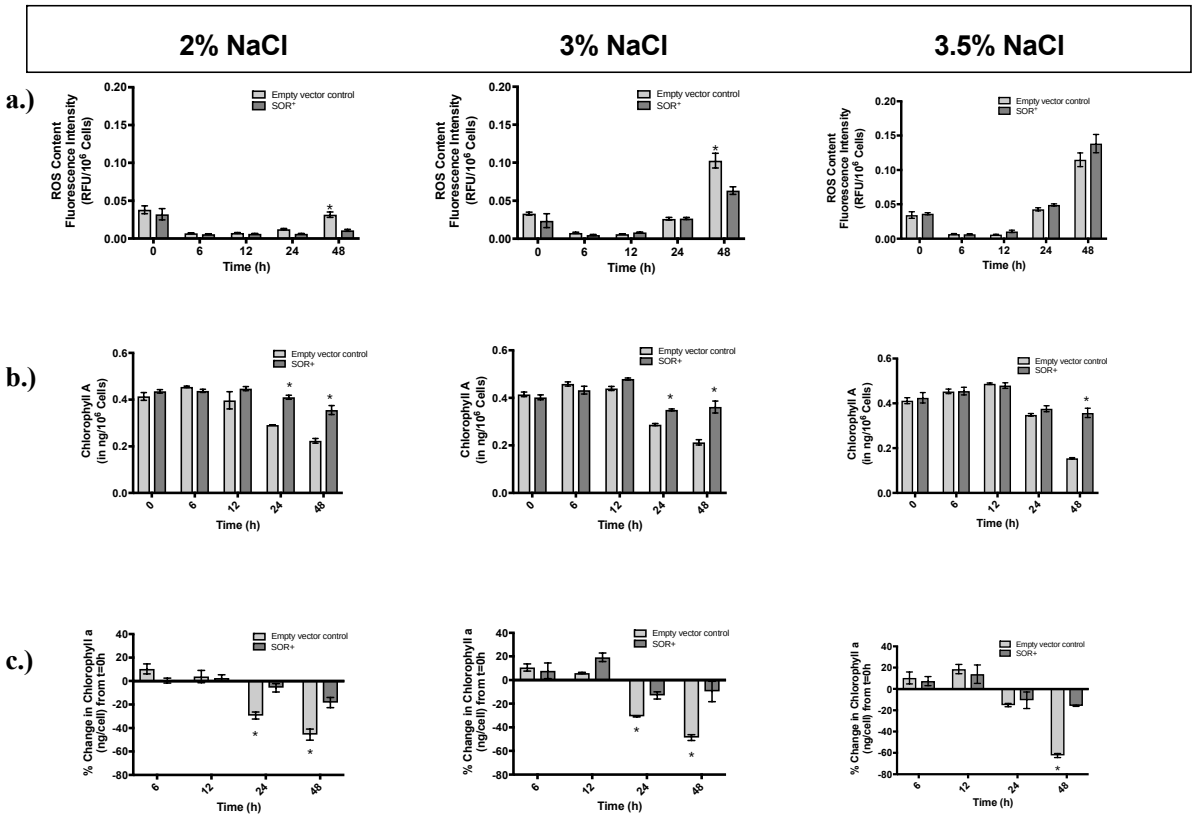

Figure 4-10. Effect of NaCl exposure on ROS content and chlorophyll a concentration. **a)** ROS content in both cell lines during 48 h treatment with 2%, 3% and 3.5% NaCl (w/v). **b)** Chlorophyll a per cell in both cell lines during treatment with 2%, 3%, and 3.5% NaCl. **c)** Percent change in chlorophyll a concentration from t = 0 h in cultures exposed to 2%, 3%, and 3.5% NaCl for 48 h. Error bars represent standard error of the mean, n = 3. Two-way ANOVA was performed in Prism software from GraphPad to determine statistical significance ($P < 0.05$), and the Šidák method was applied to correct for multiple comparisons. Data points in which the difference between the two strains was statistically significant are designated with a star (*).

Cyanobacteria have evolved with quick, robust responses to fluctuations in salinity in their surrounding environments. At the onset of salt stress, cyanobacteria accumulate compatible solutes (e.g., glucosylglycerol, glycine betaine, or proline), which are not harmful to cellular metabolism at high molar concentrations within the cell. The presence of these solutes increases osmolality inside the cell, which enables it to continue to take in water and

maintain turgor pressure following initial shrinkage of the cells resulting from NaCl exposure. Simultaneously, ion transport systems inside the cell become activated and begin exporting Na^+ and Cl^- ions (Pade et al., 2014). This immediate response to increased salinity offers some explanation for the evidence of salt tolerance that is seen in both strains for the first 12 h of exposure. From 12-48 h of continuous salt exposure, NaCl had likely accumulated in the cytoplasm leading to ROS buildup (due to alterations in photosynthetic electron transport chain) and ultimately caused inhibition of cellular metabolism, photosynthesis, and transcription / translation. Detrimental effects of salt stress were clearly demonstrated in analyses of both lines after 12 h, and visual analysis indicated that photobleaching increased proportionally with NaCl concentration (not shown). The SOR^+ line experienced less photobleaching and was less adversely affected overall than the empty vector line at all NaCl concentrations indicating enhanced tolerance to salt stress.

4.4.3.3. Solvents: isopropanol and butanol

Cyanobacteria can be engineered to produce valuable chemicals and fuel components. Isopropanol produced in cyanobacteria can easily be converted to propylene, a widely used plastic (Kusakabe et al., 2013). Short and medium chain alcohols (C_4 – C_{12}), such as butanol can be used as replacement fuels for gasoline. Branched chain hydrocarbons (C_9 – C_{23}) such as farnesene or limonene can be used as biofuels or aviation fuels (George et al., 2015; Lee et al., 2008). The antimicrobial properties of these compounds presents a significant technical roadblock to maximizing yields and cost efficiency of cyanobacterial chemical production (Dunlop et al., 2011). Exposure to solvents reduces integrity of cellular membranes leading to

disruption of energy transfer and respiration and ultimately release of cellular components (ATP, macromolecules, ions) from the cell (Dunlop, 2011). Reactive oxygen species are generated by impaired respiration, and induction of antioxidant gene expression has been shown to be a cellular response to solvent exposure (Trautwein et al., 2008).

To assess whether SOR conferred any tolerance to oxidative stress induced by solvent exposure, cultures from both cell lines were exposed to increasing concentrations of isopropanol and butanol. Figure 4-11 shows the results of a 48-h treatment with 1 g/L, 2.5 g/L, 5 g/L and 7.5 g/L isopropanol (IPA). Cell growth trends for both cell lines were similar (data not shown), with both empty vector and SOR^+ able to double culture densities by 48 h (albeit with slowed generation times) and exhibiting marked growth inhibition with 5 g/L and 7.5 g/L. At 5 g/L IPA, average generation times for the empty vector control and SOR^+ were 77.8 h and 60.9 h, respectively. At 7.5 g/L average generation times were 383.8 h for empty vector and 100.6 h for SOR^+. While generation times at 5 g/L were 2-3 times that of untreated cultures, the generation time for SOR^+ was ~ 17 h shorter than the empty vector strain. At 7.5 g/L cell division was extremely impaired, if not arrested; however, the empty vector generation time was nearly 4 times higher than that of the SOR^+ strain. The difference in generation time at these concentrations of IPA indicated that perhaps low levels of cellular metabolism continued in the presence of SOR.

In Figure 4-11a, ROS content was significantly higher in empty vector cultures at all time points when treated with 1 g/L and 2.5 g/L IPA, and at 48 h with 5 g/L and 7.5 g/L IPA. By 48 h, ROS content in the empty vector line increased significantly compared to basal levels at all IPA concentrations. At 1 g/L and 2.5 g/L IPA, the SOR^+ strain ROS concentrations had

not increased significantly over 48 h. After treating with 5 g/L IPA for 48 h, ROS content had increased by nearly 10 times in the empty vector line, while a 5-fold increase was seen in the SOR^+ strain. While ROS content increased in both strains by 48 h, the magnitude of the increase was less in SOR^+ than in the empty vector. After treatment with 7.5 g/L IPA for 48 h, ROS content in empty vector cultures had increased 4-fold throughout the study. While ROS content in SOR^+ was higher than what had been seen with any of the lower IPA concentrations, ROS content actually decreased slightly by 48 h from what was calculated at t = 0 h. The 7.5 g/L study was performed independently from the lower IPA concentrations, and the ROS concentration in the pre-treatment empty vector and SOR^+ cultures for this study were somewhat elevated compared to basal ROS in the previous study. This had been seen in some of our previous studies when the cultures were exposed to room temperature during dilution at the start of the study, or were diluted in media that had cooled to room temperature (data not shown). It is possible that exposure to lowered temperature caused some oxidative stress prior to the IPA treatment. Therefore, the decrease in ROS seen over 48 h in the SOR^+ line could be due to the possibility that the native stress response had been activated before IPA addition, and SOR was functioning in concert with the endogenous antioxidants allowing for more aggressive ROS mitigation.

As had been observed previously, chlorophyll a concentrations (Figure 4-11b) were significantly higher in the SOR^+ than in the empty vector strain at all IPA concentrations and at nearly every time point. Patterns of chlorophyll turnover were similar for both cell lines, as shown in Figure 4-11c, with loss occurring between 12 and 24 h exposure with 5 g/L IPA and

by 6 h with 7.5 g/L IPA. With the lower IPA concentrations, both lines maintained their chlorophyll a concentrations for the duration of the study.

Butanol exposure inhibited growth in both cell lines at lower concentrations than IPA (data not shown), and growth trends for SOR^+ and empty vector were similar to each other, and to what was seen with IPA. At 2.5 g/L and 5 g/L butanol, generation times for the SOR^+ cultures were much lower than empty vector, although overall culture growth was impaired. The average generation time for empty vector treated with 2.5 g/L butanol was 134.5 h, but was 82.0 h for the SOR^+ cultures. With 5 g/L butanol, average generation time increased 3.5-fold for empty vector (470.9 h) and 1.8-fold for the SOR^+ (149.5 h) cultures. This again indicates some preservation of metabolic activities in the SOR^+ cultures as was demonstrated with IPA.

Figure 4-12a shows ROS concentrations in both cell lines at all butanol concentrations. Empty vector cultures had significantly higher ROS content than SOR^+ by 48 h with all butanol concentrations. With 1 g/L butanol, ROS content decreased over 48 h in both cell lines which, when coupled to the fact that neither line lost chlorophyll during the treatment, indicated that the endogenous antioxidant response was effectively detoxifying ROS. The lower ROS content seen in SOR^+ compared to empty vector at 1 g/L butanol is likely due to additional antioxidant detoxification by SOR.

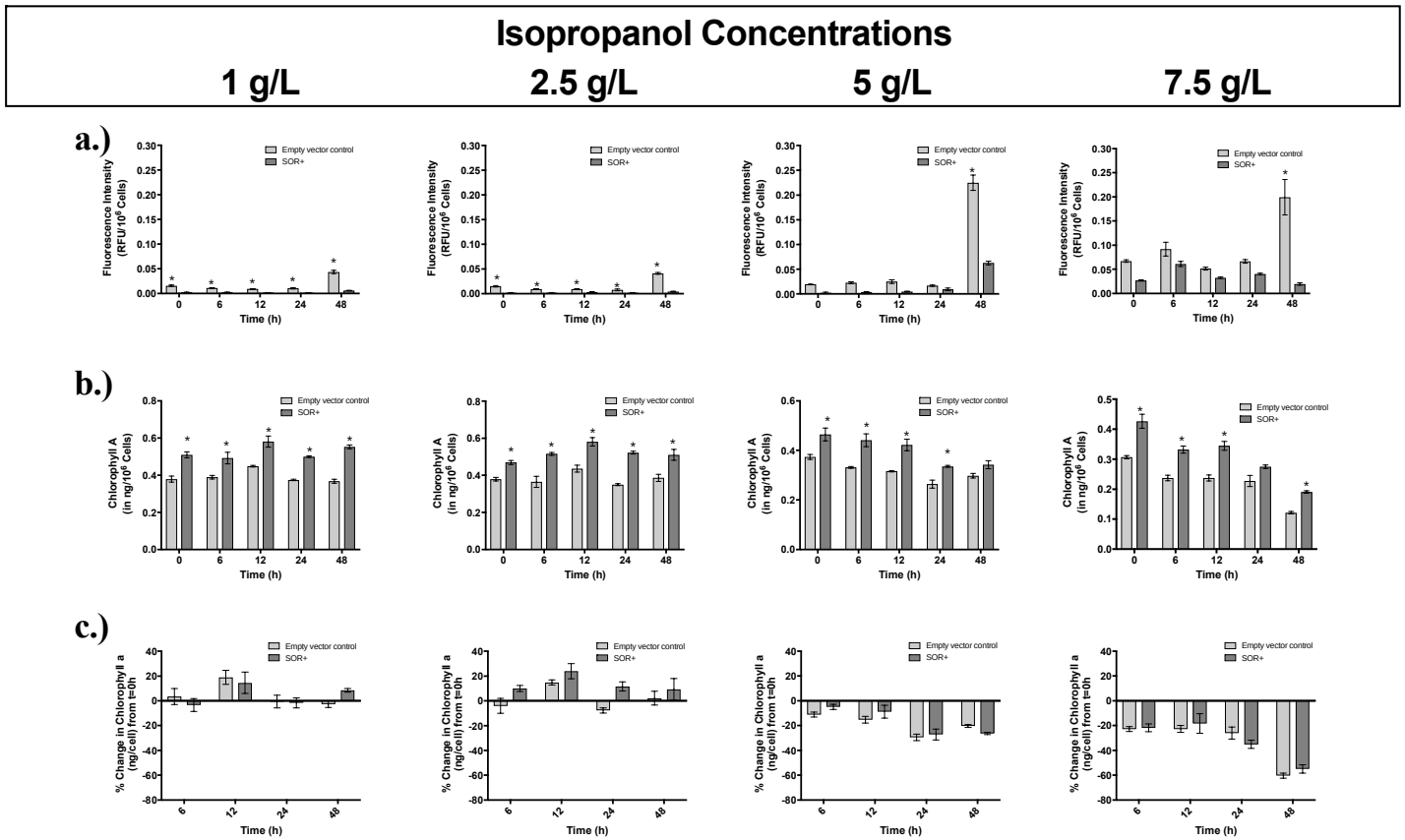

Figure 4-11. Effect of isopropanol exposure on ROS content and chlorophyll a concentration. **a)** ROS content, **b)** chlorophyll a concentration and, **c)** percent change in chlorophyll a for empty vector control and SOR$^+$ cultures grown in the presence of 1 g/L, 2.5 g/L, 5 g/L, or 7.5 g/L isopropanol for 48 h. Error bars represent standard error of the mean, n = 3. Two-way ANOVA was performed in Prism software from GraphPad to determine statistical significance ($P < 0.05$), and the Šidák method was applied to correct for multiple comparisons. Data points in which the difference between the two strains was statistically significant are designated with a star (*).

In Figure 4-12b and c, both lines increased chlorophyll a concentration by 6 h treatment with 1 g/L butanol, but had returned to baseline concentrations by 48 h, with no major chlorophyll loss for the duration of the study. By 12 h with both 2.5 g/L and 5 g/L butanol, chlorophyll turnover was evident in both lines. SOR^+ cells had significantly higher chlorophyll concentrations than empty vector with all butanol concentrations and at all time points, with the exception of 48 h at 5 g/L. With both solvents, the protective effect(s) of SOR seemed most pronounced in the ability of the cells to maintain lower ROS contents than the empty vector cultures at all solvent concentrations. It was not expected that SOR would provide protection against solvent-induced membrane damage, therefore these results are not surprising. Diminished generation times and ROS content, as well as decreased photobleaching (not shown) in SOR^+ compared to empty vector cultures does indicate some degree of tolerance conferred by SOR; however, its effects on overall culture viability have not been investigated at this time.

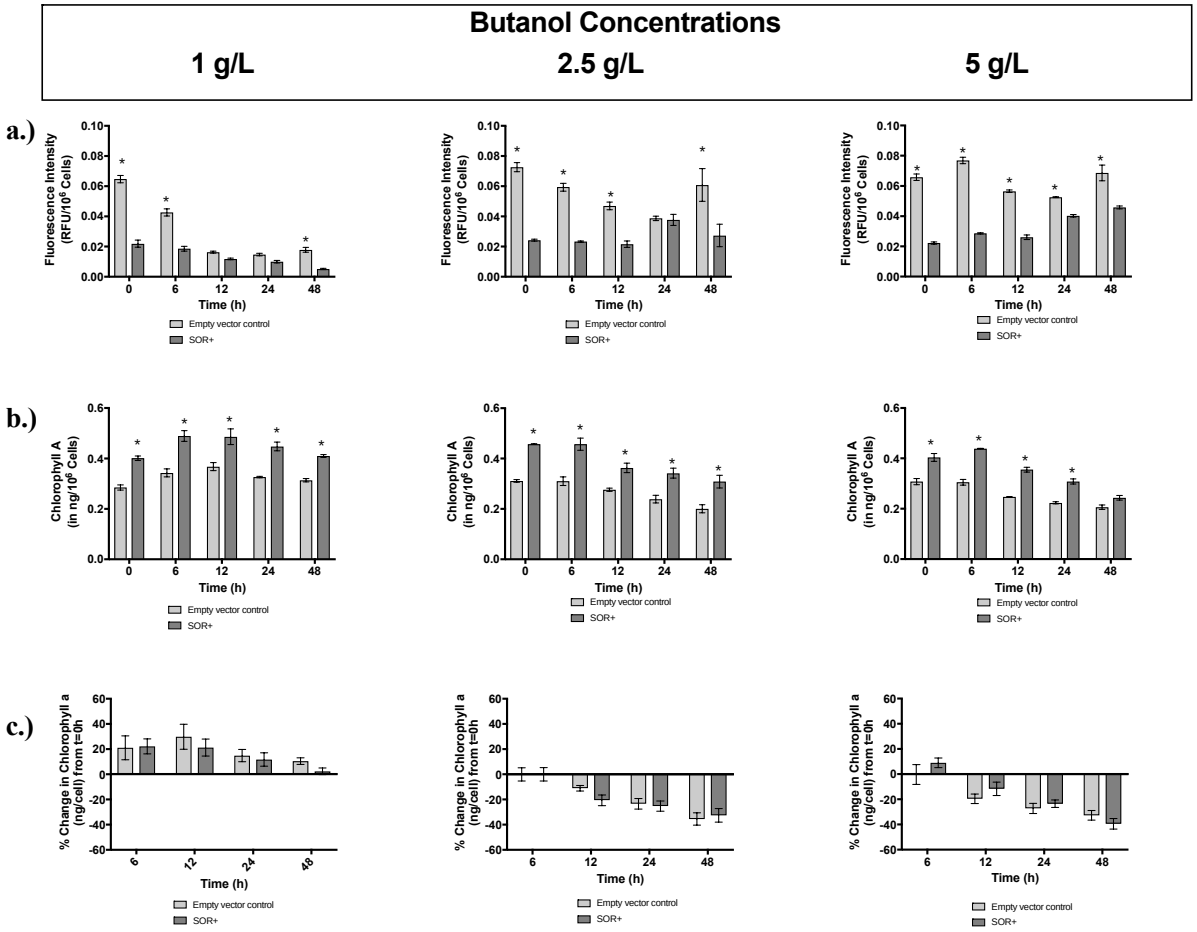

Figure 4-12. Effect of butanol on ROS content and chlorophyll a concentration. **a)** ROS content, **b)** chlorophyll a concentration, and **c)** percent change in chlorophyll a for empty vector control and SOR^+ cultures grown in the presence of 1 g/L, 2.5 g/L, or 5 g/L 2-butanol for 48 h. Error bars represent standard error of the mean, n = 3. Two-way ANOVA was performed in Prism software from GraphPad to determine statistical significance ($P < 0.05$), and the Šidák method was applied to correct for multiple comparisons. Data points in which the difference between the two strains was statistically significant are designated with a star (*).

4.4.3.4. Heat stress

To induce moderate heat shock, less than 10°C above the optimal growth temperature, cultures were grown at 42°C for 72 h. Figure 4-13a shows that both the empty vector and SOR^+ cultures increased culture density over 72 h; however, the SOR^+ cultures went through nearly

three doubling cycles and reached a final OD_{750} that was twice that of the empty vector cultures. When generation times were calculated, SOR^+ average generation time was 19.5 h at 42°C, while empty vector average generation time was 41.3 h - more than twice that of SOR^+. One possible explanation for the increase in culture density for SOR^+ at 42°C that should not be ignored, is that the OD_{750} can still increase if cells are not dividing. If cell division is arrested due to heat stress but the cells are instead able to increase biomass, an increase in OD^{750} will result, giving the false impression that the culture is growing (Červený et al., 2015). Without physically counting the cells, it is impossible to conclude from our data which situation is occurring; however, increased biomass is indicative of ongoing CO_2 fixation. Whether the SOR^+ cultures reached higher OD_{750} due to unaffected generation time or due to biomass accumulation, both possibilities indicate that the cultures are less negatively impacted by heat exposure. If biomass accumulation was the reason for increased OD_{750} in the SOR^+ cultures, this could mean that the cultures are not actually losing chlorophyll, or are not losing as much as the empty vector cultures.

As shown in Figure 4-13b, both lines lost chlorophyll a over 72 h but onset of loss occurred by 12 h in the empty vector cultures and 24 h in SOR^+ indicating at least a 12-h delay in chlorophyll turnover. At 72 h heat exposure at 42°C, the difference in chlorophyll a concentration was statistically significant, with SOR^+ containing nearly two-fold more chlorophyll. Figure 4-13c shows that, following 72 h of heat exposure at 42°C, the empty vector cultures had lost, on average, 80% of their chlorophyll concentration from t = 0 h, while SOR^+ had lost 60%. While both lines experienced chlorophyll turnover during the heat

treatment, the empty vector line was more impacted, showing negative effects on both growth and chlorophyll retention.

At 45°C, a severe heat shock at more than 10°C above optimal temperature, both cell lines were severely impacted as seen in Figure 4-13a-c. By 48 h exposure, all cultures were visibly photobleached, had lost almost all chlorophyll a, and had not increased in density, therefore the study was not continued through 72 h. Figure 4-13a (45°C) shows that neither cell line doubled in culture density over 48 at 45°C. This was likely due to the fact that cell division has been shown to be suspended during heat shock (Červený et al., 2015). The average generation time for the empty vector cultures was 208.5 h, and for SOR^+, an average of 160.0 h. While the generation time for SOR^+ is lower than for empty vector, both generation times are quite a bit longer than that of non-stressed cultures (normally ≈ 20 h). Chlorophyll a turnover began by 6 h for both cell lines, but at 12 h and 24 h SOR^+ lost significantly less chlorophyll a than the empty vector cultures (Figure 4-13b-c, 45°C). By 48 h however, both cell lines had lost nearly 100% of their starting chlorophyll concentration. The slightly lower generation time and slowed chlorophyll a turnover exhibited by the SOR^+ line could indicate a small degree of increased thermotolerance, but it is clear that neither cell line thrives at this temperature.

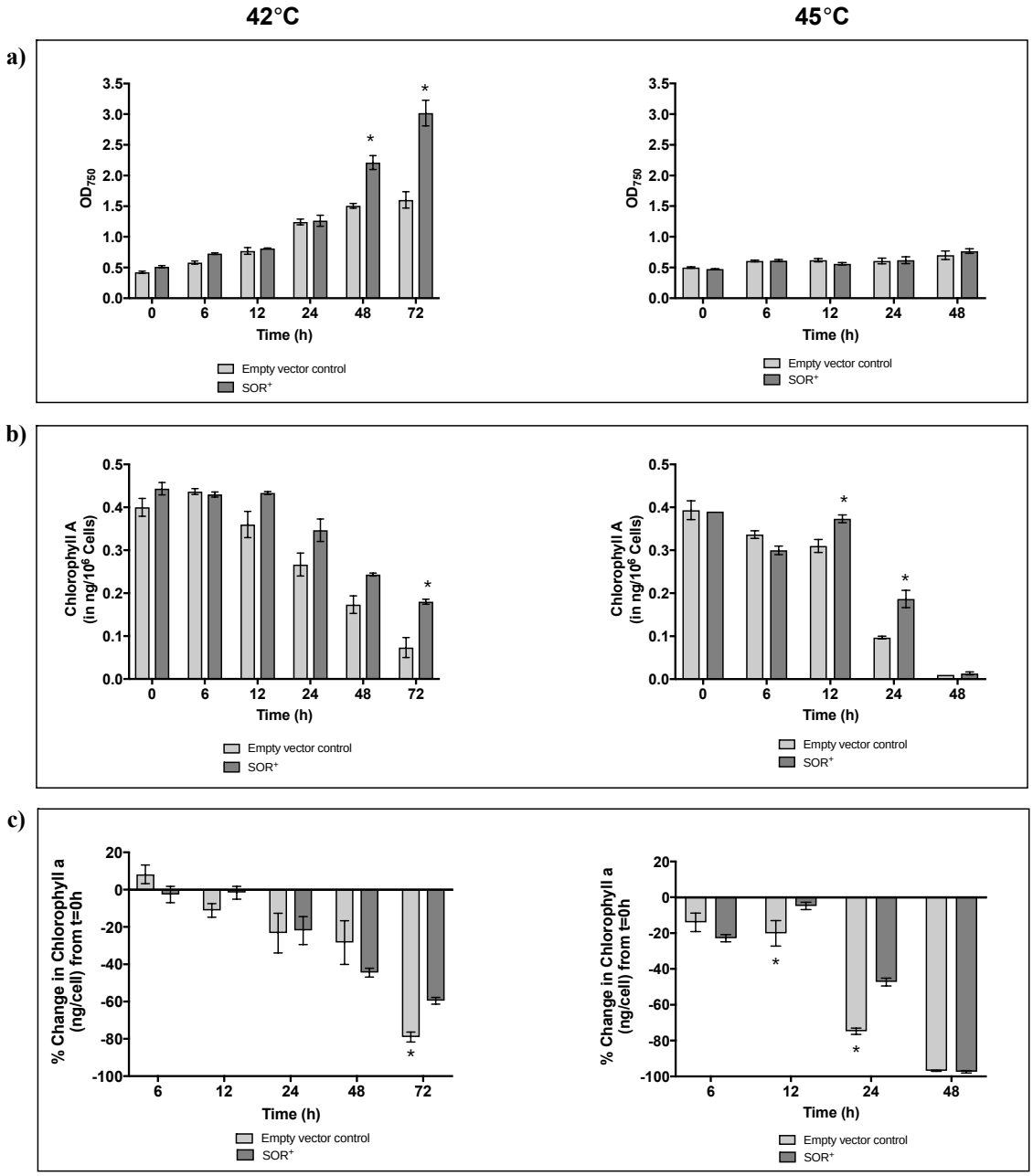

Figure 4-13. Effect of heat exposure on culture density and chlorophyll content. **a)** Culture density, **b)** chlorophyll a concentration and, **c)** percent change in chlorophyll a from t = 0 h for empty vector and SOR$^+$ cultures grown at 42°C and 45°C. Error bars represent standard error of the mean for n = 4. Two-way ANOVA was performed in Prism software from GraphPad to determine statistical significance ($P < 0.05$), and the Šidák method was applied to correct for multiple comparisons. Data points in which the difference between the two strains was statistically significant are designated with a star (*).

Prior to these heat stress experiments, short-term heat shock experiments were performed that consisted of 2- and 4-h heat treatments followed by analysis of recovery afterwards (data not shown). Obvious protective effects of SOR were not seen when these experiments were carried out. Both cell lines demonstrated minimal signs of heat-induced growth inhibition, likely due to the robust endogenous heat shock response of PCC 7942. Sustained exposure to elevated temperature can lead to a decline in photosynthetic processes, slowed metabolism, reduced membrane integrity, and accumulation of ROS (Venkataramanaiah et al., 2003; Wen et al., 2005). PSII is a vulnerable target of heat stress and damage is characterized by dissociation of the phycobilisomes from PSII and inhibition of electron transport. Cyanobacterial heat shock response (HSR) consists of several families of heat shock proteins (HSPs) that confer thermotolerance and promote recovery by repairing, re-folding, or degrading damaged proteins, protection of photosynthetic apparatus, and stabilization of membranes (Rajaram et al., 2014). In addition to the HSPs, antioxidant response is also initiated by heat stress, indicating that ROS mitigation is an important component of heat tolerance. Induction of cellular response to heat is rapid: HSP transcription has been shown to increase within the first 5-30 min of heat shock, with concentrations of the corresponding proteins increasing in the first 20-60 min of heat shock (Červený et al., 2015). It could be that the endogenous heat shock response cannot sustain prolonged heat exposure, therefore both cell lines were able to tolerate the shorter heat treatments, and the earlier h of prolonged heat exposure. This explains why our initial studies with 2- and 4-h heat treatments did not demonstrate a clear difference between the two strains, and why there was not an immediate drop in culture density or chlorophyll a concentration for the earlier time points of

prolonged heat exposure. Prolonged heat leads to increased ROS accumulation, so the protective properties of SOR could explain why SOR^+ cultures lost less chlorophyll a by 6 and 12 h heat exposure compared to empty vector.

4.4.4. Quantitative analysis of stress-induced biomarkers

4.4.4.1. Photoinhibition of PSII

Measurement of chlorophyll fluorescence can provide valuable insight into the fate of light energy absorbed by chlorophyll which can be dissipated one of three ways: 1) it can be shuttled into photosynthetic processes, 2) it can be re-emitted in the form of heat, or 3) it can be re-emitted as light (fluorescence). Chlorophyll fluorescence is therefore a measure of re-emitted light from chlorophyll in PSII. Specifically, F_0 is the measure of chlorophyll fluorescence when the PSII reaction centers are open (dark-adapted samples). F_m is a measurement of the fluorescent signal when the PSII reaction centers are closed (following exposure to saturating light). F_v is the variable fluorescence; the difference between F_m and F_0. The ratio of F_v/F_m is a measure of the maximum quantum yield of photosystem II photochemistry, or can be an indicator of photoinhibition or inactivation of PSII reaction centers (Murchie et al., 2013). In non-stressed cultures, the F_v/F_m values are expected to remain relatively consistent throughout growth cycle. As shown in Figure 4-14a, F_v/F_m fluctuated only slightly over 48 h for both cell lines, and at 24, 48, and 72 h there was very little difference between the ratios for both lines. At the earlier time points (0 h, 6 h, and 12 h), however, F_v/F_m was significantly higher in SOR^+ than in the empty vector control indicating more robust PSII reaction centers at the onset of exponential growth.

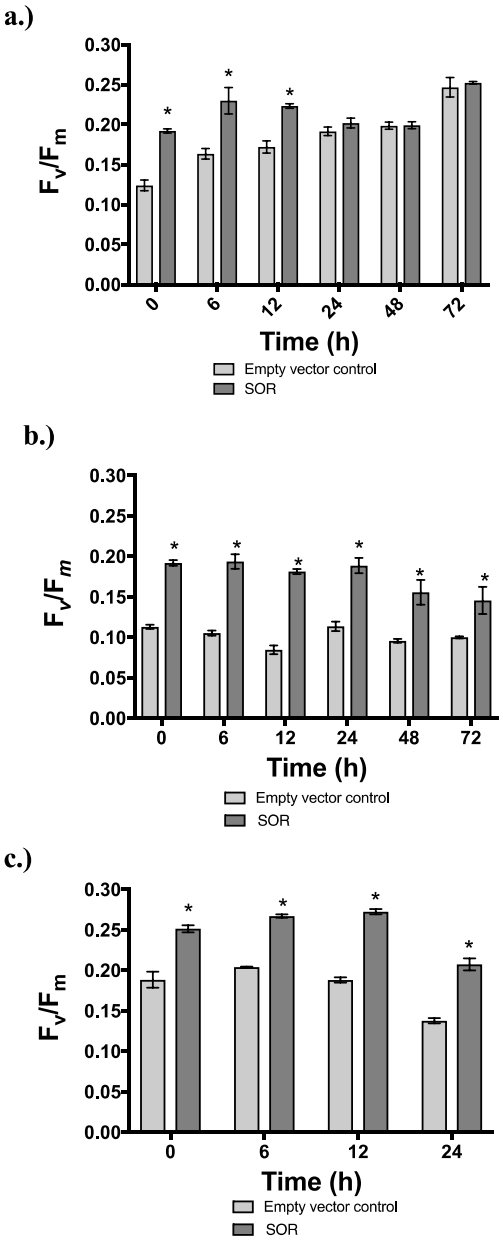

Figure 4-14. Effects of paraquat and UV-B treatments on photoinhibition of PSII. **a)** F_v/F_m ratio for untreated cultures (empty vector control and SOR+) grown under optimal conditions for 72 h. **b)** F_v/F_m ratio for cultures of both cell lines treated with 0.25 µM paraquat, and cultivated under otherwise optimal conditions for 72 h. **c.)** F_v/F_m ratio for cultures of both cell lines exposed to UV-B light constantly for 24 h. Error bars represent standard error of the mean, n = 3. To determine statistical significance ($P < 0.05$), two-way ANOVA was performed in Prism software from GraphPad was performed and the Šidák method was applied to correct for multiple comparisons. Data points in which the difference between the two strains was statistically significant are designated with a star (*).

In the presence of 0.25 µM paraquat, the F_v/F_m ratio for the empty vector control culture was significantly lower than SOR^+ for all time points, as shown in Figure 4-14b, and lower than F_v/F_m values for non-stressed empty vector control. These results are consistent with Figure 4-8, where SOR^+ maintains consistent chlorophyll a concentrations throughout the duration of the study in various concentrations of paraquat and is actually able to increase in chlorophyll a concentration by 48 h with 0.25 µM. During UV-B exposure, F_v/F_m decreased for empty vector cultures over time indicating photoinhibition, or damage to PSII, due to either UV-B exposure directly or ROS buildup (Figure 4-14c). For SOR^+, the F_v/F_m ratio was stable through t = 24 h indicating some resistance to UV-B or ROS-induced damage, or protection of PSII was taking place. These results are consistent with what was seen in the earlier UV-B study (Figure 4-9 b-c), where tolerance to UV-B was enhanced in the SOR^+ line at earlier time points during exposure. The decreased ratio at t = 24 h seen in both lines is likely due to direct damage to PSII caused by UV-exposure; against which SOR would not offer protection. The results of this study confirm that the ROS scavenging capability of SOR protects PSII from oxidative damage imparted from chemically- or UV-B-induced ROS buildup.

Tables 4-3 through 4-6 contain the raw data (F_0 and F_m) acquired via the chlorophyll fluorometer during the PSII efficiency study from which the F_v/F_m ratios were calculated. It is important to note that as the cultures grew more dense, the gain (sensitivity) had to be decreased on the fluorometer in order to keep the values for F_0 between 200 to 400 mV as recommended by the manufacturer to avoid a signal overload. Because of this, no conclusions could be drawn by examining the raw data alone, since the values varied between time points. Since the data of interest for this study are the F_v/F_m in the form of a ratio, variations in F_0 or

F_m values did not affect the outcome of the study. In addition, it was determined experimentally before the study that culture density did not affect the F_v/F_m ratio, so it was not necessary to dilute samples to a uniform culture density at each time point.

Table 4-3. Raw F_0 values (in mV) for the empty vector control (pSyn_6) and SOR^+, either untreated (optimal growth conditions) or treated (grown in the presence of 0.25 µM paraquat) over 48 h. Each value is the average of 5 replicates ± one standard deviation.

Time (h)	0	6	12	24	48 h	72 h
pSyn6 (untreated)	230.7 (±10.0)	262.5 (±57.9)	242.6 (±9.04)	275.7 (±3.43)	274.5 (±6.0)	289.1 (±55)
pSyn6 (treated)	219.7 (±7.10)	252.6 (±9.99)	277.8 (±5.67)	213.9 (±8.38)	357.4 (±22.4)	322.4 (±9.9)
SOR+ (untreated)	262.5 (±24.1)	242.8 (±18.4)	275.1 (±23.2)	314.2 (±17.3)	295.0 (±18.8)	303.6 (±17.9)
SOR+ (treated)	267.7 (±17.0)	252.5 (±13.4)	261.7 (±26.6)	223.7 (±15.4)	261.0 (±23.5)	262.1 (±12.5)

Table 4-4. Raw F_m values (in mV) for the empty vector control (pSyn_6) and SOR^+, either untreated (optimal growth conditions) or treated (grown in the presence of 0.25 µM paraquat) over 48 h. Each value is the average of 5 replicates ± one standard deviation.

Time (h)	0	6	12	24	48 h	72 h
pSyn6 (untreated)	263.9 (±14.5)	314.5 (±27.2)	293.3 (±22.9)	341.3 (±27.8)	342.5 (±21.2)	385.7 (±23.3)
pSyn6 (treated)	246.5 (±19.7)	282.3 (±15.0)	303.5 (±18.7)	241.7 (±9.79)	388.3 (±33.6)	358.5 (±31.7)
SOR+ (untreated)	325.0 (±29.8)	316.1 (±24.0)	346.3 (±36.2)	388.7 (±27.8)	368.5 (±25.0)	406.7 (±22.5)
SOR+ (treated)	338.3 (±27.2)	315.5 (±19.8)	320.0 (±31.9)	274.8 (±17.3)	307.8 (±31.6)	303.3 (±18.1)

Table 4-5. Raw F_0 values (in mV) for the empty vector control (pSyn_6) and SOR^+, either untreated (optimal growth conditions) or treated (grown under constant UV-B exposure) over 48 h. Each value is the average of 5 replicates ± one standard deviation.

Time (h)	0	6	12	24
pSyn6 (untreated)	332.4 ± 23.9	296.4 ± 38.3	324.8 ± 27.8	309.6 ± 16.7
pSyn6 (treated)	327.1 ± 31.9	278.3 ± 19.9	257.0 ± 27.9	252.7 ± 16.7
SOR+ (untreated)	407.1 ± 30.8	352.5 ± 44.4	388.6 ± 33.1	375.5 ± 21.7
SOR+ (treated)	403.5 ± 44.2	343.1 ± 30.5	316.6 ± 34.1	293.6 ± 23.4

Table 4-6. Raw F_m values (in mV) for the empty vector control (pSyn_6) and SOR^+, either untreated (optimal growth conditions) or treated (grown under constant UV-B exposure) over 48 h. Each value is the average of 5 replicates ± one standard deviation.

Time (h)	0	6	12	24
pSyn6 (untreated)	235.8 ± 36.7	239.1 ± 24.9	318.6 ± 42.6	278.5 ± 24.1
pSyn6 (treated)	244.2 ± 17.1	251.5 ± 24.1	266.9 ± 22.3	290.5 ± 17.6
SOR+ (untreated)	333.3 ± 31.2	309.3 ± 32.7	415.0 ± 57.7	365.1 ± 29.5
SOR+ (treated)	326.5 ± 25.9	343.3 ± 37.6	366.5 ± 30.6	360.3 ± 29.2

4.4.4.2. Free proline accumulation

Plants, algae, and cyanobacteria have been shown to accumulate free proline in addition to other compatible solutes in response to abiotic stress such as heat or salt (Klähn et al., 2011; A. P. Singh et al., 2005). Accumulation of free proline occurs either by biosynthesis from glutamate or ornithine, or by protein degradation (Szabados et al., 2010). Under oxidative stress conditions, proline functions more readily as a ROS scavenger capable of detoxifying •OH and quenching $^1O_2$ than an osmolyte, and proline catabolism produces energy that can feed into the electron transport chain (A. P. Singh et al., 2005).

Typically, proline quantitation is determined spectrophotometrically using a method by Bates, et al. (1973) in which cell extracts are exposed to an acidic ninhydrin solution. Ninhydrin binds free proline and forms a red product that absorbs light at 520 nm (Bates et al., 1973). Instead of this, we chose to use the the UPLC™ AccQ-Tag amino acid analysis platform from Waters Corporation (Milford, MA, USA), which allows for rapid, accurate quantitation of free amino acids in a variety of sample matrices (Fiechter et al., 2011; Waters Corporation, 2014). Utilizing this platform allowed for not only direct quantification of proline, but also allowed us to analyze 19 additional amino acid profiles in treated and untreated cultures.

It was hypothesized that free proline concentrations would increase over time in our PCC 7942 cultures during exposure to two conditions that lead to ROS formation: paraquat and UV-B. We expected to see less proline accumulation overall in our SOR^+ line which would indicate increased tolerance. This exact phenotype was seen by Geng et al. (2016) when *P. furiosus* SOR was expressed in heat-stressed ornamental dogwood trees (Geng et al., 2016). In our analyses, the interaction between the untreated cultures in the paraquat study was not deemed to be statistically significant indicating that baseline proline concentrations for the two lines were similar when grown under optimal conditions (Figure 4-15a). When treated with paraquat, free proline concentration in the empty vector line increased through 12 h, and was significantly higher than that of the SOR^+ line at all time points. The maximum proline concentration in the treated empty vector cultures was maintained between 6 and 12 h. This increased concentration by 6 h was expected, as maximum proline accumulation typically occurs within 4 h following stress onset, and subsequently declines afterward (A. P. Singh et al., 2005). The higher proline concentration seen at t = 0 h in the treated empty vector line was

unexpected, since the cultures were sampled immediately prior to paraquat addition. It is possible that the cultures were responding to brief temperature fluctuations experienced during dilution.

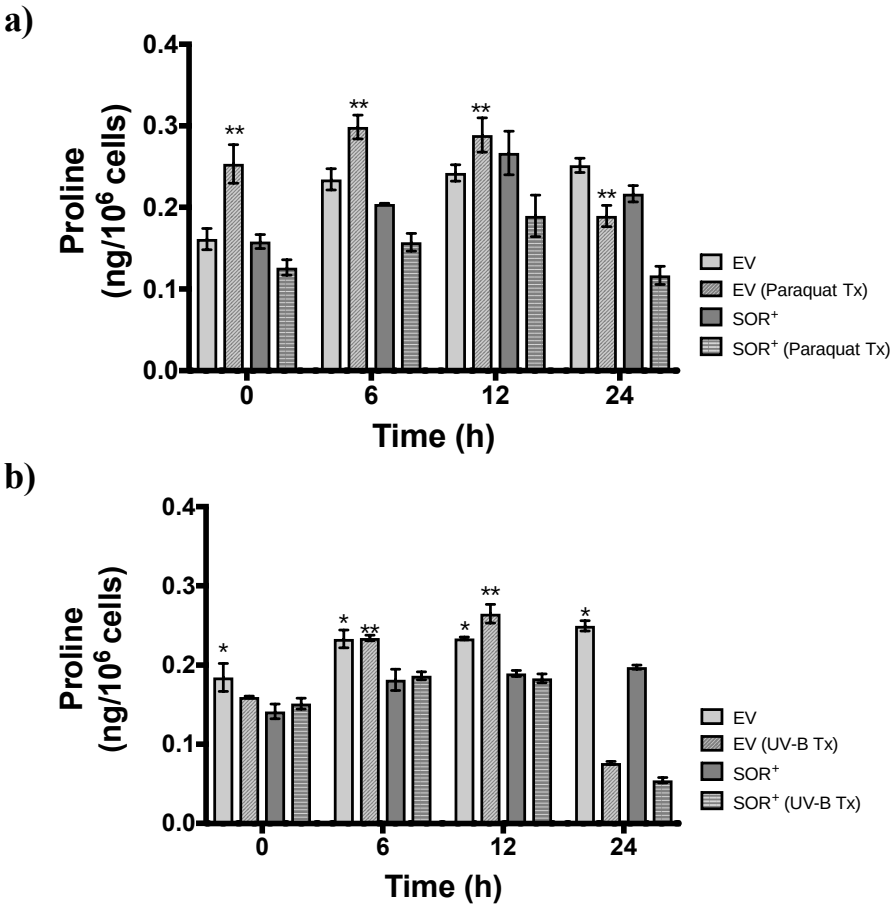

Figure 4-15. Effect of paraquat and UV-B treatment on free proline accumulation. **a)** Intracellular free proline quantitation via UPLC™ for the empty vector control and SOR$^+$, either untreated (grown under optimal conditions for 24 h), or treated (exposed to 0.25 µM paraquat for 24 h). **b)** Free proline quantitation for the empty vector control and SOR$^+$, either untreated (grown under optimal conditions for 24 h), or treated (exposed to constant UV-B radiation for 24 h). Error bars represent standard error of the mean, n = 3. To determine statistical significance ($P < 0.05$), 2-way ANOVA analysis was performed in Prism software from GraphPad and the Šidák test was applied to correct for multiple comparisons. Data points in which the difference between the two strains was statistically significant are designated with a star (*). Data points in which the difference between the two treated strains is statistically significant are designated with two stars (**).

Paraquat-treated empty vector cultures contained significantly more free proline than treated SOR^+ cultures at every time point. The maximum proline concentration in the treated SOR^+ cultures was reached by 12 h, indicating a delayed onset of stress-induced proline accumulation. At all time points, the proline concentrations in paraquat-treated SOR^+ cultures were significantly lower than in the treated empty vector cultures, which was in line with the phenotype seen in heat-treated Arabidopsis (Im et al., 2005). Less accumulation of proline overall in treated cultures coupled with delayed onset of proline accumulation indicated our hypothesis was valid, and SOR expression did confer increased tolerance to paraquat, and therefore to intracellular ROS buildup.

The results of UV-B exposure (shown in Figure 4-15b) were slightly different from what was exhibited with paraquat. At all time points, the untreated empty vector cultures contained significantly more free proline than the untreated SOR+ cultures. In the treated empty vector cultures, free proline concentration again increased between 6 and 12 h compared to the concentration at t = 0 h, however maximum proline concentration in SOR^+ cultures were reached by 6 h as well. At t = 6 h and t = 12 h, the treated empty vector cultures contained significantly more chlorophyll a than the treated SOR^+ cultures. No obvious difference in proline concentrations were observed between untreated and treated cultures of the same lines at the 0-, 6-, and 12-h time points. An explanation for this could be that cyanobacteria have several lines of defense to cope directly with UV-B radiation, instead of just responding to the resulting ROS buildup. These include changing morphology, synthesizing extracellular polysaccharides, and synthesis of protective molecules to absorb or diffuse UV-B such as carotenoids and micosporine-like amino acids (MAAs) (S. P. Singh et al., 2010). It is possible

that under UV-B exposure, cellular metabolism is directed more toward these mitigation strategies. In addition, translation is slowed during UV-B exposure due to direct damage to nucleic acids and proteins. Decreased protein translation could mean fewer amino acids are synthesized for incorporation into proteins, leaving fewer sources from which to accumulate free proline. The fact that, after 24 h UV-B exposure, an obvious decrease in proline content was visible for both treated cell lines is expected. UV-B has been shown to cause a linear decrease in intracellular protein content with continued exposure, therefore any enhancement in UV-B tolerance through ROS scavenging by proline at this time point cannot be assumed (Sinha et al., 1995).

Following proline analysis, concentrations of seven additional amino acids were analyzed to determine if there were any trends that would negate our observations of free proline accumulation due to oxidative stress (Figure 4-16a-g). All amino acid concentrations analyzed, apart from lysine, decreased more than 2-fold between 12 h and 24 h of paraquat exposure. A decrease of this magnitude was not seen with proline, indicating that while translation and amino acid synthesis were likely reduced due to oxidative stress, proline accumulation appears to be unaffected by or is independent of this.

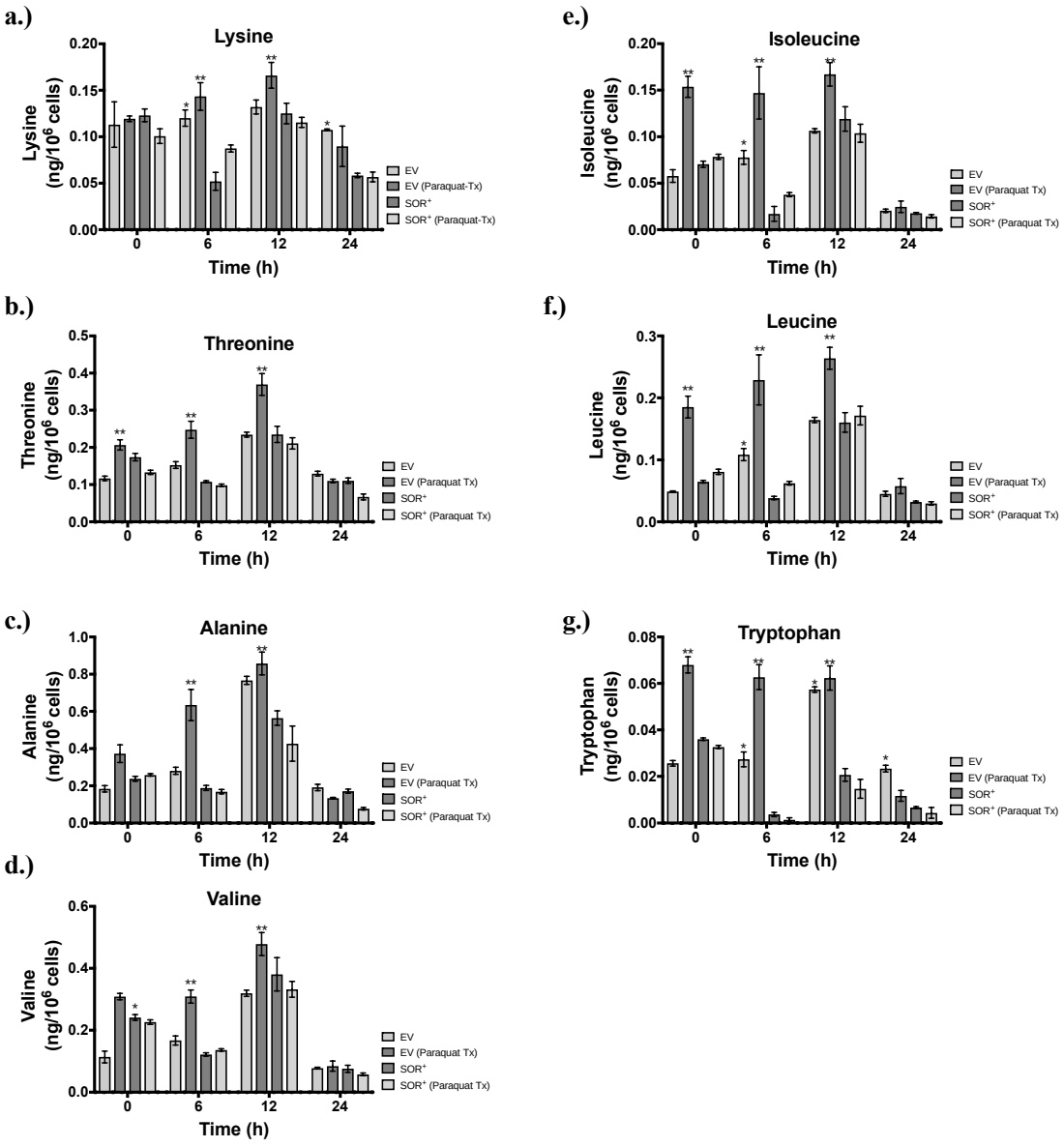

Figure 4-16. Effect of paraquat on free amino acid concentration. Results of quantification of seven additional free amino acids via UPLC™. Concentrations of **a)** lysine, **b)** threonine, **c)** alanine, **d)** valine, **e)** isoleucine, **f)** leucine and, **g)** tryptophan from 0.25 µM MV-treated and untreated empty vector and SOR$^+$ cultures. Error bars represent standard error of the mean for n = 3. To determine statistical significance ($P < 0.05$), 2-way ANOVA analysis was performed in Prism software from GraphPad and the Šidák test was applied to correct for multiple comparisons. Data points in which the difference between the two strains was statistically significant are designated with a star (*). Data points in which the difference between the two treated strains is statistically significant are designated with two stars (**).

4.4.4.3. Lipid peroxidation

Lipids that make up cyanobacterial cellular membranes are targets for ROS-induced damage during abiotic stress. Hydrogen atoms adjacent to double-bonded carbons in polyunsaturated fatty acids are particularly vulnerable to oxidation, and lead to formation of lipid radicals, rearrangement of double bonds, and ultimately loss of membrane integrity (Buege et al., 1978; S. C. Singh et al., 2002). Malondialdehyde (MDA) is one of the breakdown products of lipid peroxidation that results from formation of a lipid endoperoxide following attack by molecular oxygen. MDA from cellular extracts reacts with thiobarbituric acid (TBA) at high temperature and under acidic conditions to form an adduct that can be measured spectrophotometrically (absorbance at 530-540 nm).

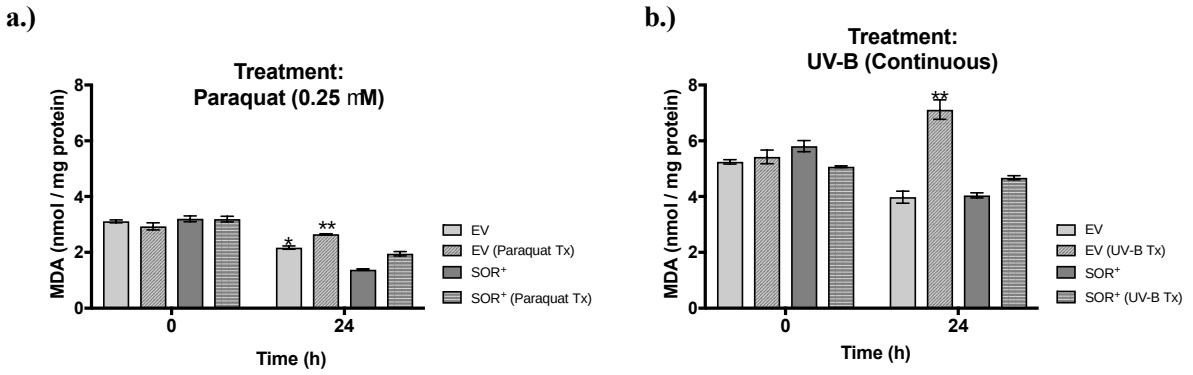

Figure 4-17. Effect of paraquat and UV-B treatments on lipid peroxidation. Malondialdehyde (MDA) concentration from the TBARS assay indicated lipid peroxidation levels in **a.)** empty vector control and SOR^+ cultures either untreated or treated with 0.25 µM paraquat and, **b.)** empty vector control and SOR^+ cultures either untreated or treated with constant UV-B exposure for 24 h. Error bars represent standard error of the mean for n = 3. To determine statistical significance ($P < 0.05$), 2-way ANOVA analysis was performed in Prism software from GraphPad and the Šidák test was applied to correct for multiple comparisons. Data points in which the difference between the two strains was statistically significant are designated with a star (*). Data points in which the difference between the two treated strains is statistically significant are designated with two stars (**).

To determine levels of lipid peroxidation in our PCC 7942 cultures, MDA formation was quantified in both cell lines, either following 24 h of growth at optimal conditions, 24 h treatment with 0.25 µM paraquat, or 24 h treatment with UV-B. Figure 4-17 shows that MDA concentrations were higher in all cultures at the pre-treatment time point for the UV-B experiment than in the paraquat experiment, indicating the cultures might have been undergoing some peroxidation as a product of normal lipid metabolism. For both treatment conditions, the t = 0 MDA concentrations were essentially the same as the untreated cultures indicative of an established baseline MDA concentration for the cultures. Following exposure to paraquat for 24 h, all MDA concentrations decreased from t = 0 h, however they were significantly higher in the empty vector cultures than in SOR^+, for both untreated and treated cultures. Following 24 h exposure to UV-B, MDA concentrations decreased from t = 0 h for untreated empty vector cultures, and for both untreated and treated SOR^+ cultures. MDA concentrations in these cultures were relatively similar and any differences were not deemed to be statistically significant. MDA concentration in the treated empty vector cultures increased significantly over 24 h indicating that more lipid damage had occurred in these cultures than in either SOR^+ cultures and the untreated empty vector cultures. The fact that there was less lipid peroxidation seen in all treated SOR^+ cultures compared to treated empty vector cultures indicated less evidence of ROS-induced lipid damage and therefore increased tolerance to both stress conditions. These results are consistent with what was seen in heat-stressed ornamental dogwood trees in which SOR expression conferred enhanced tolerance to heat (Geng et al., 2016).

4.5. Conclusion

PCC 7942 cultures expressing *P. furiosus* SOR demonstrated phenotypic evidence of enhanced tolerance to several abiotic stress conditions. When cultivated under optimal conditions, SOR^+ cultures grew at similar rates and reached similar densities as the empty vector cultures; however, they contained as much as 2 times more chlorophyll a per cell during exponential growth phase. When excess intracellular superoxide was chemically generated by exposure to paraquat, SOR^+ cultures contained more chlorophyll per cell, lost less chlorophyll over time, had lower ROS contents, accumulated less free proline, underwent less lipid peroxidation, demonstrated less damage to PSII, and were visually less photobleached than the empty vector cultures. SOR^+ cultures exhibited early ($\leq$ 12 h) tolerance to continuous UV-B exposure and contained more chlorophyll a per cell, had lowered ROS content, later onset of proline accumulation and less free proline overall, as well as less lipid peroxidation, damage to PSII, and photobleaching. When treated with varying concentrations of NaCl, SOR^+ cultures maintained more chlorophyll per cell, lost less chlorophyll, had lower ROS content, and less photobleaching than empty vector cultures. SOR^+ cultures were more tolerant of isopropanol and butanol, and exhibited lowered generation times at higher solvent concentrations, higher chlorophyll a concentrations, lower ROS content, and less visible photobleaching when compared to empty vector cultures. SOR^+ cultures exposed to long-term moderate heat either grew at faster rates than the empty vector control and reached higher culture densities, or accumulated more biomass indicative of preservation of CO_2 fixation activity. They retained more chlorophyll during the heat treatment and demonstrated less photobleaching.

While further may be useful to gain a deeper understanding of the exact physiological effects SOR expression confers on PCC 7942 cultures, these studies have provided substantial evidence for that SOR provides enhanced tolerance to a variety of abiotic stressors by maintaining lower intracellular ROS levels, and preventing or postponing detrimental consequences of ROS accumulation. We hypothesize that the benefits of improved stress tolerance could be exploited further by expressing *P. furiosus* SOR in a halotolerant/thermotolerant cyanobacterial species. Coupling SOR expression with other existing cyanobacterial stress tolerance strategies would likely improve product titers, diversify cultivation options, and encourage the utilization of cyanobacteria as a valuable resource for sustainable replacements of diminishing fossil fuels.

Acknowledgements

I would like to thank Nathan Wilson for assisting with the development of the DCFH-DA and TBARS assays; as well as Dr. Nathaniel Hentz (and the NCSU BTEC Analytical Services Lab) for allowing me to use their UPLC™ system, and for their multitude of other contributions to this research.

References

Bates, L. S., Waldren, R. P., & Teare, I. D. (1973). Rapid determination of free proline for water-stress studies. *Plant and Soil*, *39*(1), 205–207.

Breitenbach, J., Zhu, C., & Sandmann, G. (2001). Bleaching herbicide norflurazon inhibits phytoene desaturase by competition with the cofactors. *Journal of Agricultural and Food Chemistry*, *49*(11), 5270–5272.

Buege, J. A., & Aust, S. D. (1978). Microsomal lipid peroxidation. *Methods in Enzymology*, *52*(C), 302–310.

Carrieri, D., Momot, D., Brasg, I. A., Ananyev, G., Lenz, O., Bryant, D. A., & Dismukes, G. C. (2010). Boosting autofermentation rates and product yields with sodium stress cycling: application to production of renewable fuels by cyanobacteria. *Applied and Environmental Microbiology*, *76*(19), 6455–6462.

Červený, J., Sinetova, M. A., Zavřel, T., & Los, D. A. (2015). Mechanisms of high temperature resistance of *Synechocystis* sp. PCC 6803: an impact of histidine kinase 34. *Life*, *5*(1), 676–699.

Dunlop, M. J. (2011). Engineering microbes for tolerance to next-generation biofuels. *Biotechnology for Biofuels*, *4*(1), 32.

Dunlop, M. J., Dossani, Z. Y., Szmidt, H. L., Chu, H. C., Lee, T. S., Keasling, J. D., … Mukhopadhyay, A. (2011). Engineering microbial biofuel tolerance and export using efflux pumps. *Molecular Systems Biology*, *7*(487), 487.

Fiechter, G., & Mayer, H. K. (2011). Characterization of amino acid profiles of culture media via pre-column 6-aminoquinolyl-N-hydroxysuccinimidyl carbamate derivatization and ultra performance liquid chromatography. *Journal of Chromatography*, *879*(17–18), 1353–1360.

Fujii, T., Yokoyama, E., Inoue, K., & Sakurai, H. (1990). The sites of electron donation of photosystem I to methyl viologen. *BBA - Bioenergetics*, *1015*(1), 41–48.

Geng, X.-M., Liu, X., Ji, M., Hoffmann, W. A., Grunden, A. M., & Xiang, Q.-Y. J. (2016). Enhancing heat tolerance of the little dogwood *Cornus canadensis* L. f. with introduction of a superoxide reductase gene from the hyperthermophilic archaeon *Pyrococcus furiosus*. *Frontiers in Plant Science*, *7*, 26.

George, K. W., Alonso-Gutierrez, J., Keasling, J. D., & Lee, T. S. (2015). Isoprenoid drugs, biofuels, and chemicals—artemisinin, farnesene, and beyond. In *Advances in biochemical engineering/biotechnology* (Vol. 148, pp. 355–389).

Hagemann, M. (2011). Molecular biology of cyanobacterial salt acclimation. *FEMS Microbiology Reviews*, *35*(1), 87–123.

Hakkila, K., Antal, T., Rehman, A. U., Kurkela, J., Wada, H., Vass, I., … Tyystjärvi, T. (2014). Oxidative stress and photoinhibition can be separated in the cyanobacterium *Synechocystis* sp. PCC 6803. *Biochimica et Biophysica Acta (BBA) - Bioenergetics*, *1837*(2), 217–225.

He, Y.-Y., & Häder, D.-P. (2002). UV-B-induced formation of reactive oxygen species and oxidative damage of the cyanobacterium *Anabaena* sp.: protective effects of ascorbic acid and N-acetyl-l-cysteine. *Journal of Photochemistry and Photobiology B: Biology*, *66*(2), 115–124.

He, Y.-Y., Häder, D.-P., Perewoska, I., Mate, Z., Nagy, F., Etienne, A. L., … Leun, J. C. van der. (2002). Reactive oxygen species and UV-B: effect on cyanobacteria. *Photochem. Photobiol. Sci.*, *1*(10), 729–736.

Hsieh, P., Pedersen, J. Z., & Bruno, L. (2014). Photoinhibition of cyanobacteria and its application in cultural heritage conservation. *Photochemistry and Photobiology*, *90*(3), 533–543.

Im, Y. J., Ji, M., Lee, A. M., Boss, W. F., & Grunden, A. M. (2005). Production of a thermostable archaeal superoxide reductase in plant cells. *FEBS Letters*, *579*(25), 5521–5526.

Im, Y. J., Ji, M., Lee, A. M., Killens, R., Grunden, A. M., & Boss, W. F. (2009). Expression of *Pyrococcus furiosus* superoxide reductase in Arabidopsis enhances heat tolerance. *Plant Physiology*, *151*(2), 893–904.

Imlay, J. A. (2003). Pathways of oxidative damage. *Annual Review of Microbiology*, *57*(1), 395–418.

Jenney, F. E., Verhagen, M. F., Cui, X., & Adams, M. W. (1999). Anaerobic microbes: oxygen detoxification without superoxide dismutase. *Science*, *286*(5438).

Johnson, T. J., Halfmann, C., Zahler, J. D., Zhou, R., & Gibbons, W. R. (2016). Increasing the tolerance of filamentous cyanobacteria to next-generation biofuels via directed evolution. *Algal Research*, *18*, 250–256.

Kitchener, R. L., & Grunden, A. M. (2017). *Chapter 3: Methods for enhancing cyanobacterial stress tolerance to enable improved production of biofuels and industrially relevant chemicals*. *Submitted for publication*. North Carolina State University.

Klähn, S., & Hagemann, M. (2011). Compatible solute biosynthesis in cyanobacteria. *Environmental Microbiology*, *13*(3), 551–562.

Kuan, D., Duff, S., Posarac, D., & Bi, X. (2015). Growth optimization of *Synechococcus elongatus* PCC7942 in lab flasks and a 2-D photobioreactor. *Canadian Journal of Chemical Engineering*.

Kuhlgert, S., Austic, G., Zegarac, R., Osei-Bonsu, I., Hoh, D., Chilvers, M. I., … Kramer, D. M. (2016). MultispeQ Beta: a tool for large-scale plant phenotyping connected to the open PhotosynQ network. *Royal Society Open Science*, *3*(10).

Kusakabe, T., Tatsuke, T., Tsuruno, K., Hirokawa, Y., Atsumi, S., Liao, J. C., & Hanai, T. (2013). Engineering a synthetic pathway in cyanobacteria for isopropanol production directly from carbon dioxide and light. *Metabolic Engineering*, *20*, 101–108.

Latifi, A., Ruiz, M., & Zhang, C. C. (2009). Oxidative stress in cyanobacteria. *FEMS Microbiology Reviews*, *33*(2), 258–278.

Lee, S. K., Chou, H., Ham, T. S., Lee, T. S., & Keasling, J. D. (2008). Metabolic engineering of microorganisms for biofuels production: from bugs to synthetic biology to fuels. *Curr Opin Biotech*, *19*.

Life Technologies. (2013). GeneArt® Synechococcus Protein Expression Kit. *Instruction Manual*.

McCord, J. M., & Fridovich, I. (1969). Superoxide dismutase. An enzymic function for erythrocuprein (hemocuprein). *Journal of Biological Chemistry*, *244*(22), 6049–6055.

Meeks, J. C., & Castenholz, R. W. (1971). Growth and photosynthesis in an extreme thermophile, *Synechococcus lividius* (Cyanophya). *Archiv Für Mikrobiologie*.

Mittler, R., & Tel-Or, E. (1991). Oxidative stress responses in the unicellular cyanobacterium *Synechococcus* PCC 7942. *Free Radical Research Communications*, *12–13 Pt 2*(October), 845–50.

Molina-Heredia, F. P., Houée-Levin, C., Berthomieu, C., Touati, D., Tremey, E., Favaudon, V., … Nivière, V. (2006). Detoxification of superoxide without production of H2O2: antioxidant activity of superoxide reductase complexed with ferrocyanide. *Proc Natl Acad Sci U S A.*, *103*(40), 14750–14755.

Mulo, P., Sakurai, I., & Aro, E.-M. (2012). Strategies for psbA gene expression in cyanobacteria, green algae and higher plants: From transcription to PSII repair. *Biochimica et Biophysica Acta (BBA) - Bioenergetics*, *1817*(1), 247–257.

Murata, N., Takahashi, S., Nishiyama, Y., & Allakhverdiev, S. I. (2007). Photoinhibition of photosystem II under environmental stress. *Biochimica et Biophysica Acta (BBA) - Bioenergetics*, *1767*(6), 414–421.

Murchie, E. H., & Lawson, T. (2013). Chlorophyll fluorescence analysis: A guide to good practice and understanding some new applications. *Journal of Experimental Botany*, *64*(13), 3983–3998.

Nair, U., Thomas, C., & Golden, S. S. (2001). Functional elements of the strong psbAI promoter of *Synechococcus elongatus* PCC 7942. *Journal of Bacteriology*, *183*(5), 1740–1747.

Nozzi, N. E., Oliver, J. W. K., & Atsumi, S. (2013). Cyanobacteria as a platform for biofuel production. *Frontiers in Bioengineering and Biotechnology*, *1*, 7.

Pade, N., & Hagemann, M. (2014). Salt acclimation of cyanobacteria and their application in biotechnology. *Life (Basel, Switzerland)*, *5*(1), 25–49.

Pinto, E., Sigaud- Kutner, T. C. S., Leitao, M. A. S., & Okamoto, O. K. (2003). Heavy metal-induced oxidative stress in algae. *J. Phycol.*, *39*, 1008–1018.

Porra, R. J., Thompson, W. a, & Kriedemann, P. E. (1989). Determination of accurate extinction coefficients and simultaneous-equations for assaying chlorophyll-a and chlorophyll-b extracted with 4 different solvents - verification of the concentration of chlorophyll standards by atomic-absorption spectroscopy. *Biochimica et Biophysica Acta*, *975*(3), 384–394.

Rajaram, H., Chaurasia, A. K., & Apte, S. K. (2014). Cyanobacterial heat-shock response: role and regulation of molecular chaperones. *Microbiology*, *160*(Pt_4), 647–658.

Rastogi, R. P., Singh, S. P., Häder, D.-P., & Sinha, R. P. (2010). Detection of reactive oxygen species (ROS) by the oxidant-sensing probe 2′,7′-dichlorodihydrofluorescein diacetate in the cyanobacterium *Anabaena variabilis* PCC 7937. *Biochemical and Biophysical Research Communications*, *397*(3), 603–607.

Rodrigues, L. H. R., Arenzon, A., Raya-Rodriguez, M. T., & Fontoura, N. F. (2011). Algal density assessed by spectrophotometry: A calibration curve for the unicellular algae *Pseudokirchneriella subcapitata*. *Journal of Environmental Chemistry and Ecotoxicology*, *3*(8), 225–228.

Schieber, M., & Chandel, N. S. (2014). ROS function in redox signaling and oxidative stress. *Current Biology*, *24*(10).

Sheng, Y., Abreu, I. A., Cabelli, D. E., Maroney, M. J., Miller, A.-F., Teixeira, M., & Valentine, J. S. (2014). Superoxide dismutases and superoxide reductases. *Chemical Reviews*, *114*(7), 3854–3918.

Shestakov, S. V, & Khyen, N. T. (1970). Evidence for genetic transformation in blue-green alga *Anacystis nidulans*. *Molecular and General Genetics MGG*, *107*(4), 372–375.

Singh, A. P., Asthana, R. K., Kayastha, A. M., & Singh, S. P. (2005). A comparison of proline, thiol levels and GAPDH activity in cyanobacteria of different origins facing temperature-stress. *World Journal of Microbiology and Biotechnology*, *21*(1), 1–9.

Singh, S. C., Sinha, R. P., & Häder, D.-P. (2002). Role of lipids and fatty acids in stress tolerance in cyanobacteria. *Acta Protozool*, *41*, 297–308.

Singh, S. P., Häder, D.-P., & Sinha, R. P. (2010). Cyanobacteria and ultraviolet radiation (UVR) stress: Mitigation strategies. *Ageing Research Reviews*, *9*(2), 79–90.

Sinha, R. P., Kumar, H. D., Kumar, A., & Hader, D. P. (1995). Effects of UV-B irradiation on growth, survival, pigmentation and nitrogen-metabolism enzymes in cyanobacteria. *Acta Protozoologica*, *34*(3), 187–192.

Sobiechowska-Sasim, M., Stoń-Egiert, J., & Kosakowska, A. (2014). Quantitative analysis of extracted phycobilin pigments in cyanobacteria—an assessment of spectrophotometric and spectrofluorometric methods. *Journal of Applied Phycology*, *26*(5), 2065–2074.

Su, H.-Y., Chou, H.-H., Chow, T.-J., Lee, T.-M., Chang, J.-S., Huang, W.-L., & Chen, H.-J. (2017). Improvement of outdoor culture efficiency of cyanobacteria by over-expression of stress tolerance genes and its implication as bio-refinery feedstock. *Bioresource Technology*.

Szabados, L., & Savouré, A. (2010). Proline: a multifunctional amino acid. *Trends in Plant Science*, *15*(2), 89–97.

Thermo Fisher Scientific. (n.d.). Gibco® BG-11 Media: Optimized for Cyanobacteria (Formulation). Retrieved from https://www.thermofisher.com/us/en/home/technical-resources/media-formulation.353.html

Thomas, D. J., Avenson, T. J., Thomas, J. B., & Herbert, S. K. (1998). A cyanobacterium lacking iron superoxide dismutase is sensitized to oxidative stress induced with methyl viologen but is not sensitized to oxidative stress induced with norflurazon. *Plant Physiology*, *116*(4), 1593–602.

Trautwein, K., Kühner, S., Wöhlbrand, L., Halder, T., Kuchta, K., Steinbüchel, A., & Rabus, R. (2008). Solvent stress response of the denitrifying bacterium *Aromatoleum aromaticum* strain EbN1. *Applied and Environmental Microbiology*, *74*(8), 2267–2274.

Venkataramanaiah, V., Sudhir, P., & Murthy, S. D. S. (2003). Effect of high temperature on photosynthetic electron transport activities of the cyanobacterium *Spirulina platensis*. *Photosynthetica*, *41*(3), 331–334.

Waters Corporation. (2014). AccQ.Tag Ultra Derivatization Kit. Milford, MA, USA.

Wen, X., Gong, H., & Lu, C. (2005). Heat stress induces an inhibition of excitation energy transfer from phycobilisomes to photosystem II but not to photosystem I in a cyanobacterium *Spirulina platensis*. *Plant Physiology and Biochemistry*, *43*(4), 389–395.